9-1983

Improved Methods and Guidelines for Modeling Stormwater Runoff from Surface Coal Mined Lands

Digital Object Identifier: https://doi.org/10.13023/kwrri.rr.147

Michael E. Meadows
University of Kentucky

George E. Blandford
University of Kentucky

Research Report No. 147

IMPROVED METHODS AND GUIDELINES FOR MODELING STORMWATER RUNOFF FROM SURFACE COAL MINED LANDS

By

Michael E. Meadows
George E. Blandford
Principal Investigators

Project Number: B-069-KY (Completion Report)

Agreement Number: 14-34-0001-0222 (FY 1980)

Period of Project: October 1979 - September 1983

Water Resources Research Institute
University of Kentucky
Lexington, Kentucky

September 1983

The work upon which this report is based was supported in part by funds provided by the United States Department of the Interior, Washington, D.C., as authorized by the Water Research and Development Act of 1978. Public Law 95-467.

DISCLAIMER

Contents of this report do not necessarily reflect the views and policies of the United States Department of the Interior, Washington, D.C., nor does the mention of trade names or commercial products constitute their endorsement or recommendation for use by the U.S. Government.

ABSTRACT

The investgations, developments and guidelines for several hydrologic modeling strategies are presented. Investigations were conducted to determine appropriate event curve numbers for surface mined disturbed watersheds; and performance of four synthetic unit hydrograph models (SCS curvilinear, SCS single triangle, Williams and TVA double triangle) on 38 USDA experimental watersheds in 14 physiographic provinces using in excess of 270 events. A second test using only the SCS curvilinear unit hydrograph on 11 small watersheds and 48 events was conducted to investigate the excess rainfall pattern simulated with the curve number model. A procedure for developing a unit hydrograph using the time area method and a two parameter gamma distribution is presented for ungaged watersheds or watersheds undergoing land use changes. The development of a coupled explicit finite difference Green and Ampt infiltration-implicit finite element kinematic wave model is presented. The deterministic overland flow model includes a variable width which is essential for the accurate modeling of the watershed geometry. Both impervious and pervious watershed simulations are presented for the deterministic overland flow model.

DESCRIPTORS: Storm Water*, Strip Mines*, Mathematical Models*, Hydrologic Models, Synthetic Hydrology, Small Watersheds, Model Studies

IDENTIFIERS: Curve Number, Unit Hydrographs, Kinematic Runoff, Green-Ampt Infiltration, Finite Element, Modified Newton-Raphson Iteration, Excess Rainfall Pattern

ACKNOWLEDGEMENTS

The investigators wish to express their sincere gratitude to the United States Department of the Interior for supporting this project with research funding from the Office of Water Research and Technology (Grant No. B-069-KY) and the Office of Surface Mining (Grant No. G5115213). Furthermore, the investigators are grateful to the following graduate students for their work on this project during the past four years: Allen Chestnut, Kevin Howard, Duane Johnson, Bernard Jones, Nathaniel Peters, II, Katheleen Regan, Patrick Reinert and Gary Royalty. Finally, and especially, the investigators wish to thank Ms. Elaine Powell, Ms. Margaret Schwartzel, Ms. Jill Jensen, and Beverly Mullins for their professional typing of this manuscript.

TABLE OF CONTENTS

LIST OF TABLES

LIST OF FIGURES

CHAPTER 1

INTRODUCTION

1.1 Background

As mandated by Federal and state regulations and local ordinances, before certain actions that create a land use change are approved, a management plan for minimizing hydrologic impacts is required. Specific to surface mining, the permit process requires plans for runoff and sediment control and a determination of the probable hydrologic consequences (PHC) of surface mining. These requirements differ little conceptually from the requirements for urban activities; only the setting is different. Surface mining is often conducted in a harsh environment, usually disturbs a large area, can involve major changes in topography, ground cover and soil profile, and is performed in an area where little or no hydrologic information is available. As such, mathematical models that account for the changes in watershed hydrologic response due to these modifications are required for planning management strategies and evaluating thir effectiveness.

Available models include discrete (single event) and continuous (daily flow) models. Generally, the design of stormwater and sediment controls requires only single event information; whereas, PHC's require daily flow variations, an indicator of long term impacts to the coupled surface-subsurface drainage system. Further, available models can be classed as distributed and lumped parameter models. Distributed parameter models, also identified as deterministic models in some references (Overton and Meadows, 1976), account for spatial variability in watershed characteristics. They have a theoretical structure based

on physical laws and measures of initial and boundary conditions and input. When conditions are adequately described, the output from such models should be known with a high degree of certainty. However, because of the complexity of hydrologic processes, simplifications and approximations have been made; thereby introducing coefficients and parameters that cannot be directly or easily measured. This requires that a model be verified by checking simulation results against actual watershed data wherever the model is to be applied.

Lumped parameter models evaluate the response of an entire whatershed as a single hydrologic unit. Model equations generally are descriptive of a concept of the runoff process, not necessarily governing physical laws. As such, model parameters are not always defined as measurable physical entities although they generally are rational. Parameter values are determined through calibration studies.

Both distributed and lumped parameter models require data before the model can be employed. The significant difference is where the data must be located. Distributed parameter models require data at the site of application. Lumped parameter models avoid this requirement through a two-step approach. The optimal model parameters can be determined at locations where data are available. There parameter values can then be correlated with physical watershed and event characteristics. When this is done over several watersheds within a geographic (physiographic) area, the model is said to be regionalized. Once regional relationships are available, it is possible to measure the site characteristics on watersheds where insufficient hydrologic data is available and to predict reliable model parameters. This allows scientifically based simulations. These models of course are limited to watersheds within the

same geographical area, and to those with similar geomorphic and land use characteristics.

Some of the models that are currently used for surface mine simulation are shown in Table 1.1. The data in this table was taken in part from a larger table included in the ASCE task committee report on quantifying land use change effects (ASCE, 1983). The evaluation data for each model is based on questionnaire responses by typical model users. This is not an exclusive list. Those models listed are considered typical of the range of available models. Other notable models such as SEDIMOT II (Wilson, et al., 1982) are not considered only because they were not included in the original questionnaire responses.

These results emphasize the problems of using available models for surface mine simulation. First, though not evident from the table, is the fact that most models were developed and calibrated on data from agricultural, forest, or urban watersheds. Second, the distributed parameter models require a large number of measures, and/or calibration at the site of application. Of the lumped parameter models, only two, TVA HYSIM and TENN II, were calibrated using surface mined watershed data and hence, are regionalized to surface mining. However, they are restricted to surface mined watersheds in the Cumberland Plateau section of the Applachian Plateau Province. Also, it is recommended that they still be calibrated locally for confidence in simulation results. This recommendation is based on the fact that the quality of some of the available data in the New River basin is questionable. (Betson, et al., 1981). Third, key component model parameters, e.g. the SCS curve number, have not been evaluated on surface mined data. A quick look at the user's guides published since 1980 for models applicable to surface mining areas reveals the user must select the appropriate curve number

Table 1.1 Evaluation of Selected Models Used for Quantifying Surface Mining Effects. (Excerpted from ASCE (1983))

	References*		Description**				Application			
Model	Primary	Comparison	Dist.	Lumped	Disc	Cont	#Par/Meas	Easily Det	Cal Needed	Regionalized
SCS CN	SCS, 1972	Hawkins, 1978		X	X		2	Yes	No	No
SCS TR-20	SCS, 1969	Damushkedi, 1979		X	X		12	Yes	No	No
HSPF	Johnson, et al., 1980		X		X	X	$\leq$ 100	No	No	No
TVA HYSIM	Betson et al., 1980	Betson, et al., 1981		X	X	X	$\leq$ 28	Yes	No	Yes
FESHM	Ross, et al., 1978	Curwick & Jennings, 1981	X		X		17	Some	Yes	No
TENN II	Overton, 1980	Curwick & Jennings, 1981		X	X		7	Yes	Yes	Yes
USGS-DSA	Alley, et al., 1980	Sneider, 1981	X			X	7	Yes	Yes	No

* Numbers correspond to List of References

** Abbreviated terms are:

Dist = Distributed

Disc = Discrete (single event)

Cont = Continuous (daily flow)

#Par/Meas = Number of parameters or measures required

Easily Det = Easily Determined

Cal Needed = Calibration Needed

from available tables for agricultural, forest and urban land uses. Finally the number of published comparison studies evaluating the capability of models to simulate in the absence of calibration data is very limited, regardless of land use. As noted in the ASCE task committee report, there are probably a number of reasons why. Most obvious are the constraints of cost and difficulty of obtaining the necessary data to objectively estimate each model parameter to test several models. Published comparison studies, such as Curwich and Jennings (1981), used hypothetical catchment data to overcome these difficulties.

1.2 Confidence in Simulation Models

The choice of which model to use is often an expression of user confidence in individual models. Confidence has been defined as "the belief in the reliability or credibility of the results and exists either consciously or subconsciously in the minds of the model user or clientele" (ASCE, 1983). This belief is derived from experiences in the use, development, or testing of a model, from user understanding of watershed hydrologic processes and model representation of these processes, and from confidence in authority, e.g., textbooks, technical journals, and federal agency recommendations. Ultimately, confidence is founded on verification studies at the watershed where the simulations are required.

When local verification is not possible, the user is encouraged to evaluate models based on comparison studies, model regionalization, and the internal verification provided by the model developers in the parent document.

1.3 Purpose and Outline of Report

The purpose of this report is to present the results of research designed to develop improved methods and guidelines for modeling stormwater runoff from surface mined watersheds. Three primary areas of hydrologic modeling are considered. Namely, the SCS curve number method synthetic unit hydrograph models and kinematic wave modeling of overland flow.

Chapter 2 on the SCS curve number method begins with the theory (section 2.2.1) and the development (section 2.2.2) of curve number models for simulating stormwater runoff. Section 2.3 deals with surface mine curve numbers obtained from rainfall simulation. In particular, the runoff data obtained by Lusby and Toy (1976) for unmined and reclaimed mine spoil sites at two coal mines in Wyoming are presented and discussed.

Chapter 3 deals with synthetic unit hydrograph models. Section 3.2 presents the theory (section 3.2.1) and developments (section 3.2.2) associated with synthetic unit hydrograph models. Section 3.3 presents the two parameter gamma distribution and its relationship to synthetic unit hydrograph models. In section 3.4, four popular synthetic unit hydrograph models are presented. In particular, the Williams' model (section 3.4.1), the TVA double triangle model (section 3.4.2), the SCS single triangle model (section 3.4.3) and the Hahn model (section 3.4.4) are presented and discussed. In excess of 270 storm events on 38 USDA experimental watersheds in 14 physiographic provinces were analyzed using these four synthetic unit hydrographs. The data base and methodology for these events is presented in section 3.5. Section 3.6 presents and discusses the results of these analyses for each of the four synthetic unit hydrograph models. Section 3.7 presents the

investigation of rainfall pattern on the SCS hydrograph results with particular reference to utilizing the curve number model as an infiltration model (section 3.7.1) and the influence of the curve number model on watershed hydrology (section 3.7.2). The results of this portion of the investigation on 11 small watersheds and 48 events is presented in section 3.7.3. Section 3.8 presents a method for estimating unit hydrographs for ungaged watersheds utilizing time-area curves (section 3.8.1) and the results of the McCuen and Bondelid (1983) study (section 3.8.2). This discussion is followed by a proposed method for surface mined disturbed watersheds in section 3.8.3.

Chapter 4 presents the development of a coupled Green-Ampt infiltration and kinematic wave model for the deterministic simulation of overland flow. An explicit finite difference Green-Ampt infiltration model is developed in section 4.2. The kinematic wave approximation for a variable width plane is presented in section 4.3. Section 4.4 presents the finite element spatial and temporal discretization of the variable width kinematic wave approximation. An implicit time discritization of the finite element equations results in a system of nonlinear equations. The modified Newton-Raphson iteration strategy used to solve these nonlinear equations is presented in section 4.5. Section 4.6 discusses the finite element simulations utilizing impervious plane (section 4.6.1) and multi-plane pervious (section 4.6.2) data. Section 4.7 discusses the applicability of the deterministic finite element overalnd flow model to surface mined watersheds.

Chapter 5 summarizes the developments and conclusions which were obtained during this investigation (section 5.1) as well as presenting answers of future research (section 5.2).

CHAPTER 2

SCS CURVE NUMBER METHOD

2.1 Introduction

Simply stated, the SCS curve number (CN) is an index of the runoff potential for a given watershed. The SCS first devised the CN method for estimating direct storm runoff from small, generally ungaged, watersheds using daily rainfall data. From that beginning, the method has evolved into a widely accepted procedure for estimating runoff volume for any rainfall event and is an integral part of many rainfall-runoff models. This has occurred, in part, because the SCS, to the extent possible, determined CN values for gaged watersheds where soils, cover, and hydrologic conditions were known (SCS, 1972). Today, design CNs are determined easily from published tables as a function of hydrologic soil group, land use, and antecedent moisture condition. Further, the research watersheds from which data were used are located in various parts of the United States, so that the CNs apply throughout the country (Rallison, 1980). (Note: They apply better in the more humid regions; there is some doubt about their applicability in arid regions.)

Due to its general acceptance, ease of use and the fact that most models for rainfall abstractions include parameters that are not easily quantified, the CN method is applied widely in surface mining runoff simulations. Popular models, such as SEDIMOT II (Wilson, et al., 1982) and TENN II (Overton, 1980), use the CN model in determining the excess rainfall distribution for convolution with a unit hydrograph in simulating the event runoff hydrograph. It is presented as the technique to use in such authoritative texts as "Applied Hydrology and

Sedimentology for Disturbed Areas" (Barfield, et al., 1981).

The major problem in using the CN method is that CNs have not been determined and tabulated for typical surface mined watershed conditions. This is due to an insufficient data record at controlled surface mined watersheds on which to base CN determinations and the lack of a procedure for determining CN values from limited records or from mixed land use watershed data. The best available data identified during this study are rainfall simulation data on small plots in Wyoming. These data are evaluated following a review of the CM method.

2.2 Curve Number Runoff Model

2.2.1 Theory

The CN runoff model is a simple algebraic equation that evolved from efforts to generalize plots of accumulated rainfall and runoff. Analysis indicated a threshold rainfall depth which must be exceeded before any runoff occurs. The SCS interpreted this as the depth (volume) of rain required to satisfy interception, depression storage and initial high rate infiltration. This depth was termed the initial abstractions (Ia) and is the rainfall before any runoff is recorded at the watershed outfall. After runoff begins, additional loss of rain occurs mainly to infiltration.

For large storms, when accumulated runoff is plotted versus accumulated rainfall, the runoff becomes asymptotic to a line of 45 degrees slope. In other words, as the total actual watershed retention (F) increases to some limiting maximum value (S), the runoff (Q) also increases and approaches P-Ia, where P is the total precipitation. The SCE modeled this conceptually as

$$\frac{Q}{P-Ia} = \frac{F}{S} \qquad (2.1)$$

In the limit, as P->∞, the ratio Q/(P-Ia)->1 and F/S->1. Also, as P->0, Q/(P-Ia)->0 and F/S->0. Since the relationship is valid at the two end points, the SCS assumed it also holds for all intermediate points. An obvious omission in this equation is time, which was not included for two reasons (Rallison, 1980). First, sufficient reliable data were not available to define curves of infiltration capacity versus time for a wide range in soil, land use and cover conditions. Second, if time had been incorporated, it would have required a determination of the time distribution of rainfall in storms for which runoff was to be estimated. In the majority of cases, rainfall records did not permit determinations of the time distribution of individual storms. This is still true and is one reason why synthetic rainfall distributions and frequency rainfalls are used in analysis and design.

After runoff begins, all rainfall becomes actual retention or runoff. That is,

$$P - Ia = F + Q \tag{2.2}$$

Solving Eqs. 2.1 and 2.2 for Q when P > Ia yields

$$Q = \frac{(P - Ia)^2}{P - Ia + S} \tag{2.3}$$

To eliminate the necessity of estimating both variables (Ia and S) in Eq. 2.3, field data were used to correlate Ia and S. The field data indicated that

$$Ia = 0.2\ S \tag{2.4}$$

where the 0.2 factor was determined from the intercept of a median line on a log-log plot of Ia and S. This value has been challenged (Golding, 1979), but no indisputable alternate has survived the test of peer review. Thus, this relationship has persisted and is applied widely in design. Substitution of Eq. 2.4 into Eq. 2.3 gives the more familiar

form of the SCS curve number runoff model.

$$Q = \frac{(P - 0.2\ S)^2}{P + 0.8S} \tag{2.5}$$

The watershed retention factor, S, is limited by either the rate of infiltration at the soil surface or the available soil moisture storage, whichever gives the smaller S value. S is related to CN by the identity

$$S = \frac{1000}{CN} - 10 \tag{2.6}$$

where CN is an index of watershed runoff potential and is documented in various SCS handbooks and technical reports (SCS, 1972, 1975) as a function of land use, soil type and cover condition, and antecedent moisture content.

2.2.2 Development of Curve Numbers

The SCS established CNs by analyzing rainfall and runoff measurements from a large number of experimental watersheds having various known soil and cover types. For each watershed, the maximum one day runoff volume in each year was plotted against that day's total rainfall. A grid of plotted CNs for Ia = 0.2S was laid over each plot, and the median CN selected. The published curve numbers represent the averages of median site values for hydrologic soil groups, cover, and hydrologic conditions. Not all conditions were represented from watershed data; therefore, the SCS interpolated data to complete the information contained in the tables (SCS, 1972). The variablility in CN was considered to be due to infiltration, evapotranspiration, soil moisture, lag time, rainfall intensity, temperature, etc. The SCS chose the antecedent soil moisture condition (AMC) to represent this variability. Though the CN varies continually with soil moisture, the SCS defined only three AMC classes: AMC I for dry conditions; AMC II

for average conditions; the AMC III for wet conditions. Part of the criticism of the CN model stems from this discontinuous relationship and is founded on the failure of handbook values to reproduce observed runoff volumes from known rainfalls. In defense of this apparent shortcoming, the SCS developed the CN model to compare the effects of different land treatment and stormwater management practices on runoff, and not to recreate the specific features of individual storms.

2.3 Surface Mine Curve Numbers from Rainfall Simulation

One approach to obtaining basic information on the runoff generation characteristics of a land use where little or no data are available is to use rainfall simulation. A small site typical of the area soils and cover conditions is selected. Either a sprinkler system is deployed on a grid pattern within the selected site or a movable apparatus with overhead mounted sprinklers is used. The sprinklers have nozzles to produce raindrop sized droplets and pressure regulating valves to maintain constant pressure. Usually they can be adjusted to vary rainfall intensities. A "rainfall" then is simulated and appropriate runoff quantities measured.

2.3.1 Data

In a Bureau of Land Reclamation funded study, Lusby and Toy (1976) used a fixed grid rainfall simulator to obtain runoff data from unmined and reclaimed mine spoil sites at two coal mines in Wyoming. The purpose of their study was to evaluate the effects of different reclamation practices on surface hydrology. Prior to a simulation, they surveyed the site to develop a topographic map and to determine the type and extent of vegetative cover. Soil samples were taken for laboratory determination of textural composition, antecedent moisture content, and

moisture holding capacities. During a simulation, the rainfall was measured by a series of gages and an average rainfall intensity computed with the Thiessen polygon method. Runoff was routed through a flow measuring device and recorded at 1 minute intervals. From these measurements a runoff hydrograph was constructed from which the total runoff volume was determined.

The sites selected for study were at the Dave Johnston coal mine near Glenrock, Wyoming and the Big Horn mine near Sheridan, Wyoming. The characteristics of the study areas and results of the rainfall simulations are summarized in Table 2.1.

The Dave Johnston coal mine is located within the Great Plains Physiographic Province at the southern extremity of the Powder River Basin. The region in the vicinity of the mine can generally be classed as semi-arid, with an average annual precipitation of approximately 15 inches. Most of the rainfall occurs during the growing season as thunderstorms with locally high intensities. Prior to the opening of the mine in 1958, the dominant land use was grazing native grasses. The rehabilitation program began in 1965 and as of June, 1975, some 750 acres of mined land had been reclaimed. Reclamation included several phases. First, spoil banks were regraded so that slopes were less than 33%. Second, 4 to 6 inches of top soil were applied to the surface and mulched at the rate of 2 to 3 tons per acre. Finally, a seed mixture was drilled into the soil using standard farm equipment. Once the vegetation was established, the area was pastured in horses.

The Big Horn coal mine also is located within the Great Plains Physiographic Province but is a part of the Tongue River Drainage Basin. The climate of the area is similar to that at the Dave Johnston mine.

Table 2.1

Characteristics of the Study Sites and Results of Application of 1.5 Inches of Rainfall in 45 Minutes at Two Areas in Wyoming

(Source: Lusby and Toy, 1976)

Item	Dave Johnston Mine		Big Horn Mine	
	Natural	Reclaimed	Natural	Reclaimed
Area (sq.ft.)	2364	3083	2953	2020
Slope (%)	17.6	22.7	14.9	20.5
Clay in Topsoil (%)	20	48	25	35
Bare Soil and Rock (%)	30	13	35	48
Runoff (Inches)				
Dry Soil	0.78	0.60	0.03	0.64
Wet Soil	0.85	1.23	0.13	0.82

The reclamation also is similar with two notable exceptions. Typically there was no mulching of the reclaimed slopes and trees and shrubs common in the area were planted throughout the reclaimed site. Surface mining began in 1943 and the first reclamation was undertaken in 1952.

2.3.2 Results

The event curve number for each simulation is given in Table 2.2 along with the percentage difference in curve number between natural and reclaimed mine spoil conditions. The CN values were computed as those that preserve continuity between measured rainfall and runoff volumes. The relationship was derived by solving Eq. 2.5 for S and then solving Eq. 2.6 for CN.

The results for the Dave Johnston mine indicate little difference in runoff potential between the natural and reclaimed mine spoil sites. Insights are found in the data in Table 2.1. The reclaimed site has a greater slope and higher percentage of clay in the topsoil; both cause increased runoff. However, this site has the lesser percentage of bare soil indicating better vegetative cover which tends to retard runoff and enhance infiltration, especially under dry soil conditions. The effect of the increased clay is most evident when the soil is wet. Then the clay is "tight" and the runoff potential is a maximum. The clay was added to provide a better soil for vegetation, but has the negative impact of increasing the runoff.

The results for the Big Horn mine are more dramatic. The runoff potential at the reclaimed site is more than 25% greater than at the natural site. The data in Table 2.1 point out the obvious reason--the reclamation did not restore the mined land to natural hydrologic conditions. The overland slope was increased 5%, the percentage clay in

the topsoil 10%, and the bare soil 13%. Each change results in increased runoff.

The curve numbers in Table 2.2 were compared with published values to relate them to known agricultural, forested and urban land use curve numbers. For the Dave Johnston mine, the curve numbers for both the natural and reclaimed sites are equivalent to the curve number for cultivated land without conservation in D soils. The natural site at Big Horn has curve numbers equivalent to cultivated land with conservation practices in A and B soils, while the reclaimed site behaves as the reclaimed site at the Dave Johnston mine. These results suggest that until better data are available which can be used to quantify surface mined land curve numbers, the appropriate agricultural (disturbed) land use curve number should be used.

Table 2.2

Surface Mine Curve Numbers for Two Wyoming

Mine Sites Derived From Rainfall Simulations

Soil Condition	Dave Johnston Mine			Big Horn Mine		
	Natural	Reclaimed	% Difference	Natural	Reclaimed	% Difference
Dry	91.7	88.4	-3.6	64.9	89.2	37.4
Wet	92.8	97.5	5.1	73.0	92.3	26.4

CHAPTER 3

SYNTHETIC UNIT HYDROGRAPH MODELS

3.1 Introduction

The promulgation of federal regulations pertaining to the probable hydrologic consequences of surface mining necessitates hydraulic structure design, flood forecasts, and water quality impact studies before proposed mining activities are permitted. Each of these analyses requires the simulation of stormwater runoff hydrographs for presecribed design storm events. Lumped parameter synthetic unit hydrograph models are probably the most widely accepted tools for this task. They are popular because they are simple, requiring only easily determined watershed and land use measures, and because several important design quantities are generated in the output, including the runoff volume, the peak flowrate, and the time distribution of runoff. Although they treat the watershed as a single hydrologic unit, unit hydrograph models can be applied at a subwatershed level when spatial variability is important. Thus, they are viewed as useful tools for simulating stormwater runoff from watersheds undergoing land use change.

Perhaps the greatest problem confronting the model user is the choice of model for a given situation. The literature is replete with models developed and tested internally for specific geographic areas and land uses. Most recently, research has focused more on developing new techniques rather than comparing and contrasting existing ones, thereby, increasing the number of available models. Consequently, the user is faced with a multitude of unit hydrograph models, each based on unique assumptions, on particular watersheds, in a specific region, for a

regional rainfall pattern.

Recognizing that surface mining creates a drastic environmental change, how well models developed and tested on watersheds in agricultural, forested and urban land use apply to surface mining is not known. Moreover, the applicability of models developed in one physiographic region to another is unknown. Before model application to a different land use can be tested objectively, regional performance must be understood.

This portion of the study was designed to test the regional application of four popular synthetic unit hydrograph models. These test results are presented, along with the results of a second test to study the effects of rainfall pattern on simulation accuracy of the SCS runoff hydrograph methodology. Finally, a procedure for determining a unit hydrograph on ungaged watersheds, where regionalized equations are inadequate, is outlined.

3.2 Synthetic Unit Hydrograph Theory

3.2.1 Unit Hydrograph Theory

Sherman (1932) is generally credited with the development of the unit hydrograh concept. He defined a "unit" graph as a hydrograph representing one inch of runoff from a twenty-four hour rainfall, i.e., a unit duration. Once determined for a watershed, this graph was utilized to derive runoff hydrographs for storms of any duration by following the "summation process of nature." For example, if the runoff hydrograph from a two day rain was desired, two unit graphs were constructed. Their ordinates then were adjusted until the volumes under each equalled the volumes of precipitation excess for the first and

second days of the storm, respectively. The second unit graph then was lagged in time one day from the storm start and the ordinates of the two graphs summed to yield the runoff hydrograph for the two day event. Today, the term unit denotes one inch of rainfall excess (runoff) rather than a specified duration. Nonetheless, the basic process of lagging and summing unit hydrograph ordinates to construct the runoff hydrograph has not changed.

Unit hydrograph theory is founded on the following assumptions:

1. For the given drainage basin, the duration of surface runoff is essentially constant for all uniform intensity storms of the same length, regardless of differences in the total volume of surface runoff.
2. For a given drainage basin, if two uniform intensity storms of the same length produce different total volumes of surface runoff, then the rates of runoff at corresponding times on the two hydrographs are in the same proportion to each other as the total volumes of surface runoff.
3. The time distribution of surface runoff from a given storm period is independent of concurrent runoff from antecedent storm periods.

More generally, the unit hydrograph concept says that for a given land use, initial moisture content and rainfall excess duration, the unit hydrograph will be the same for each storm on a watershed. In systems terminology, this means that a unit hydrograph represents a linear and time invariant system (Dooge, 1973). The essence of linearity is the principle of superposition, literally, that hydrographs

from different storm periods are additive. A system is time invariant if its parameters do not change with time. In hydrograph simulation, this assumes the various processes involved in runoff generation are stationary during the runoff duration.

It is well documented that the assumptions of linearity and time invariance are not strictly correct. Much evidence has been reported that has shown the unit hydrograph is also a function of rainfall excess intensity, for example, the data in Minshall (1960) and kinematic wave theory, see Chapter 4 of this report. This simply means the system is nonlinear. However, these assumptions still are made because of the simplication they introduce. Without the assumption of time invariance, it would not be possible to use past records of rainfall and runoff to predict the runoff from a given rainfall. The assumption of linearity allows the prediction of runoff from a storm pattern unlike any other observed in the past. The storm can be decomposed into individual components that are analyzed and summed to yield the runoff hydrograph.

3.2.2 Development of Synthetic Unit Hydrographs

Sherman's unit graphs were developed for a given watershed using observed runoff events. The goal then, as now, was to predict the stormwater hydrograph from a drainage basin where insufficient rainfall and streamflow records are available for the derivation of a unit hydrograph. This requires a procedure (basis) for transferring data from similar, but gaged, watersheds to the watershed in question using map data, i.e., watershed land use, soils, and physiographic data that are readily determined from published maps and reports. Regionalized parameter prediction equations that statistically relate unit hydrograph shape parameters and map data are the basis for this procedure. These

equations are used to predict the unit hydrograph shape parameter values, thereby predicting the unit hydrograph on the ungaged watershed. A unit hydrograph developed in this manner is referred to as "synthetic."

There are three major steps in the development of a synthetic unit hydrograph technique. First, a shape for the unit hydrograph is chosen or derived. It commonly is described with an equation or simple geometric form, e.g., triangle. Next, a procedure is established whereby the parameters governing the shape are determined from obserrved hydrographs. Fig. 3.1 shows the general form of a unit hydrograph and defines the standard unit hydrograph parameters, i.e., peak flowrate, time of peak, lag time, etc. These parameters often are estimated directly from an observed runoff hydrograph that closely approximates a unit hydrograph in that it has a volume of roughly one inch and resulted from a continuous rainfall that ended before the time of peak discharge. A more objective approach is to use a mathematical optimization technique which determines the parameter values that result in the "best-fit" between predicted and observed hydrographs. This is preferred when many hydrographs are to be analyzed, or the rainfall and runoff hydrograph do not satisfy the previously mentioned constraints. Finally, the optimal unit hydrograph parameters are correlated with the watershed physical measures to develop the parameter prediction equations.

Current synthetic unit hydrograph techniques have developed basically along two different approaches (Dooge, 1973). One approach is based on the assumption that every watershed has a unique unit hydrograph, and the other on the assumption that all unit hydrographs

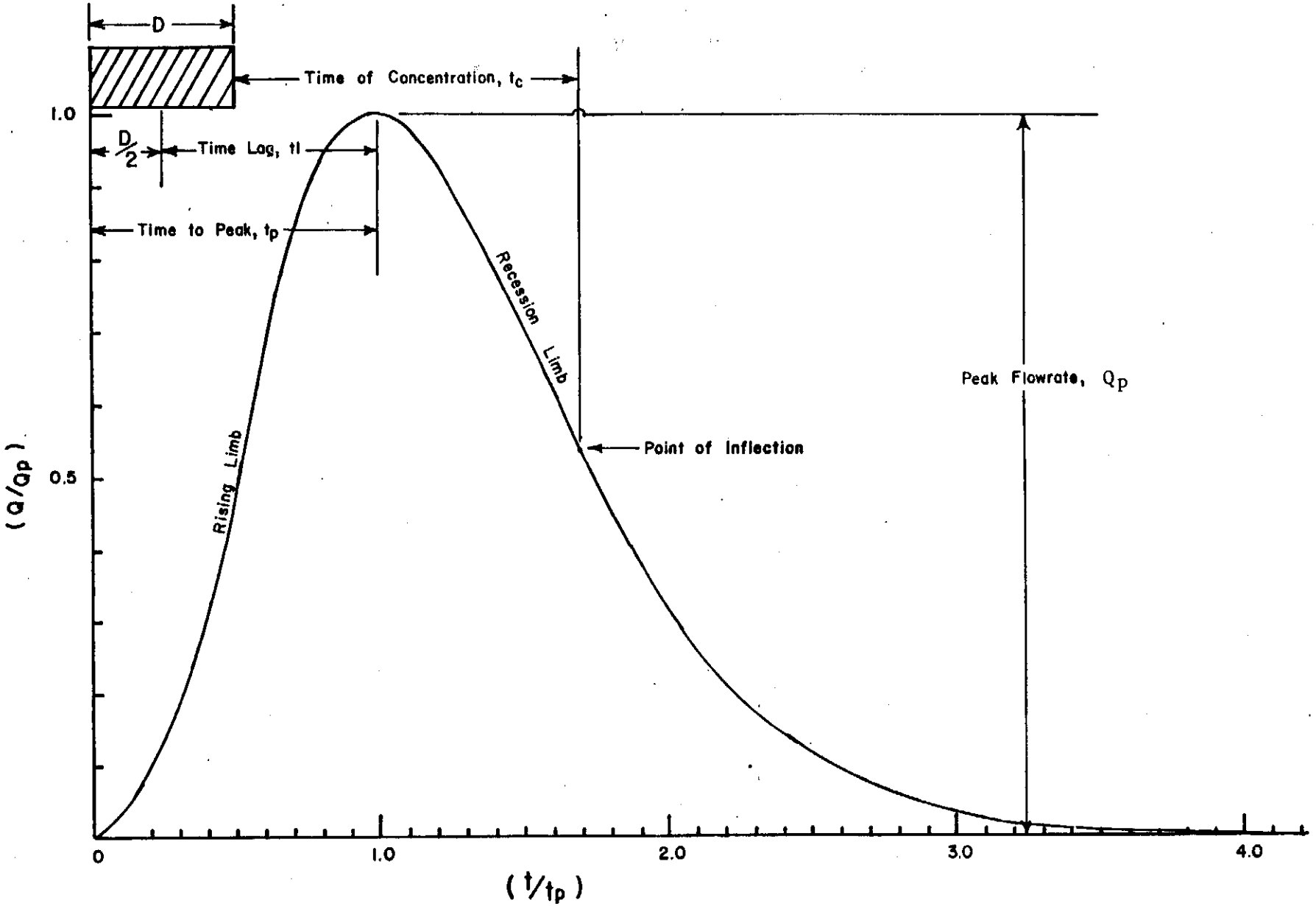

Fig. 3.1 - Typical Unit Hydrograph Parameters

for all watersheds can be represented by either a singe curve, a family of curves, or a single equation. The first line of development arose from efforts to modify the rational method to allow for nonuniform rainfall intensities and irregularities in catchment shapes. A procedure evolved which requires the construction of a time-area curve and a rainfall intensity curve. The rainfall intensity curve is plotted to the same scale as the time-area curve but in the reverse direction. The storm hydrograph is obtained by superimposing the two curves. The zero point of the rainfall curve is placed on the abscissa of the time-are curve at each time, t, and the ordinates summed. As the curves are shifted relative to each other a graphical convolution is performed. As such, the time-area curve serves as a synthetic unit hydrograph.

The second line of unit hydrograph development is not readily apparent. This class of synthetic unit hydrographs includes the empirical techniques which ignored the variation in unit hydrograph shape among watersheds and sought a unique shape or set of shapes which would be applicable to all watersheds. An excellent example is the popular SCS dimensionless unit hydrograph, (SCS, 1972). Because the shape and volume of these unit hydrographs are fixed, only one parameter, usually the peak discharge or time of peak, is required. Other parameters are determined from geometry and volume constraints.

Techniques that sought a family of unit hydrographs generally have been two parameter techniques. It was discovered that working with a family of curves is tedious and that simulation is simplified if the family of curves can be described with an equation. The most common equation that has developed is the two parameter gamma distribution.

3.3 Two Parameter Gamma Distribution

A discussion of the two parameter gamma distribution is presented to better understand its role in the evolution of synthetic unit hydrograph methods, and to develop important shape and timing characteristics. During this research, it was discovered that many of the popular unit hydrograph models were derived directly from this distribution or have shape characteristics that can be explained functionally with it.

3.3.1 Origin and Application

Edson (1950) is credited as the first to use the two parameter gamma distribution to describe the unit hydrograph shape. In fact, he was the first to use a general equation to represent a family of shapes (Dooge, 1973). Prior to this, unit hydrographs were constructed graphically once peak ordinates and other shape characteristics were specified, or dimensionless unit hydrographs were used. His equation resulted from efforts to describe the generally parabolic shape of different watershed time area curves. Although the exact form of his model equation was not applied widely, Edson's approach profoundly affected the work of others.

The most recognized form of the two parameter gamma distribution is the Nash model (Nash, 1959). He developed an equation for unit hydrograph shape with the conceptual model of routing an instantaneous imput of one inch of rainfall excess through a series of linear reservoirs. His equation is

$$Q = \frac{V}{\Gamma(n)K^n} t^{n-1} e^{-t/K} \qquad (3.1)$$

where Q is stormwater discharge, t is time from the beginning of runoff, V is the runoff volume (=1, for a unit hydrograph), and n and K are model parameters, interpreted as the number of conceptual linear reservoirs and reservoir storage coefficient, respectively. Eq. 3.1 and Edson's equation have the same form, demonstrating that the two lines of unit hydrograph development, time area methods and empirical methods, are convergent (Dooge, 1973).

The Nash model has been a workhorse in watershed runoff modeling. The principal question raised has been how many equal linear reservoirs are needed in using this model. Most reported results indicate that from 1 to 5 reservoirs are satisfactory (Overton and Meadows, 1976).

The two parameter gamma distribution has been widely applied in recent years. Gray (1961) used it to develop a synthetic unit hydrograph technique applicable to three regions in the United States (1) Nebraska-Western Iowa, (2) Central Iowa-Missouri-Illinois-Wisconsin, and (3) Ohio. He obtained a set of optimal K values by statistically best fiting the distribution to the dimensionless unit hydrographs from 33 watersheds. These values then were correlated with watershed hydraulic length and average channel slope to develop a prediction equation for K. n was related to K and tp mathematically by equating the first derivative of Eq. 3.1 to zero.

$$K = \frac{t_p}{n-1} \tag{3.2}$$

Wu (1963) extended the utility of the gamma distribution by expressing it in dimensionless form. He used the relationship in Eq. 3.2 to remove the storage coefficient, K, in terms of n and t_p.

The dimensionless equation he obtained is

$$\frac{Q}{Q_p} = \left(\frac{t}{t_p} e^{1-t/tp}\right)^{n-1} \qquad (3.3)$$

where Q_p is the peak flowrate, and the other parameters are as defined previously.

In applying this equation to Indiana watersheds, he modified the recession limb past the inflection point to represent recession exponentially

$$Q = Qo\ e^{\frac{-t - to}{K1}} \qquad (3.4)$$

where to is time at the inflection point, Qo is discharge at the inflection point, and K1 is a storage parameter, representative of withdrawal from valley and bank storage. Wu related K1 and n graphically, and completed his technique by developing synthetic prediction equations for K1 and t_p. Williams (1968) adopted the work of Wu, with modification, to USDA-ARS experimental watersheds in the midwest and south. His work resulted in the computer model, HYMO, and is discussed later in this report.

More recently, Haan (1970) used the dimensionless form to develop families of curves in terms of Q_p, t_p and n. McCuen & Bondelid (1983) demonstrated using the gamma distribution with time area curves to develop unit hydrographs in watersheds where the SCS hydrograph methods are suspect, e.g., coastal watersheds. A similar application for surface mined watersheds is considered in this report.

3.3.2 Shape, Peak Rate and Timing Characteristics

It has been documented that unit hydrograph shapes vary considerably within and among watersheds (TVA, 1973; Overton and Meadows, 1976), thus any model equation must describe a wide range of shapes and variations in peak rate and timing. Mathematical functions, such as the two parameter gamma distribution, have great flexibility for shape, but generally are fixed in shape once the peak coordinates are fixed. In this section, the shape characteristics and relationships among peak rate, time of peak and shape are examined.

The variation of unit hydrograph shape with the shape parameter, n, is best determined with the dimensionless form of the two parameter gamma distribution, Eq. 3.3. For t_p=1, values of Q x t_p in terms of t/t_p were determined for a range of n values. These results are given in Table 3.1. Note the variation in runoff duration. The ordinates Q x t_p, rather than the dimensionless ordinates Q/Q_p, are preferred because the resulting shapes are properly scaled and the volume under each curve is one inch of runoff. These results illustrate the gamma distribution can depict long duration, low peaked hydrographs as well as flashy, short duration, high peaked ones.

The relationship between peak rate and shape is determined as follows. The functional relationship among time of peak, shape parameter and storage coefficient is found by setting the first derivative with respect to time of Nash's model, Eq. 3.1. to zero. This gives Eq. 3.2. which then is used to remove K from the Nash model in terms of n and t_p. The following expression for Qp is obtained for $Q-Q_p$ at $t=t_p$

Table 3.1

Coordinates for Two Parameter Gamma Function Unit Hydrograph

	Shape Parameter								
	2	3	4	5	6	7	8	9	10
t/t_p	$Q \cdot t_p$								
0.00	0.000	0.000	0.000	0.000	0.000	0.000	0.000	0.000	0.000
0.25	0.195	0.151	0.100	0.061	0.036	0.021	0.012	0.007	0.004
0.50	0.303	0.368	0.376	0.361	0.334	0.302	0.270	0.238	0.208
0.75	0.354	0.502	0.600	0.672	0.726	0.768	0.800	0.825	0.844
1.00	0.368	0.541	0.672	0.781	0.877	0.963	1.042	1.116	1.185
1.25	0.358	0.513	0.620	0.701	0.766	0.820	0.863	0.900	0.930
1.50	0.334	0.448	0.506	0.535	0.546	0.546	0.538	0.524	0.506
1.75	0.304	0.370	0.379	0.365	0.338	0.307	0.275	0.243	0.214
2.00	0.270	0.293	0.267	0.229	0.189	0.153	0.122	0.096	0.075
2.50	0.205	0.168	0.117	0.076	0.047	0.029	0.018	0.010	0.006
3.00	0.149	0.089	0.045	0.021	0.010	0.004	0.002	0.001	0.000
3.50	0.106	0.045	0.016	0.005	0.002	0.001	0.000	0.000	0.000
4.00	0.073	0.021	0.005	0.001	0.000	0.000	0.000	0.000	0.000
5.00	0.034	0.005	0.001	0.000					
6.00	0.015	0.001	0.000						
7.00	0.006	0.000							
8.00	0.003								
9.00	0.001								
10.00	0.000								

$$Q_p = \frac{V(n-1)^n}{(n-1)!\ e^{n-1}} \frac{1}{tp} \tag{3.5}$$

$$= \frac{BV}{tp} \tag{3.6}$$

where B is a peak rate factor and is a function only of the shape parameter, n. For Q in cfs, tp in hours, and V in square mile-inch, this relationship is more conveniently written

$$Q_p = \frac{645.33\ BAQ}{t_p} \tag{3.7}$$

where A is the watershed area in square miles, and Q is the runoff volume in inches, equal to 1 inch for the unit hydrograph. With this equation, the peak discharge for a given shape is evaluated. Alternately, the shape (n) is known once the peak rate and time are fixed.

There is an obvious relationship among the shape parameter, the peak rate factor, and the proportion of the runoff under the rising limb of the unit hydrograph. This is evaluated as the time integration of the unit hydrograph from incipient runoff to the time of peak, tp. Using the dimensionless form for the gamma distribution, the following integral is obtained

$$p = 645.33BAQ \int_o^{t_p} \frac{1}{t_p}\left[\frac{t}{t_p} e^{1-t/t_p}\right]^{n-1} dt$$

where p is the volume (proportion) of runoff under the rising limb. This equation must be integrated numerically for noninteger values of n. Table 3.2 gives the relationship among n, B and p for n values from 1.5

to 10. The significance of these data are discussed with the SCS and Haan unit hydrographs, and in the section on developing a unit hydrograph for an ungaged watershed, Section 3.8.

Finally, it is important to investigate the relationship between the unit hydrograph time of peak and watershed time of concentration. With unit hydrograph methods, one definition for the time of concentration is the time from the end of a rainfall burst of duration, D, to the inflection point on the recession limb of the runoff hydrograph generated by that burst. This is illustrated in Fig. 3.1. The time at the inflection point, t_o, is determined when the second derivative with respect to time of the gamma distribution vanishes. This is given by

$$t_o = t_p \left[1 + \sqrt{\frac{1}{n-1}}\right] \tag{3.8}$$

The fundamental relationships for lag time, t_l, and t_p, and t_c and t_o are also indicated in Figure 3.1.

$$t_p = t_l + D/2 \tag{3.9}$$

$$t_c = t_o - D \tag{3.10}$$

Using these relationships and the constraint that burst duration be less than or equal to two-tenths lag time, Eq. 3.8 becomes

$$t_c = t_p \left[0.818 + \sqrt{\frac{1}{n-1}}\right] \tag{3.11}$$

TABLE 3.2
Variation of Peak Rate Factor and Volume
in Rising Limb with Shape Factor

Shape Factor (n)	Peak Rate Factor (B)	Proportion in Rising Limb (p)
1.50	0.2417	0.1959
2.00	0.3675	0.2632
2.50	0.4621	0.2996
3.00	0.5409	0.3230
3.50	0.6097	0.3398
4.00	0.6715	0.3525
4.50	0.7282	0.3626
5.00	0.7808	0.3708
6.00	0.8766	0.3837
7.00	0.9629	0.3933
8.00	1.0421	0.4009
9.00	1.1157	0.4071
10.00	1.1847	0.4122

TABLE 3.3
Variation of Time Characteristics with Shape Factor

Shape Factor (n)	to/t_p	t_c/t_p
1	-	-
2	2.00	1.82
3	1.71	1.53
4	1.58	1.40
5	1.50	1.32
6	1.45	1.27
7	1.41	1.23
8	1.38	1.20
9	1.35	1.17
10	1.33	1.15

Table 3.3 gives values of t_o/t_p and t_c/t_p for various n values. These values are important when relating empirical equations for watershed lag time and time of concentration to unit hydrograph time parameters.

3.4 Synthetic Unit Hydrograph Models

The unit hydrograph techniques tested were selected based on three criteria. First, and most important, the methods must represent the diversity of popularly used models. Second, only techniques in current use for surface mining runoff simulation or readily available for use were considered. Since unit hydrograph techniques require lengthy repetitive computations, the final criterion was computer applicability. The techniques chosen are the Williams (1968), SCS single triangle (SCS, 1972), Tennessee Valley Authority double triangle (Betson, et al., 1980), and Haan (1970) unit hydrograph models.

3.4.1 Williams Model

The synthetic unit hydrograph technique developed by Williams (1968) is available in the computer model (Williams and Haan, 1973). This technique utilizes the two parameter gamma distribution coupled with exponential recession for the unit hydrograph form. The parameter prediction equations were developed from thirty four watersheds, principally in agricultural land use, in Texas, Oklahoma, Arkansas, Louisiana, Mississippi, and Tennessee.

Williams used three equations to describe the shape of his unit hydrograph. He adopted Wu's formulation of the two parameter gamma distribution for the unit hydrograph ordinates. Because he did not abstract base flow from the calibration storm events, this equaion performed poorly in predicting the recession limb. Thus, Williams added

an exponential decay curve, Eq. 3.4, to the recession limb after the inflection point. Later, he extended the length of the hydrograph recession limb with a second exponential decay curve, i.e.,

$$Q = Q1\ e^{\frac{t-t1}{3K1}} \tag{3.12}$$

where Q1 is the discharge at time t1, t1 is time arbitrarily taken at 2K after the inflection point, and K1 is the recession constant defined in Eq. 3.4.

Williams related the parameters K1 and tp to watershed physical characteristics through multiple regression and obtained the following equations

$$K1 = 27.0\ A^{0.231}\ SLP^{-0.777}\ \left(\frac{L}{W}\right)^{0.124} \tag{3.13}$$

$$t_p = 4.63\ A^{0.422}\ SLP^{-0.46}\ \left(\frac{L}{W}\right)^{0.133} \tag{3.14}$$

where A is the drainage area in square miles, SLP is the ratio of the change in elevation from the most remote point on the drainage divide to the watershed outlet (feet) to the watershed hydraulic length width ratio (approximated by the ratio of the square of the hydraulic length to the watershed area) and K1 and t_p are as defined previously.

Williams adopted a graphical relationship developed by Wu (1963), as simplified by Delleur (1964), to determine the unit hydrograph shape parameter, n, from the ratio of K1 and t_p (see Figure 3.2).

The remaining unit hydrograph parameter, the peak discharge rate, Q_p, was determined from the volume constraint. By integrating Eqs. 3.3, 3.4 and 3.12, Williams obtained an equation equivalent to Eq. 3.7. His

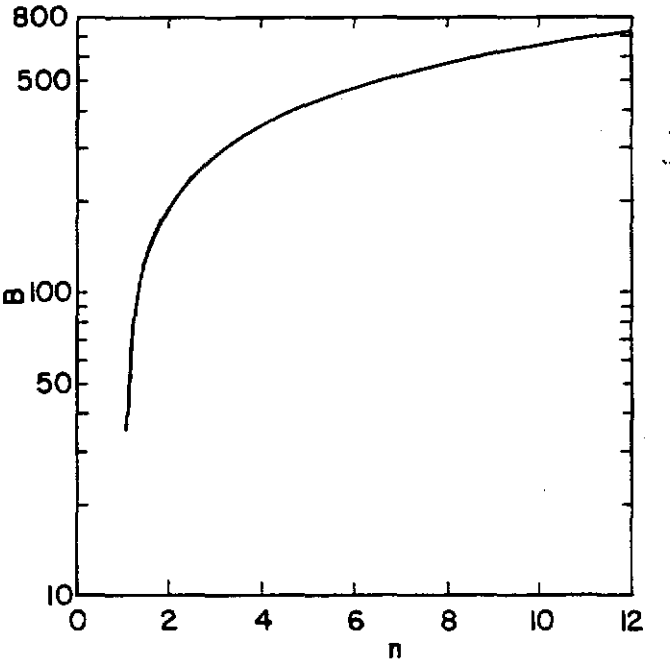

Fig. 3.3 - Relationship Between Dimensionless Shape Parameter n and Watershed Parameter B.

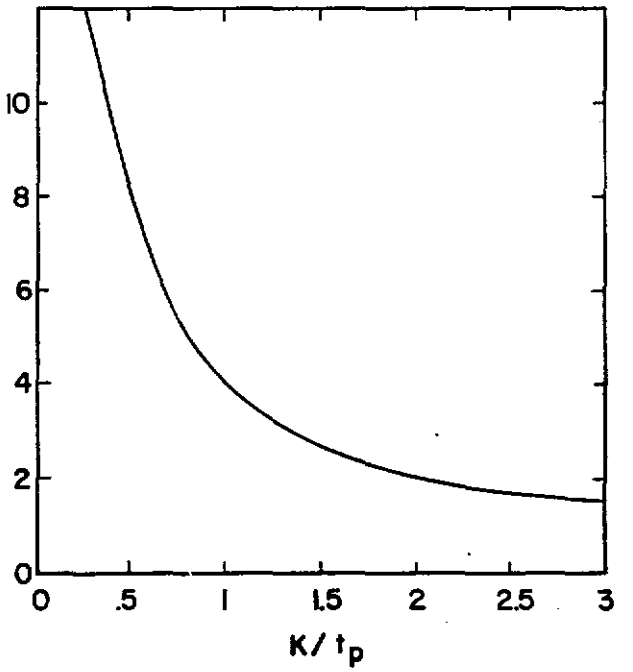

Fig. 3.2 - Relationship Between Dimensionless Shape Parameter and Recession Constant/ Time to Peak.

B value is given in Fig. 3.3.

This formulation for the unit hydrograph shape was programmed with the SCS curve number runoff equation as the computer model HYMO.

3.4.2 TVA Double Triangle Model

The TVA double triangle unit hydrograph technique is available in the computer model HYSIM (Betson, et al., 1980). This technique was developed with data principally from watersheds in the Tennesee River Valley, which includes portions of the older Applachians, Ridge and Valley Province, and Cumberland Plateau. Available surface mined watershed data were from the Cumberland Plateau region only. Therefore, due to limited testing outside this region, the TVA cautions its use elsewhere.

The shape of the double triangle unit hydrograph was derived from the partial area runoff concept, which states the heaviest runoff into a stream emanates first from the riparian wet areas (Ardis, 1972). The remaining areas contribute flow later as their soils become saturated. A unit hydrograph must represent these two separate influences, the immediate and delayed responses. TVA assumed that each watershed response could be represented by a simple triangular shape. It was arbitrarily required that the peak of the delayed response triangle occur at the end of the initial respose triangle. Superimposing these graphs resulted in a quadrilateral unit response function which is known as the double triangle unit hydrograph.

The double triangle unit hydrography is shown in Fig. 3.4. The hydrograph parameters are defined as:

I - The precipitation excess intensity in inches per hour. Since the volume of input is one basin-inch, I = I/DT.

DT - The convolution interval.

UP - The ordinate of the double-triangle model at T1, generally the peak, in inches per hour.

UR - The ordinate of the double-triangle model at T2 in inches per hour.

T1 - The time to peak of the initial response in hours.

T2 - The time base of the initial response and the time to peak of the delayed response in hours.

T3 - The time base of the delayed response and the time base of the double-triangle model in hours.

$p_e(t)$ - The precipitation excess as a function of time, t, in inches per hour.

q(t) - The double-triangle ordinate as a function of time, t, in inches per hour.

The various model parameters are predicted using watershed physical measures and event runoff. The time of concentration, t_c, is related to watershed characterics and a storm runoff intensity parameter, PEIN,

$$t_c = A(PEIN)^B$$

where A and B are predicted from watershed characterics as shown in

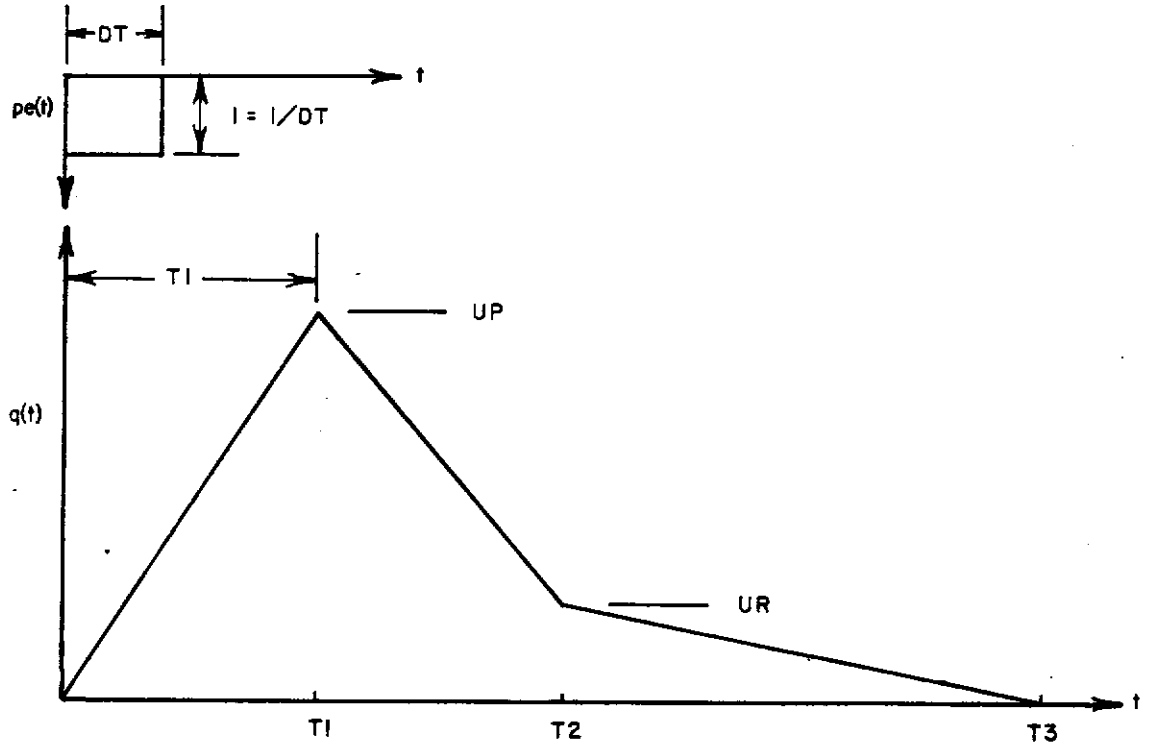

Fig. 3.4 - The Double-Triangle Unit Hydrograph

Table 3.4 and PEIN is defined as

$$PEIN = [\Sigma(PE_i)^2 / \Sigma(PE_i)] / [\Sigma(PE_i) / TRF] \quad (3.15)$$

PE_is the "it^{h}" increment of precipitation excess and TRF is the total storm rainfall.

TVA defined the watershed lag time, lt, as the time between the occurrence of fifty percent of an incremental volume of precipitation excess and fifty percent of the unit hydrograph volume. It related to the time of concentration as

$$lt = 0.6t_c \quad (3.16)$$

Hence, the lag time may be predicted as

$$lt = 0.6\ A(PEIN)^B \quad (3.17)$$

The unit hydrograph parameters UP and T2 are related to the lag time and basin characteristics as power functions

$$UP = C(lt)^D \quad (3.18)$$

$$T2 = E(lt)^F \quad (3.19)$$

where C, D, E and F are related to watershed parameters as shown in Table 3.4. Note that separate equations for A, B, C, D, E, and F were developed for watersheds with drainage areas less than two-square miles.

The unit hydrograph time base, T3, is predicted with

$$T3 = 6.0621t^{0.818}\ DA^{0.113} \tag{3.20}$$

where DA is the watershed drainage area in square miles.

The geometry of the double-triangle is used to determine T1 and UR from the predicted values of UP, T2, and T3. The following geometric relationships hold

$$t_{50} < T1,\ t_{50} = (\frac{T1}{UP})0.5 \tag{3.21}$$

$$t_{50} < T2,\ t_{50} = T3 - (\frac{T3 - T2}{UR})0.5 \tag{3.22}$$

$$T1 < t_{50} < T2, \tag{3.23}$$

$$t_{50} = [UP-(UP^2-[1-AA]\ [BB/CC])^{0.5}](CC/BB)+T1 \tag{3.24}$$

where t_{50} is the time to the occurrence of fifty percent of the unit hydrograph volume and

$$AA = UP - T1 \tag{3.25}$$

$$BB = UP - UR \tag{3.26}$$

$$CC = T2 - T1 \tag{3.27}$$

When t_{50} is greater than T2, UR is determined directly from Eq. 3.22. T1 is found from the requirement that the volume of the unit hydrograph equals one inch of precipitation excess

$$T1 = \frac{-(2 - UP \cdot UR)}{UR} + T3 \tag{3.28}$$

Table 3.4 Regionalized Equations for Predicting Coefficients in the TVA Double-Triangle Unit Hydrograph Equations for TL, UP, and T2

Coefficient*	Constant	Exponent on Basin Characteristic									
		DA	CN	PCM	PERM	CSLOPE	DD	AWA	SHAPE	FOR	SINU
		DA less than or equal to two square miles									
A	330.9	0.047	-1.389	-2.081	1.270						
B	-.0046	-.240		3.116		0.358	1.634	-0.724			
C	0.290		0.115	0.361	-.082		0.179				
D	-1.215	0.073	0.109					0.132			
E	2.989	0.092		-1.039	0.415	-.154					
F	1.802				0.140		-.395		0.195	0.049	
		DA greater than two square miles									
A	147.5	0.072	-0.581			-.158			0.150	0.935	0.438
B	-8.79E-6		2.483		-.057	0.072			-.521		
C	0.708	-.030				0.032		-0.020	-.085		
D	-1.655		-.135		0.078			0.088			0.149
E	3.742					-.228		0.334	0.158		0.300
F	40.62		-0.711			-.100	-.224				

*The coefficients are predicted as follows:

For coefficient "A" for DA greater than two square miles -

$$A = 147.5 DA^{0.072} CN^{-.581} CSLOPE^{-.158} SHAPE^{0.150} FOR^{0.935} SINU^{0.438}$$

The parameters are defined as:

DA = drainage area in square miles

CN = SCS curve number

PCM = a measure of the percentage of mined land in the study watershed

PERM = average soil permeability of the study watershed in inches per hour

CSLOPE = average channel slope in feet per mile

DD = drainage density in miles per square mile

AWC = average available water holding capacity of study watershed soils in inches

SHAPE = a measure of watershed shape

FOR = a measure of the percentage of forested land in the study watershed

SINU = a measure of the mainstream sinuosity

If t_{50} is less than T2, T1 is computed by Eq. 3.21. If t_{50} is less than the T1 computed, then Eq. 3.21 holds and UR is computed from the volume relationship Eq. 3.27. If t_{50} is greater than T1, then Eq. 3.23 applies and a trial and error solution for T1 and UR employing Eq. 3.23 and 3.27 is necessary.

HYSIM uses a modified version of the SCS curve number technique to distribute runoff. Since the value of IA at the beginning of storms and during lulls in multiple burst storms is often too large, a rainfall constant loss parameter PHI was introduced. PHI is subtracted from each time increment of precipitation, P_i, to yield a new rainfall increment, NP_i, subject to the constraint that

$$NP_i \geq 0 \tag{3.29}$$

The NP_i are summed over the storm duration to yield an adjusted accummulated rainfall volume and the curve number is redetermined, CNPE, to maintain runoff volume. The time incremental values of precipitation excess are then determined as

$$PE_i = SRO_i - SRO_{i-1} \tag{3.30}$$

$$SRO_i = \frac{(NP_i - 0.2S)^2}{NP_i + 0.8S} \tag{3.31}$$

where S is the watershed retention.

PHI is estimated with the equation

$$PHI = 0.0567-0.0003PCF1-0.0971SINU-0.0150Q+0.0332 PKARST+0.0314(P-Q)+0.0240(P/DURATION) \tag{3.32}$$

where PCF1 is the percent of watershed under forest cover, Q is the runoff volume in inches, an PKARST is a term representing losses to carbonate rock systems, P is the total accumulated precipitation (inches) and DURATION is the length of the rainfall event (hours). The remainder of the parameters are defined in Table 3.4.

3.4.3 SCS Single Triangle Model

The SCS single triangle unit hydrograph is based on a straight line approximation to the SCS curvilinear unit hydrograph (SCS, 1972). This is shown in dimensionless form in Fig. 3.5. The single triangle is defined by three parameters; the peak flowrate, Q_p, the time to peak, t_p; and the time base, t_b. Since the single triangle and curvilinear unit hydrographs must have a common point of rise, peak flowrate, and time of peak, the rising limb is readily defined. The length of the time base is fixed by the volume constraint.

Unfortunately, the SCS did not publish a derivation or justification for the shape of the curvilinear unit hydrograph other than to note "it was derived from a large number of natural unit hydrographs from watersheds varying in size and geographic locations" (SCS, 1972). Therefore, it is not possible to identify fully the assumptions underlying the single triangle.

In developing the model equations, the SCS required the same volume under the rising limbs of the single triangle and the curvilinear unit hydrographs. This was determined from the mass curve as 0.375 inches, or 37.5 percent of the volume. From the geometric and volume relationships, the two following equations were obatined.

$$t_b = 2.67\ t_p \tag{3.32}$$

$$Q_p = \frac{0.75}{t_p} \tag{3.33}$$

A comparison of Eq. 3.33 with Eq. 3.6 reveals a peak rate factor, B=0.75, which corresponds to a two parameter gamma function shape factor, n=4.70 (see Table 3.2). The two curves are compared in Fig. 3.5. For watershed drainage area, DA, in square miles and t_p in hours, Eq. 3.33 becomes

$$Q_p = \frac{484\ DA}{t_p} \tag{3.34}$$

The SCS defines t_p in terms of lag time and burst duration as illustrated in Fig. 3.1 and given by Eq. 3.9. The burst duration is constrained to be less than or equal to two-tenths of lag time.

The SCS investigated a large number of natural unit hydrographs over a "broad set of conditions ranging from heavily forested watersheds with steep channels and a high percent of runoff resulting from subsurface or interflow and meadows providing a high retardance to surface runoff, to smooth land surfaces and large paved parking areas" (SCS, 1972). It was found that the unit hydrograph lag time can be related to three parameters: (1) the average watershed slope, Y, in percent; (2) the watershed hydraulic length, L, in feet; and (3) the watershed retention factor, S, as determined with the curve number runoff model. The resulting equation for predicting lag time is

$$tl = \frac{L^{0.8}(S+1)^{0.7}}{1900\ Y^{0.5}} \tag{3.35}$$

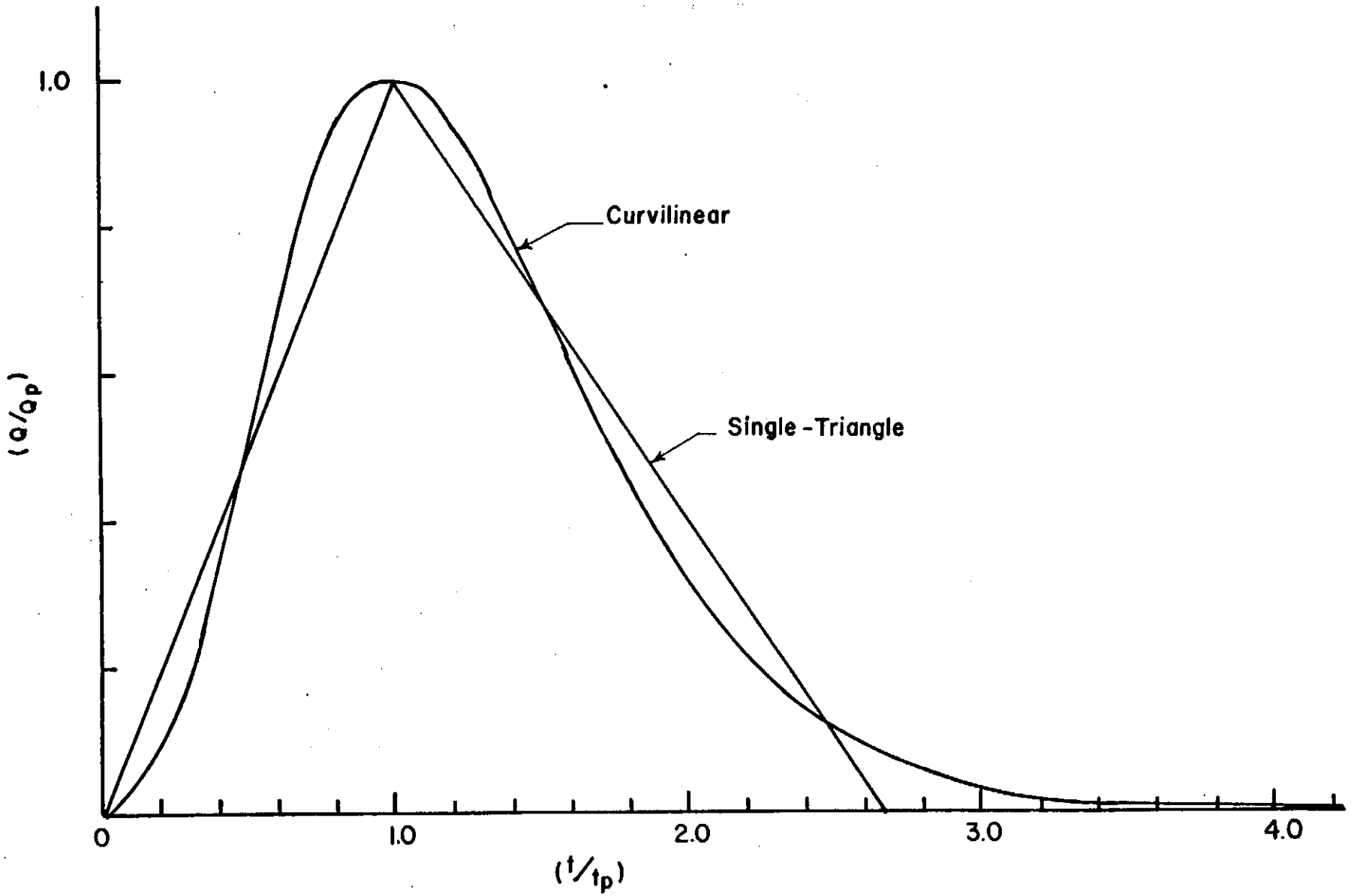

Fig. 3.5 - A Comparison of the SCS Curvilinear and Single-Triangle Unit Hydrographs

where tl is in hours.

3.4.4 Haan Model

Haan (1970) proposed a dimensionless unit hydrograph equation based on the two parameter gamma distribution. Utilizing a simple procedure by Bloomsburg (1960), he reduced the gamma distribution to a dimensionless form equilvalent to Eq. 3.3. His model parameters are Q_p, t_p and C3tp, where C3tp equals n-1. To generate the shape parameter, he developed a graphical solution for C3tp in terms of Q_p and t_p; the resultant curve is identical to the data given in Table 3.2. Because the Haan model equation is a mathematical function, fixing the peak coordinates also fixes the shape.

Rather than developing his own regionalized equations for Q_p and t_p, Haan adopted the SCS equations discussed previously with the single triangle model. This results in a peak rate factor, B=0.75, corresponding to a gamma function shape factor, n=4.70, also discussed with the single triangle. Therefore, the Haan model, when the SCS peak rate and time of peak equations are used, becomes essentially the SCS curvilinear unit hydrograph. This is shown in Fig. 3.6. The Haan model was applied in this fashion during this research.

The computer algorithm for the Haan model was taken from the WASH subroutine of the DEPOSITS sediment pond model (Ward, et al., 1979).

3.5 Data Base and Methodology

3.5.1 Data Base

The main purpose for this study was to determine the regional applicability of four synthetic unit hydrograph techniques. This

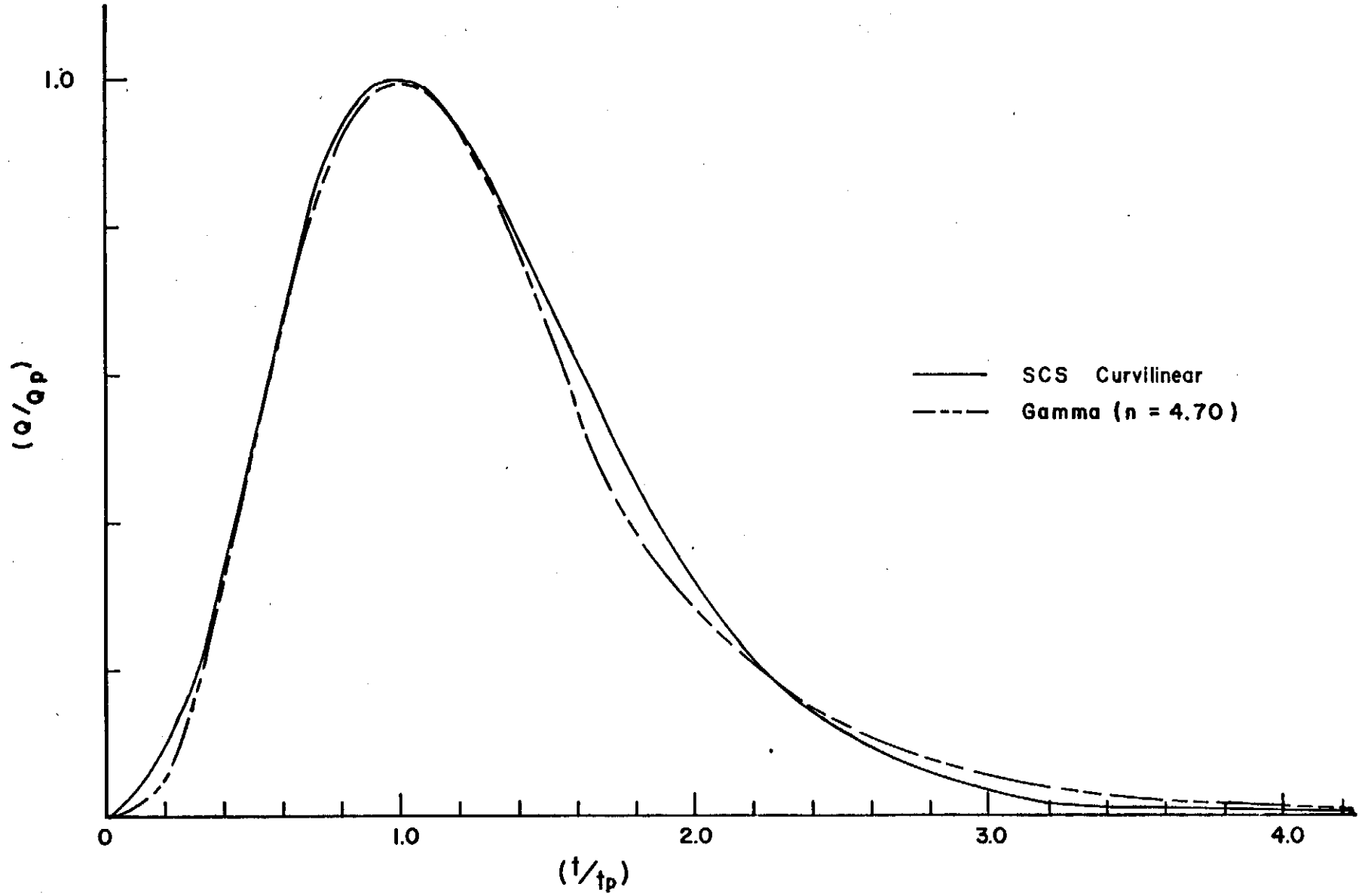

Fig. 3.6 - A Comparison of the SCS Curvilinear and Two Parameter Gamma Function (n = 4.7) Unit Hydrographs

required a complete, quality data set that is characteristic of the hydrology in the major coal producing regions. As noted by Betson, et al. (1981), evidence of questionable data restricts the conclusions which can be made regarding model performance. Therefore, the data base had to be of unquestionable quality. (No data set for watershed hydrology is unquestionable. Rather some are less questionable than the others.) Further, to test several models simultaneously required the data be sufficiently complete to allow determination of all model parameters. Several potential data sets were identified, but only the expermimental watershed hydrologic data published by the U.S. Department of Agriculture, Agricultural Research Service (ARS) met these three conditions.

The ARS data were selected because they are reliable, systematically organized, complete, and representative of the hydrology of the major land use and physiographic provinces east of the Rocky Mountains. These data are published in a series of reports entitled "Hydrologic Data for Experimental Watersheds in the United States." A listing of the volumes in the series is given in Table 3.5 Each section of a report is devoted to a particular experimental station and the following data are given for each watershed at the station:

(1) A description of the watershed.

(2) A table of monthly precipitation and runoff values for the watershed.

(3) A table of the average monthly precipitation and runoff for the period of record.

(4) A listing for the annual maximum flows.

Table 3.5

Publications in the Series:
"Hydrologic Data for Experimental Watersheds in the United States"

Reference Number	For Calendar Year (19--)	Miscellaneous Publication Number	Year Published	Total Pages	Title and Information
1	23 - 57	------	1957	691	"Monthly Precipitation and Runoff for Small Agricultural Watersheds in the United States" 334 watersheds at 60 locations in 27 states
2	23 - 57	------	1958	330	"Annual Maximum Flows from Small Agricultural Watersheds in the United States" 332 watersheds at 59 locations in 27 states
3	33 - 59	------	1960	374	"Selected Runoff Events for Small Agricultural Watersheds in the United States" Runoff events from 68 watersheds at 40 locations in 25 states
4	56 - 59	------	1963	672	"Hydrologic Data for Experimental Watersheds in the United States" 134 runoff events

Table 3.5
(continued)

Publications in the Series:
"Hydrologic Data for Experimental Watersheds in the United States"

Reference Number	For Calendar Year (19--)	Miscellaneous Publication Number	Year Published	Total Pages	Title and Information
5	60 - 61	994	1965	496	"Hydrologic Data for Experimental Watersheds in the United States" 133 runoff events
6	62	1070	1968	447	"Hydrologic Data for Experimental Watersheds in the United States" 136 runoff events
7	63	1164	1970	465	"Hydrologic Data for Experimental Watersheds in the United States" 142 runoff events
8	64	1194	1971	460	"Hydrologic Data for Experimental Watersheds in the United States" 143 runoff events

Table 3.5
(continued)

Publications in the Series:
"Hydrologic Data for Experimental Watersheds in the United States"

Reference Number	For Calendar Year (19--)	Miscellaneous Publication Number	Year Published	Total Pages	Title and Information
9	65	1216	1972	568	"Hydrologic Data for Experimental Watersheds in the United States" 122 runoff events
10	66	1226	1972	399	"Hydrologic Data for Experimental Watersheds in the United States" 106 runoff events
11	67	1262	1973	634	"Hydrologic Data for Experimental Watersheds in the United States" 174 runoff events
12	68	1330	1976	542	"Hydrologic Data for Experimental Watersheds in the United States" 116 runoff events

Table 3.5
(continued)

Publications in the Series:
"Hydrologic Data for Experimental Watersheds in the United States"

Reference Number	For Calendar Year (19--)	Miscellaneous Publication Number	Year Published	Total Pages	Title and Information
13	69	1370	1979	602	"Hydrologic Data for Experimental Watersheds in the United States" 139 runoff events
14	70	1380	1979	515	"Hydrologic Data for Experimental Watersheds in the United States" 113 runoff events

(5) For some watersheds, tables of the daily temperature extremes, daily precipitation, and discharge.

(6) The time record of accumulated rainfall and runoff along with antecedent rainfall and runoff and land use conditions for at least one event.

(7) Graphs for selected runoff events.

(8) A map of the drainage basin.

It was not possible to analyze all the watersheds for which data are available. Only watersheds less than 10 square miles and within or proximate to the principal coal producing regions were considered. In all, 38 watersheds and 270 events were chosen. Table 3.6 lists the watersheds according to ARS experiment watershed research station, and gives their drainage area, land resource code, and the number of events analyzed. The ARS uses a land resource map, shown in Fig. 3.7, to represent the various regions of the U.S. This map closely follows the physiographic map of the U.S. Table 3.7 gives the correspondence between the land resource regions for the 38 watersheds and the physiographic provinces and principal coal producing regions.

A complete listing of the watersheds and events, and discussion of the analysis technique are given in Meadows, et al. (1983).

3.5.2 Methodology

The computer model HYMO (Williams and Hann, 1973) was modified to include algorithms for all four of the synthetic unit hydrograph techniques. This model was adopted because it is very easy to add

Table 3.6 Agricultural Research Service Watersheds Selected for Analysis

ARS Research Station	Watersheds Selected			
	Name	Drainage Area (Acres)	Region Code*	Number of Events
Blacksburg, Virginia	Powells	182	P	8
	L.Winas	1,471	P	8
	Pony Mt.	192	S	8
	Chub Run	2,023	N	8
	Fosters	389	S	8
Edwardville, Illinois	W4	209	M	4
Coshocton, Ohio	10	122	N	8
	5	349	N	9
	92	920	N	6
	94	1,520	N	7
	95	2,570	N	7
	97	4,580	N	7
Fennimore, Wisconsin	WI	330	M	8
	W2	23	M	7
Stillwater, Oklahoma	W1	17	H	8
	W3	92	H	8
	W4	206	H	8
Riesel, Texas	C	579	J	8
	D	1,110	J	8
	G	4,380	J	8
Hastings, Nebraska	W3	481	H	9
	W5	411	H	5
	W8	2,086	H	11
	W11	3,490	H	7
Stafford, Arizona	W11	682	D	7
	WV	723	D	6
Colorado Springs, Colorado	W4	36	G	4
Albuquerque, New Mexico	WI	246	D	4

Table 3.6 cont.

Oxford Mississippi	W4	2,000	P	8
	W10	5,530	P	8
	W19	243	P	8
	W24	512	P	8
	W30	113	P	3
Tombstone, Arizona	W3	2,220	D	7
	W4	560	D	4
North Danville, Vermont	W2	146	R	6
	W3	2,067	R	8
Chickasha, Oklahoma	612	563	H	7

*See Fig. 3.7

Table 3.7 Land Resource Regions, Physiographic Provinces and Coal Production Regions

Region Code	Land Resource Region	Principal Physiographic Province	Coal Producing Region
D	Western Range and Irrigated Region	Basin and Range	San Juan River Reg.
G	Western Great Plains Range and Irrigate Reg.	Great Plains	Fort Union Reg.
H	Central Great Plains Winter Wheat and Range Reg.	Great Plains	Western Interior Reg.*
J	Southwestern Prairies, Cotton, and Forage Reg.	Coastal Plain	Texas Reg.
M	Central Feed Grains and Livestock Reg.	Central Lowlands	Eastern and Interior Reg.
N	East and Central General Farming and Forest Reg.	Applachian Plateau	Northern and Central Applachian Plateau
P	South Atlantic and Gulf Coast Cash Crop, Forest, and Livestock Reg.	Coastal Plain	Texas Reg.
R	Northeastern Forage and Forest Reg.	Ridge and Valley	Northern and and Central Applachian Plateau
S	North Atlantic Slope Truck, Fruit, and Poultry Reg.	Piedmont	Northern Applachian Plateau*

*Most proximate coal producing region. This land resource region presently is not a coal producing region.

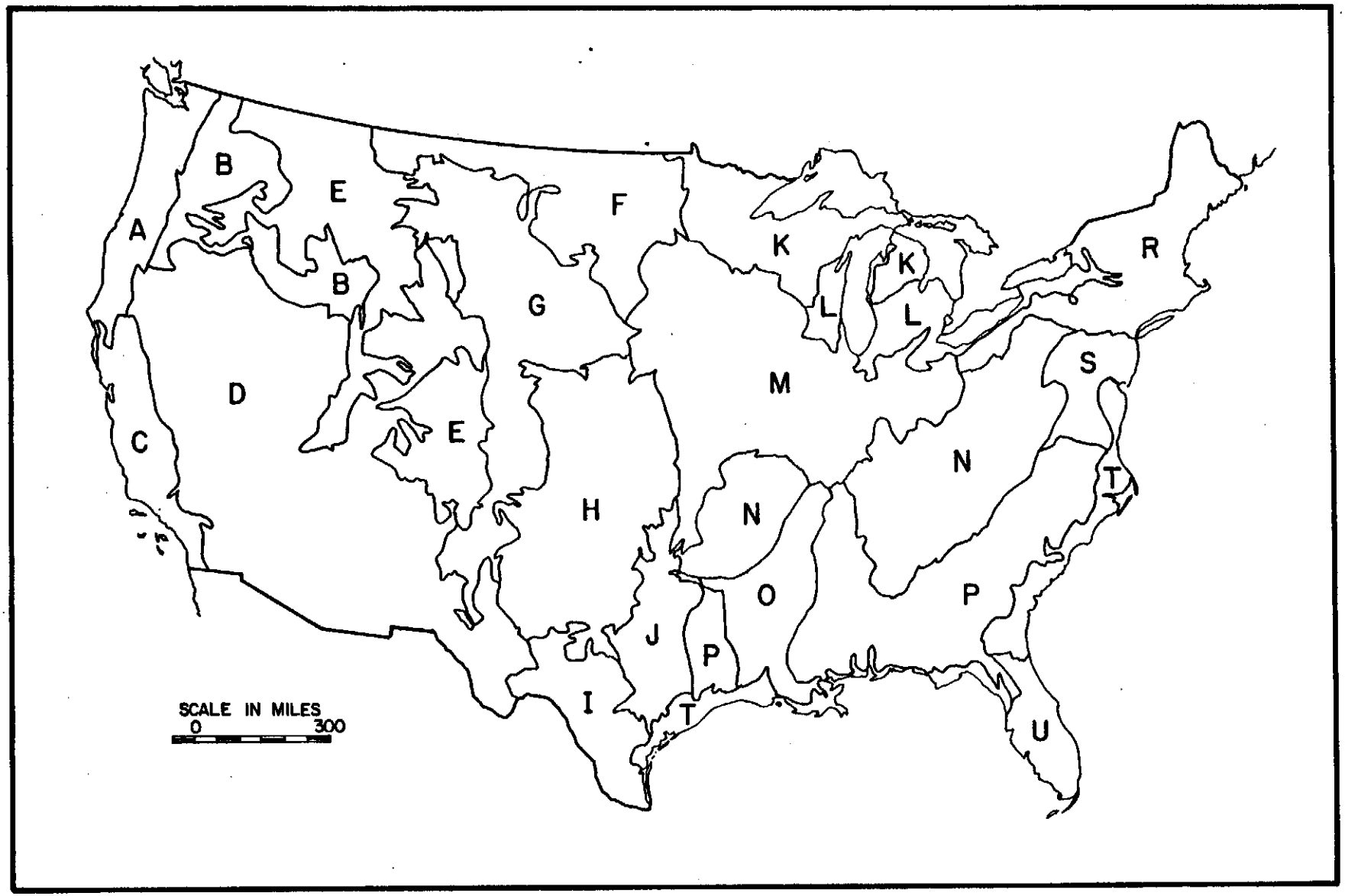

Fig. 3.7 - Map of the United States Showing USDA-ARS Land Resource Regions

subroutines and the sequence of functions to be executed are input with the data. The algorithms for the TVA and Haan methods were abstracted from the computer models HYSIM (Betson, et al., 1980) and WASH (Ward, et al., 1979), respectively, and added to HYMO. A subroutine was written for the SCS single triangle unit hydrograph and added to HYMO.

A preprocessor program was developed to organize the rainfall, runoff and watershed physical data into a format compatible with the HYMO program. Output from this program were written to a file that was read by HYMO. In addition to organizing the data, this program determined computional time increments and the event curve number. The event curve number was used to preserve volume.

Simulation results were printed in tabular and graphical form. Statistical data were determined for peak discharge rates and times of peak. Subjective judgments of simulated shape quality were made and recorded.

3.6 Results

A statistical summary of the results by land resource region is given in Table 3.8. More detailed results and discussion are given in Meadows, et al. (1983). The statistics for mean percent error and standard deviation of percent error are measures of model accuracy and precision, hence indicators of the confidence that a user can place in a given model applied to a specific region. To illustrate, consider the results for peak flowrate in the Southwestern Prairies, Cotton and Forage Region. The Williams model had the smallest standard deviation meaning it was the most precise. However, its accuracy was worse than the SCS and Haan models. They averaged overpredicting the peak by less than 20 percent while the Williams model averaged underpredicting the

peak by 40 percent.

A discussion of each model performance follows.

3.6.1 Williams Model

The Williams unit hydrograph model demonstrated a tendency to underpredict outflow hydrograph peak flowrates. This is, in part, because his unit hydrograph model does not round the unit hydrograph time to peak to the nearest convolution interval. When the unit hydrograph is lagged and summed a portion of the peak is usually lost. This has an added undesirable effect of destroying runoff volume.

Allowing the hydrograph recession limb to fix the hydrograph shape and hence peak flowrate also contributes to the model tendency to underpredict peak flowrates. The two exponential decay recession limbs shift runoff from the rising limb and reduce the peak flowrate. The long hydrograph time base created by the exponential decay equations occasionally exceeded allotted computer storage space. The resulting truncation caused a loss of runoff volume.

This model has the simplest parameter inputs of the unit hydrograph techniques tested. Very little parameter preparation or estimation time is required to use this model.

Williams' unit hydrograph model outperformed the SCS, Haan, and TVA models in the East and Central General Farming and Forest Region (specifically at Coshocton, Ohio). It was generally acceptable at Oxford, Mississippi in the South Atlantic and Gulf Slope Cash Crop, Forest, and Livestock Region.

Table 3.8 Statistical Analysis by Land Resource Region

Resource Region (Code)	Unit Hydrograph Technique	Percent Error			
		Peak Flowrate		Time of Peak	
		Mean	Standard Deviation	Mean	Standard Deviation
Arid Lands (D,G)	Williams	-63.16	40.53	106.52	186.43
	SCS	-51.43	63.06	201.74	345.38
	TVA	-21.04	82.40	-95.15	289.01
	Haan	-49.78	64.37	201.78	352.33
Central Great Plains Winter Wheat and Range Region (H)	Williams	-49.97	17.98	34.36	56.67
	SCS	-8.87	35.75	33.28	57.15
	TVA	25.18	81.73	-22.51	36.44
	Haan	-6.31	36.69	32.23	57.83
Southwestern Prairies, Cotton, and Forage Region (J)	Williams	-40.70	13.23	7.42	38.92
	SCS	15.87	25.77	8.62	40.73
	TVA	196.29	248.15	-22.03	40.46
	Haan	19.30	26.67	7.56	40.21
South Atlantic and Gulf Slope Cash Crop, Forest, and Livestock Region (P)	Williams	-36.30	29.27	21.01	47.85
	SCS	7.60	53.98	25.03	63.30
	TVA	-7.33	54.13	2.32	56.58
	Haan	10.65	55.62	23.23	1.75
Central Feed Grains and Livestock Region (M)	Williams	-52.14	20.34	47.16	50.44
	SCS	-24.78	27.14	69.86	76.41
	TVA	-44.49	32.78	55.96	173.16
	Haan	-22.01	28.26	70.47	76.28
East and Central General Farming Region (N)	Williams	46.60	107.74	-6.27	19.17
	SCS	69.16	90.16	-8.22	22.11
	TVA	-27.56	44.61	4.42	37.72
	Haan	72.61	91.86	-8.34	22.10

Table 3.8 Statistical Analysis by Land Resource Region (Cont.)

Resource Region (Code)	Unit Hydrograph Technique	Percent Error			
		Peak Flowrate		Time of Peak	
		Mean	Standard Deviation	Mean	Standard Deviation
Northeastern Forage and Forest Region (R)	Williams	224.37	114.84	112.31	367.55
	SCS	189.37	102.68	122.71	375.30
	TVA	96.70	122.54	-15.41	48.59
	Haan	195.97	103.25	122.61	373.02
North Atlantic Slope Truck, Fruit, and Poultry Region (S)	Williams	21.86	40.13	-0.88	27.31
	SCS	41.02	83.07	10.72	32.46
	TVA	44.07	114.76	-6.84	27.48
	Haan	44.25	86.04	9.72	32.91

3.6.2 SCS and Haan Models

Since the SCS synthetic equations were used with the Haan unit hydrograph there was little or no difference in the magnitude or timing of the peak coordinates for these models. As a rule, the Haan model produced a better overall hydrograph shape.

When these models were programmed for inclusion into the HYMO computer program a rounding routine was added that forces the peak flowrate to occur at an even convolution interval thus there were no volume loss problems with these models.

With the exception of the average watershed slope, the input parameters required by these models were simple to determine. The SCS does not identify any technique for determining average watershed slope with their equations. The grid technique utilized in this study was reasonable and consistent but extremely tedious.

The SCS and Haan models outperformed the Williams and TVA procedures at Oxford, Mississippi (the South Atlantic and Gulf Slope Cash Crop, Forest, and Livestock Region), at Riesel, Texas (the Southwestern Prairies, Cotton and Forage Region), and at Hastings, Nebraska and Stillwater, Oklahoma (the Central Great Plains Winter Wheat and Range Region).

3.6.3 TVA Double Traingle Model

The most striking feature of the TVA unit hydrograph model was the extreme variation in its predictions. This is evidenced by the consistently higher standard deviations. This variation is attributed, in part, to the rainfall constant loss parameter, PHI, on the rainfall excess pattern. In the HYSIM model, the PHI parameter caused volume losses whenever it was sufficiently large to make CNPE greater than 100.

In this study, to overcome these losses, PHI was forced to zero whenever CNPE reached 100. As a result some simulations were made with and some without PHI.

It was noted that TVA relied heavily upon rainfall/runoff event data reported at one hour time intervals in the development of their regionalized equations. During this study, the TVA model was applied to rainfall/runoff event data of much smaller time intervals. This may have influenced the results.

One further observation with the TVA model concerns the time base prediction equation. In numerous instances a very long time base was predicted. This shifted runoff volume to the recession limb and reduced the peak flowrate. This was considered a reason why the model frequently underpredicted the runoff hydrograph peak.

The TVA model requires three times the watershed parameters as any other model tested. Depending on the availability of maps and soil surveys, the time required to develop parameter estimates often exceeded the time required to complete the simulations with the other three models.

The TVA double-triangle unit hydrograph model did not produce outstanding results in any region studied. It did, however, outperform the other models in regions with unusual hydrologic characteristics, i.e., the arid southwest and New England watersheds near North Danville, Vermont.

3.6.4 Summary

The Haan two-parameter gamma distribution unit hydrograph coupled with the SCS parameter prediction equations was, in general, the best

synthetic unit hydrograph technique tested. It was simple and straight forward, easy to use, and gave acceptable predictions in terms of peak coordinates and outflow hydrograph shape. It demonstrated broader application, than the other techniques. With the exception of hydrograph shape the same holds true for the SCS single triangle unit hydrograph.

The Williams synthetic unit hydrograph technique worked very well at Coshocton, Ohio. Watersheds at Coshocton, Ohio are typical of much of the Appalachian Plateau. This technique should be applicable in that region. Potential users should, however, consider correcting the hydrograph scheme as discussed previously.

In the HYSIM user's guide, the TVA explictly outlined the region of applicability for their model (Betson, et al., 1980).

> "The regionalized relationships incorporated in TVA-HYSIM were derived using hydrologic data collected in the Tennessee Valley and surrounding area. This region includes six physiographic provinces: Blue Ridge, Valley and Ridge, Cumberland Plateau, Highland Rim, Central Basin, and Mississippi Embayment. . . To the extent that conditions are similar to those within this region, the model will apply elsewhere. Its applicability, however, should be verified."

This study provided limited testing in other regions. Based on the results of this study, further work is required in other regions before the TVA model can be confidently applied. The model was included because it is the only model having a parameter for the percent of mined land. No watershed tested was disturbed by mining; therefore, the

advantages of this additional parameter could not be assessed.

It should be noted that the TVA model did well at North Danville, Vermont which is in the Ridge and Valley Province, one of the provinces within its region of applicability.

In closing, it is requested that the reader note the extreme variations in the synthetic unit hydrograph peak flowrate and time of peak predictions in Table 3.8. Any potential user of unit hydrograph techniques should realize that a + 25 percent prediction of an event is the rule rather than the exception. This is the price that one pays for the simplifying assumptions of linear theory and spatial uniformity of rainfall. One should be careful in attaching absolute significance to the hydrograph produced by any one technique for a particular watershed.

3.7 Rainfall Pattern and SCS Hydrograph Results

The results of this study, though inconclusive due to the limited number of events analyzed, indicate regional applicability for each model, with the SCS curvilinear unit hydrograph generally performing best overall. Since event curve numbers were used, hydrograph volumes were predicted exactly. For each model, simulated shapes compared well with observed shapes; but, predicted peaks and times of peak varied widely. A sensitivity analysis revealed that peak rate and timing are more sensitive to curve number than to the unit hydrograph shape parameters.

Based on the sensitivity analysis and criticism of the curve number model for determining the rainfall excess distribution, a second study was conducted to test the hypothesis that the simulation errors were due to the rainfall excess pattern predicted with the curve number model, i.e., due to using the curve number model as an inflitration model.

Forty-eight events on 11 small watersheds at the Central Great Plains Experimental Watershed at Hastings, Nebraska, were selected for the study. The results of the first study indicate that the SCS curvilinear unit hydrograph model performs well within this region, see Table 3.8, and therefore should be applicable to these watersheds. Thus, these watersheds were chosen to reduce spatial variation in rainfall, soils, land use, etc., and to reduce channel routing effects. Minimization of these sources of variability should insure objective test results.

3.7.1 Curve Number Model as an Infiltration Model

The general application of the SCS curve number runoff model and methods for determining curve numbers are discussed in Chapter 2 of this report. The following discussion pertains to the performance of the curve number model in determining the rainfall excess distribution for a known rainfall.

To determine the rainfall excess distribution, the curve number model is applied to successive time levels of the accummulated rainfall curve. During any time interval, Δt, the incremental volume of rainfall excess is

$$\Delta Q = Q(t + \Delta t) - Q(t) \tag{3.36}$$

which also can be written as

$$\Delta Q = \Delta P\left[1 - \frac{S^2}{(P(t) + 0.8S)^2 + \Delta P\ (P(t) + 0.8S)}\right] \tag{3.37}$$

where $P = P(t + \Delta t) - P(t)$. During the same time interval, the rain lost

to infiltration is

$$\Delta F = \Delta P \frac{S^2}{(P(t) + 0.8S)^2 + \Delta P(P(t) + 0.8S)} \tag{3.38}$$

The average rate of infiltration (and other abstractions) during the time interval is $\Delta F/\Delta t$. In the limit as $\Delta P/\Delta t \to i$, the instantaneous rainfall intensity, and $\Delta F/\Delta t \to f$, the instantaneous infiltration rate, Eq. 3.38 becomes

$$F = i \left[\frac{S}{P + 0.8S}\right]^2 \tag{3.39}$$

which is the curve number infiltration equation (Hawkins, 1980).

Several limitations to the curve number model are evident in Eq. 3.39. First, note that f varies directly with i, regardless of the magnitude of rainfall intensity. This is consistent with modern theories of infiltration only when the rainfall intensity is less than the potential (capacity) rate of infiltration; otherwise, the infiltration rate equals the capacity rate. Further note that as P becomes large, $f \to 0$. This is consistent with modern theory when either rainfall or soil moisture storage are limiting; otherwise the capacity rate asympototically approaches a steady final rate equal to soil saturated hydraulic conductivity. Also, during lulls when $i \to 0$, $f \to 0$, and the curve number model fails to predict the infiltration of water ponded on the watershed, i.e., surface runoff. Thus, the curve number model should perform best on short duration rainfalls without lulls or extended periods of rainfall intensity less than the soil saturated hydraulic conductivity.

3.7.2 Curve Number Model and Watershed Hydrology

Further insight to the application of the curve number model is gained by considering model performance in terms of watershed hydrology. There are currently four views on the mechanics of runoff generation. They are: (1) surface runoff due to rainfall excess, i.e., rainfall intensity exceeds infiltration capacity; (2) shallow subsurface flow through a highly permeable soil layer; (3) surface runoff from the emergence of subsurface flow in a region of saturated soil or at the outcrop of a confining impermeable layer; and (4) deep subsurface flow through the saturated zone. These viewpoints can be generalized as hydrographs dominated volumetrically by surface and subsurface flow.

Hydrographs dominated by surface runoff generally have sharp peaks and short recession limbs. Also, the flowrate is sensitive to changes in rainfall intensity. On the other hand, hydrographs dominated by subsurface flow generally have rounded peaks and protracted recession limbs, and exhibit little sensitivity to temporal variations in rainfall. To determine whether the hydrograph is dominated by surface or subsurface flow, Dunne (1978) recommended fitting the following equation to the recession limb

$$Q = Q_p K^t \tag{3.40}$$

where Q is the discharge at time, t, Q_p is the peak discharge, and K is a recession constant. Dunne analyzed hydrographs from controlled watersheds, where the sources for flow dominating the hydrographs were known, to establish values for the recession constant. For watersheds approximately one square mile in area, K greater than 0.7 indicates subsurface flow dominance; and K less than 0.3, surface dominance.

Figures 3.8 and 3.9 are plots of event accummulated rainfall,

runoff, and total abstraction, F+Ia, for watersheds dominated hydrologically by surface and surface flow, respectively. Figure 3.8 is for the storm event of June 7, 1953, on watershed W-3 at Hastings, Nebraska (USDA-ARS, undated). W-3 is a 401 acre watershed on 5% slope, with silty clay loam topsoil over a silt loam subsoil. This watershed is considered to be dominated by surface runoff because of the recession constant value, 0.30, and the results of the kinematic runoff model reported in Chapter 4 on the smaller watersheds at Hastings. The kinematic model is based on surface runoff only.

Figure 3.9 is for the storm event of August 16, 1971, on a 380 acre watershed in the Santee Experimental Forest located in the Coastal Plain northeast of Charleston, South Caroline (Medina and Mohns, 1978). This watershed is flat, average slope less than 0.5%, with loamy to sandy topsoil overlaying a clay subsoil. The average recession constant value is 0.90, indicating subsurface dominance of runoff.

Also shown on each figure is the accumulated runoff predicted by the curve number model before and after routing with the unit hydrograph procedure. These curves are labelled Q,CN and Q,CN-ROUTED. For each event, the observed and precidted Q curves differ significantly. The F+Ia curves indicate a buildup of storage within the watersheds that is released with the runoff hydrograph. For the watershed where surface runoff dominates the runoff hydrograph, Fig. 3.8, the routed Q curve nearly matches the observed; whereas, for the case of subsurface dominance, Fig. 3.9, the routed and observed curves match only to hour 13, approximately the time of peak runoff. During the recession limb, the observed curve lags the predicted by several hours. Around hour 18, the difference between the two curves is about 0.35 inches of runoff.

The simulated hydrograph for the event in Fig. 3.8 resulted in a 4.9 percent overprediction in peak rate, eight minute lag in time of peak, and a shape correlation of 0.96. Comparative statistics for the event in Fig. 3.9 are 71 percent overprediction in peak rate, 1.5 hours lag in time of peak, and shape correlation of 0.63. The lags in time of peak are four and eight percent of the runoff duration, respectively.

These results suggest that curve number model and SCS curvilinear unit hydrograph properly lags and attenuates the rainfall excess, regardless of the previously mentioned criticisms.

Several hydrographs were analyzed from Pony Mountain Branch near Blacksburg, Virginia, and from watersheds in the New River basin of the Cumberland Plateau region of Tennessee. These were selected because of their proximity to coal mining regions and their mountainous topography. The data for the New River basin were collected on watersheds up to twenty percent mined, but under the old mining practices that did not require return to contour (Betson, et al., 1981). Almost every event analyzed indicated subsurface, or analygous, dominance. This suggests that the standard SCS curvilinear unit hydrograph methodolgy does not apply to watersheds in this condition. If, however, an alternate unit hydrograph shape is used that better mimics the natural attenuation and dispersion characteristics, the method can be adapted and reliable simulations made. No suitable data for current mining practices was identified in time for this report. Therefore, no conclusions can be offered about the performance of any unit hydrograph model on surface mined watersheds.

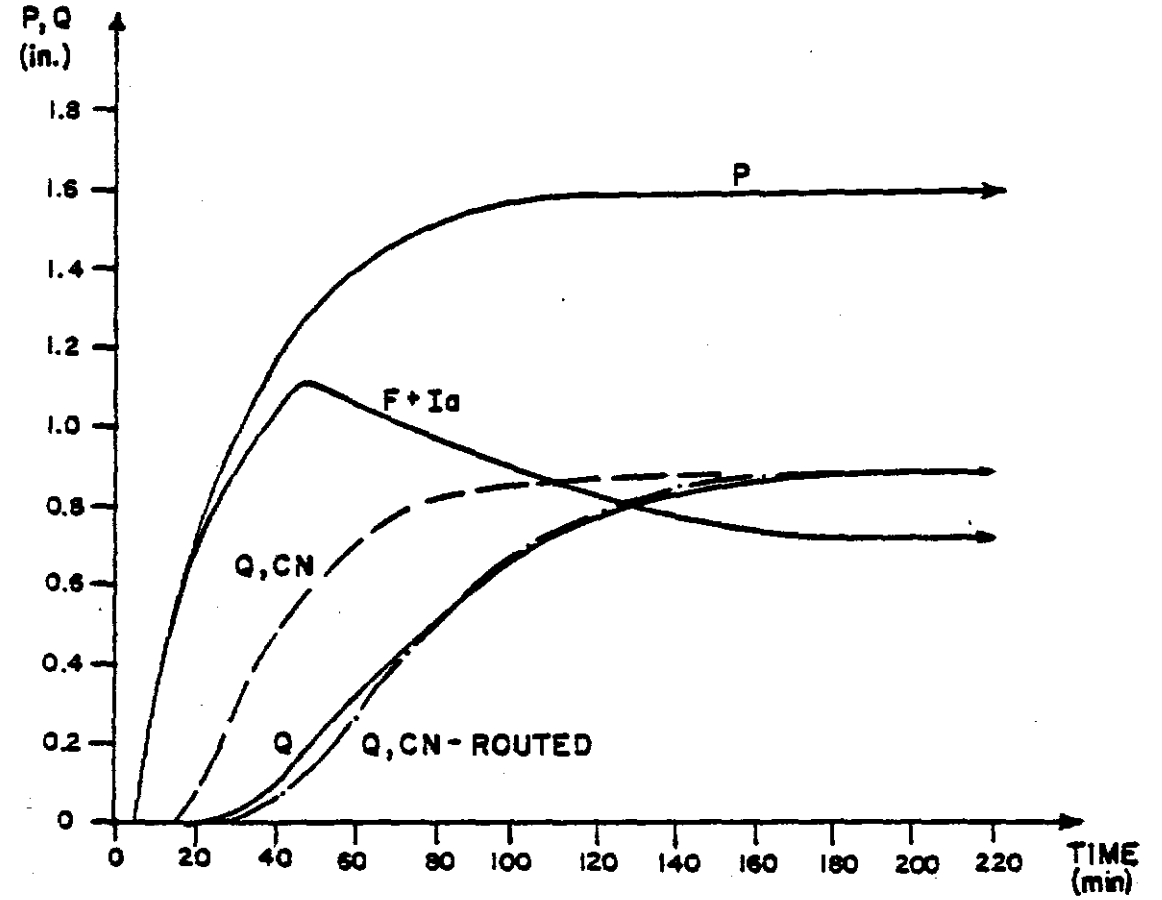

Figure 3.8 Event of June 7, 1953 on Watershed W-3.

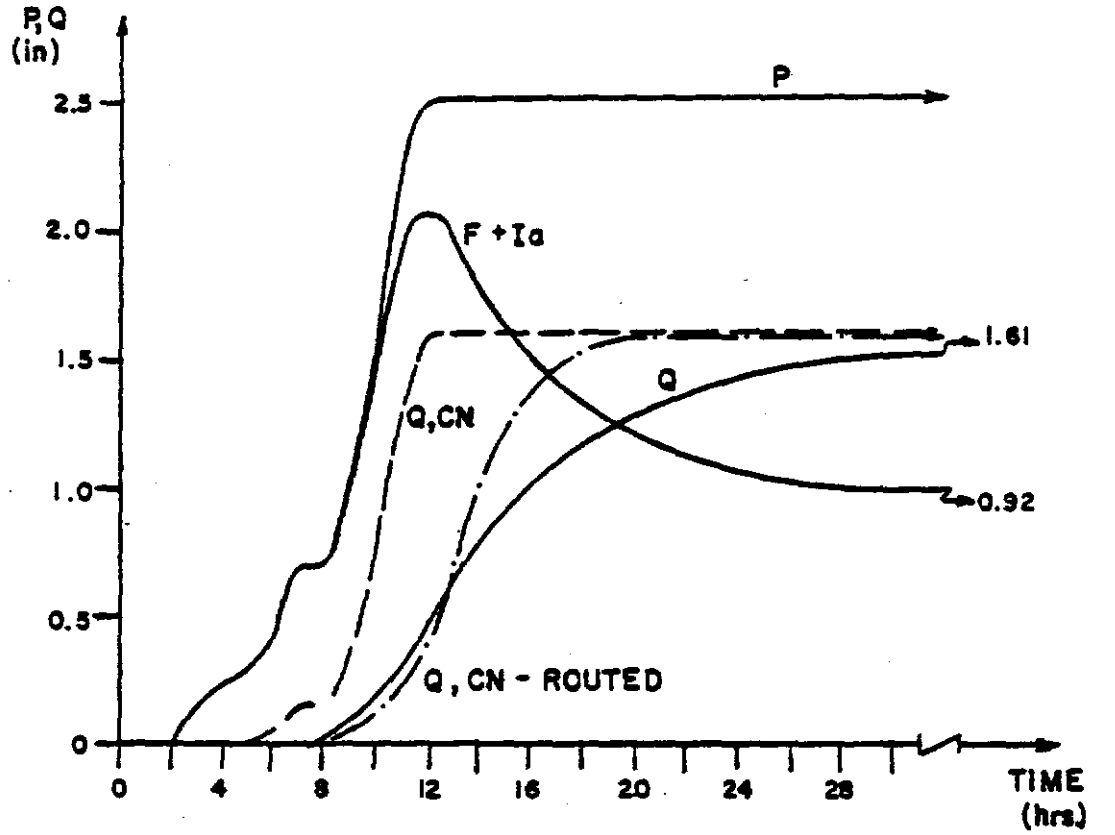

Figure 3.9 Event of August 16, 1971 on Santee Watershed.

3.7.3 Results

The test watersheds were less than five acres, in varying agricultural land use, and with average slopes ranging from 3.8 to 7.2 percent. Watershed soils were similar to those described previously for watershed W-3. The rainfall events were grouped into three categories: (1) continuous events without lulls or extended periods of rainfall intensity less than soil hydraulic conductivity; (2) events ending with an extended period (tail) of rainfall intensity less than soil hydraulic conductivity; and (3) events with one or more lulls. The runoff hydrographs were simulated using the event curve number. The results for peak flowrate and time of peak predictions are summarized in Table 3.9. The results were best for continuous events without lulls or extended periods of rainfall intensity less than soil hydraulic conductivity. The average error in peak flowrate was 13.5% for the continuous events, with a range from 2.7 to 30.8 percent. This error was at least 2.5 times greater for rainfalls with a "tail" or lull. Also, the ranges in percent error were 2.8 and 4.4 times greater. These results support the notion that the curve number runoff model works better for the continuous rainfall pattern. To test this idea further, those events with tails were simulated again, but with a portion of the rainfall in the tail deleted. The amount deleted was selected to approximate the rainfall after rainfall and surface runoff became limiting for capacity rate infiltration. The peak rate prediction error for 75 percent of the events was reduced within the range of error for continuous events. These results are encouraging; but, further study is required before a firm rule-of-thumb is identified. No approach to improve the error in peak rate for events with lulls has tested successfully.

Table 3.9

Simulation Results As A Function of Rainfall Pattern

Rainfall Pattern	Number of Events	%Abs Error in Peak Rate Average	Range	Avg. Error Time of Peak (minutes)
Continuous	14	13.5	2.5 - 30.8	2.7
Tail	19	37.4	5.0 - 83.1	4.0
Lull	15	34.9	1.5 -125.0	4.5

3.8 A Method for Estimating Unit Hydrographs for Ungaged Watersheds

The inherent regional applicability of synthetic unit hydrograph techniques developed for agricultural, forested and urban watersheds gives rise to three basic questions concerning their application to surface mines watersheds: (1) How well does a model developed in one region apply in another region, when the watershed land use is similar?; (2) How well does a model that applies to agricultural, forested and urban watersheds in one region apply to a different land use condition in the same region?; and (3) How does one determine the unit hydrograph on an ungaged watershed where the model parameter prediction equations do not hold?

This study provides a partial answer to the first question. The results in Table 3.8 clearly indicate which model performed best within each region and can be used as a basis for recommending a model. The second question cannot be answered until a sizeable, quality data base for current mining practice has been compiled for model testing. This requires several years of data collection under controlled conditions. Data collected under current permit requirements is insufficient; and further, the data quality is highly questionable. An added complication is the continuously changing land use conditions, oftentimes interrupted by rescheduled mining operations. A proposed answer to the third question is to modify the procedure suggested by McCuen and Bondelid (1983). They recommend using the time area method to develop an instantaneous unit hydrograph, which is then used to derive a dimensionless unit hydrograph for use with the SCS method. It is proposed that this procedure be followed and the gamma distribution be sued rather than the SCS dimensionless unit hydrograph.

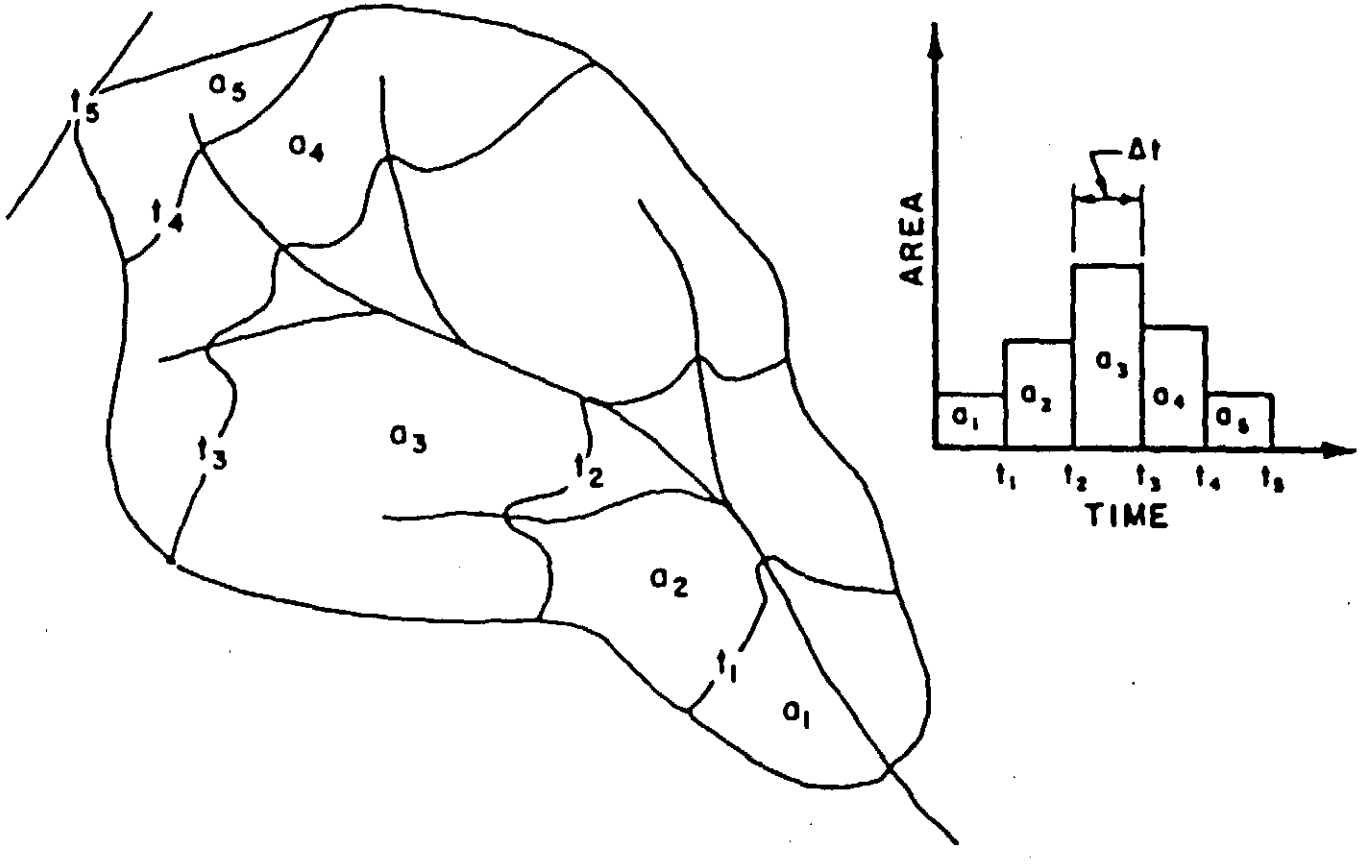

Fig. 3.10 Watersheds Showing Isochromes and Time Area Diagram (Source: Barfield, et al., 1981)

3.8.1 Time-Area Curves

The elements of a typical time area curve are shown in Fig. 3.10. The curve is obtained by drawing isochrones (lines of equal time) on the watershed map with the isochrones separated in time by equal increments, t. The value of time on each isochrone represents the travel time of runoff from the isochrone to the watershed outlet. Once the isochrones are drawn, the incremental areas between consecutive lines are determined by planimetry or other means. Each area represents that portion of the watershed that begins to contribute to the outflow hydrograph during the corresponding time period. A time area diagram is then constructed by plotting the areas in terms of corresponding isochronal times. The time area curve is obtained by drawing a smooth curve through the time area diagram.

As discussed previously, time area methods were devised to extend the rational method to unsteady rainfalls and irregularly shaped watersheds. Generally, a topographic map and Manning's equation are used to construct the isochrones. An alternative to Manning's equation is the SCS upland method for watershed time of concentration (SCS, 1975). This method relates runoff velocities, watershed slopes, and land use conditions. Regardless of the method used to determine the travel times, time area curves are based only on translation time for overland and channel flow. Hydrograph dispersion and attenuation due to internal storage effects are neglected. As such, the peak flow rates of storm hydrographs produced with these curves almost always are overpredicted. For this reason, they are not used widely.

3.8.2. The McCuen and Bondelid Method

In a study of the SCS curvilinear unit hydrograph method, McCuen

and Bondelid (1983) found it consistently overpredicts runoff rates from coastal watersheds. With this model, the unit hydrograph peak discharge is given by Eq. 3.7, which they wrote as

$$Q_p = \frac{Df\ A\ Q}{t_p} \tag{3.41}$$

in which Q_p is the peak discharge rate in cubic feet per second; A is the drainage area in square miles; Q is the runoff volume in inches; t_p is the time to peak in hours; and Df is a peak rate factor, which has units of hours-cubic feet per second per square mile per inch. For the dimensions specified for Q_p, A, Q and t_p, and the assumption that 37.5 percent of the unit hydrograph volume occurs under the rising limb, Df equals 484, as seen in Eq. 3.34. SCS (1972) indicates that Df can vary from 300-600, with a value of 300 in very flat, swampy country, and a value of 600 in steep terrain. However, no accurate, systematic method for selecting the appropriate value for Df existed before the McCuen and Bondelid study.

Supported by successful test results on six watersheds, they proposed a method for estimating Df based on the assumption that the proportions under the rising limbs of the time area curve and the unit hydrograph are equal. Recognizing that storage routing can result in significant changes in both the time to peak and peak discharge of a unit hydrograph, they assumed it has little effect on the proportion under the rising limb. Therefore, the assumption that the proportions under the rising limbs of the time area curve and unit hydrograph are equal is not critical to the accuracy of the computed unit hydrograph. They concluded a unit hydrograph can be developed by computing the time area curve for the watershed and using the proportion under the rising limb to compute the peak rate factor for the unit hydrograph. After the

peak rate factor is determined from the time area curve, one of several alternatives can be used to obtain the unit hydrograph.

McCuen and Bondelid sought a procedure that produces a unit hydrograph consistent with the SCS curvilinear unit hydrograph. They related the peak rate factor and proportion under the rising limb as

$$Df = 1290.67\ p \tag{3.42}$$

in which p is the proportion under the rising limb. The constant (Df) in Eq. 3.42 is based on units specified for Eq. 3.41, and is valid for both the SCS curvilinear and single triangle unit hydrographs. They mistakenly assumed it is also valid for a unit hydrograph represented by the two parameter gamma distribution, Eq. 3.1 (Nash's Model). The relationship between the peak rate factor and p for the gamma distribution is not Eq. 3.42, but Eq. 3.8. The constant in Eq. 3.42 is simply the ratio, 484/0.375, which holds only for the SCS unit hydrographs.

Since they assumed Eq. 3.42 is valid for the gamma distribution, McCuen and Bondelid chose it to represent the unit hydrograph shape. The value of the shape factor, n, is determined from the relationship in Table 3.2 between n and the proportion under the rising limb. The unit hydrograph peak is computed with Eqs. 3.41 and 3.42. For proportions under the rising limb of the time area curve different from 0.375, the unit hydrograph peak is scaled upward or downward accordingly. Because the gamma distribution time base varies with n (see Table 3.1), they specified truncating or lengthening the time base to the dimensionless time of 5 and adjusting the ordinates to preserve the unit hydrograph volume. This method was tested on six watersheds and provided good agreement with measured data.

Criticisms to this method include the misinterpretation of the relationship between the gamma function peak rate factor and the proportion under the rising limb, and the requirements to lengthen or truncate the time base and adjust the ordinates to preserve volume. Seemingly, it is advisable to use the gamma distribution directly, without modification.

3.8.3. The Proposed Method

It is proposed that the procedure by McCuen and Bondelid be followed, but use the gamma function and its characteristics as developed in Section 3.3.2. of this report rather than modify it to approximate the SCS curvilinear unit hydrograph. The steps for this procedure are: (1) Construct the time-area curve for the watershed; (2) Use the proportion under the rising limb of the time-area curve and Table 3.2 to obtain the gamma distribution shape and peak rate (b) factors; (3) Estimate the watershed time of concentration, t_c, with the SCS upland method (SCS, 1975) and use the relationship in Table 3.3 between t_c and t_p to determine the unit hydrograph time to peak; (4) Determine the unit hydrograph peak flowrate with Eq. 3.7; and (5) Construct the unit hydrograph with Eq. 3.3.

The validity of this method has been tested by calibrating the gamma distribution model on data from Pony Mountain Branch Watershed W-1 located in Culpepper County, Virginia. This is a 192 acre watershed in mixed land use, with about 50% in farm woods, predominantly hardwoods, 30% native grass, and the rest in a mixture of orchard grass, clover, alfalfa, small grain and road surfaces. Approximately 66% of the watershed has slopes less than 4%, while the remaining portion has slopes ranging from 12 to 25%. The average elevation is 2400 feet.

This watershed was selected because it is topographically similar to watersheds in the Applachian coal mining region. Further, McCuen and Bondelif tested their method on this watershed; therefore, the performances of the two methods on a common data base can be compared.

The proposed method was tested on four storm events. The shape factor that provided the best fit between the predicted and observed runoff hydrographs was determined for each event using a modified pattern search technique (Himmelblau, 1972). The best fit criterion was minimization of the sum of squared errors between the ordinates of the observed and predicted hydrographs. A shape statistic that indicates how well the ordinates of the predicted hydrograph match the ordinates of the observed hydrograph was evaluated for each event. This statistic ranges between 0 and 1, with 1 being a "perfect" fit.

The test results are given in Table 3.10. This table includes the event curve number (CN), the best fit shape factor and corresponding proportion under the rising limb, and the shape statistics for the SCS and gamma distribution unit hydrographs. An interesting correlation is noted between the event CN and the shape factor. Events with higher runoff potential, i.e. higher CN, resulted in lower shape factors, hence, lower peaked and longer tailed unit hydrographs. This contradicts the premise that events with the greatest runoff potential have a "flashy" unit hydrograph response. It must be noted that the runoff depths were small, less than 0.50 inches. One conjecture is that only a portion of the watershed generated runoff, so-called partial area runoff. Therefore, the difference in watershed area and actual contributing area resulted in a distortion of the true unit hydrograph shape and proportions. Regardless, current unit hydrograph theory applies to the entire watershed as a whole.

Table 3.10

Calibration Results for Pony Mountain Branch Watershed

Date of Storm	Event CN	Shape Factor n	Proportion Under Rising Limb, p	Shape SCS	Statistic Fitted
6/09/58	71.5	2.25	0.284	0.31	0.64
6/12/58	75.1	1.75	0.236	0.86	0.95
9/30/59	72.4	2.00	0.263	0.65	0.83
5/26/62	63.6	3.00	0.323	0.15	0.60

McCuen and Bondelid constructed the time area curve and measured the proportion under its rising limb as 0.279. The results in the fourth column indicate the fitted value varies among storms; whereas, the average is 0.277. This average agreees well with the value measured from the time area curve. The average in the McCuen and Bondelid study was based on different storm events, but was also 0.277.

The shape statistics indicate significant improvements to the accuracy of the simulated hydrographs. The increase in shape statistic value ranged from 0.09 to 0.45 (9 to 45%). The average increase was 0.26 (26%). McCuen and Bondelid did not report comparable statistics, so a comparison is not possible.

In summary, the proposed method given comparable results to the McCuen and Bondelid method while avoiding the truncation or lengthening of the time base and adjusting the ordinates to preserve the unit hydrograph volume. This volume is recommended for ungaged watersheds, or watersheds undergoing land use change, where available unit hydrograph techniques do not apply.

CHAPTER 4

FINITE ELEMENT SIMULATION OF OVERLAND FLOW

4.1 Introduction

The objective of this chapter is to present a physically-based, deterministic runoff model which includes the major rainfall abstraction, infiltration. The use of a deterministic model is not restricted by the availability (or unavailability) of historical records, thus making it ideal for mining disturbed watersheds.

Deterministic overland flow models are based upon the governing hydrodynamic equations for open channel flow, which are known as the Saint-Venant equations. The complete Saint-Venant equations yield the full dynamic wave model. However, several researchers (e.g. Woolhiser and Liggett (1967) and Ponce et al. (1978)) have shown that a simplified set of governing equations called kinematic wave approximation (KWA) is applicable to most overland flow events. Consequently, the KWA is used in the model to be presented.

Models which utilize the KWA for simulating overland flow generally involve a numerical discretization. Two popular numerical descretization schemes are the finite difference method (FDM) and the finite element method (FEM). The FDM has a long history of generating excellent results for the analysis of hydrologic events. In particular, Stoker (1953) used an explicit FDM to perform the first major work in the area of numerical flood routing. Kibler and Woolhiser (1970) used the FDM for the overland flow analysis of impervious surfaces based on the KWA. Smith (1970) coupled Richard's equation for vertical unsaturated flow to a finite difference solution of the KWA to

simulate runoff from pervious planes.

The finite element method does not enjoy the same history of use or popularity for solving hydrologic problems as does the finite difference method. Pioneering work by Zienkiewicz and Cheung (1965) paved the way for utilization of the FEM in the analysis of hydrologic problems. Zienkiewicz and Chueng used the FEM to analyze a seepage flow problem. Al-Mashidani and Taylor (1974) were among the earliest researchers to apply the FEM to surface runoff. They used the FEM to solve the non-dimensional form of the Saint-Venant equations and found that the FEM was more stable, exhibited faster convergence and required much less execution time that the other numerical methods tested.

In general, there are several advantages in using the finite element method, as opposed to other mumerical techniques such as the finite difference method. Most of the advantages are manifested in the application of the method to actual physical situations. Material properties in adjacent elements do not have to be the same, irregularly shaped boundaries can be easily approximated, and special boundary conditions present no difficulty for the finite element method. Another advantage from a computational point of view, as well as physical, is that the size and number of elements can be varied, allowing the element grid to be refined or expanded as the need arises.

For the reasons cited above, other researchers have begun utilizing the finite element method for the analysis of overland flow based on the KWA. Judah et al. (1975) and Ross (1978) used the Galerkin method of weighted residuals to develop an explicit, finite element, kinematic wave model for overland and channel flow. Ross' formulation included linear, quadratic, and cubic Lagrangian elements. Ross accounted for infiltration by using the empirical Holtan equation to generate excess

intensities.

Jayawardena and White (1977) also utilized the Galerkin method to generate a finite element, kinematic wave model for overland flow, but they used an implicit time integration scheme. Jayawardena and White presented both linear and quadratic element formulations. Flow from a hypothetical uniform plane was analyzed and the results compared very well with an analytic solution. Jayawardena and White (1979) applied the same finite element, kinematic wave model to a natural watershed. However, the watershed studied had a top soil layer of highly porous peat, on which overland flow was not likely to occur. Therefore, a finite element throughflow model, which was also developed in the first paper (1977), was used to route the flow from the slopes. The finite element kinematic wave model was subsequently used only for channel routing.

The deterministic model of this report is based on the kinematic wave approximation coupled with an explicit Green-ampt infiltration equation. The Green-Ampt infiltration equation parameters are obtained using the USDA-ARS parameter estimation technique which is based on soil-moisture tension data.

The numerical discretization of the kinematic wave approximation for simulating overland flow on small watersheds utilizes the Galerkin finite element formulation. The finite element formulation includes linear, quatratic and cubic one-dimensional Lagrangian spatial elements. A linear variation in time is assumed for the evaluation of the time integral. The time integration scheme includes both explicit and implicit time marching algorithms. The particular scheme to be used depends on the choice of the time weighting parameter. The choice of an

implicit time algorithm results in a system of nonlinear equations. The resulting nonlinear equations are solved using a modified Newton-Raphson iteration scheme. Explicit time integration yields a linear system of equations, but a small time increment must be used to insure solution stability.

The overland flow model development is presented in the following three sections. Each section deals with a distinct step in the development of an overland flow model. The first step (Section 4.2), determining excess intensity, is accomplished by utilizing a Green-Ampt infiltration model. The second step (Section 4.3), the mathematical representation of overland flow, utilizes the kinematic wave approximation. The third step (Section 4.4), uses the finite element method (FEM) to generate a system of equations which approximate the mathematical overland flow equations. Sections 4.5 and 4.6 present the solution strategy for generating approximate outflow hydrographs and sample results obtained using the developed model, respectively.

4.2 Green and Ampt Infiltration

Green and Ampt infiltration is based on Darcy's law as applied to vertical unsaturated flow. Many studies, including those by Bouwer (1969) and Mein and Larson (1971 and 1973), have demonstrated the usefulness of the Green and Ampt equation for modeling infiltration. Mein and Larson (1973) obtained very good correlation between values of cumulative infiltration predicted by the Green and Ampt equation and those values computed by a finite difference solution of the Richard's equation.

Referring to Fig. 4.1, Darcy's law for vertical unsaturated flow can be written as

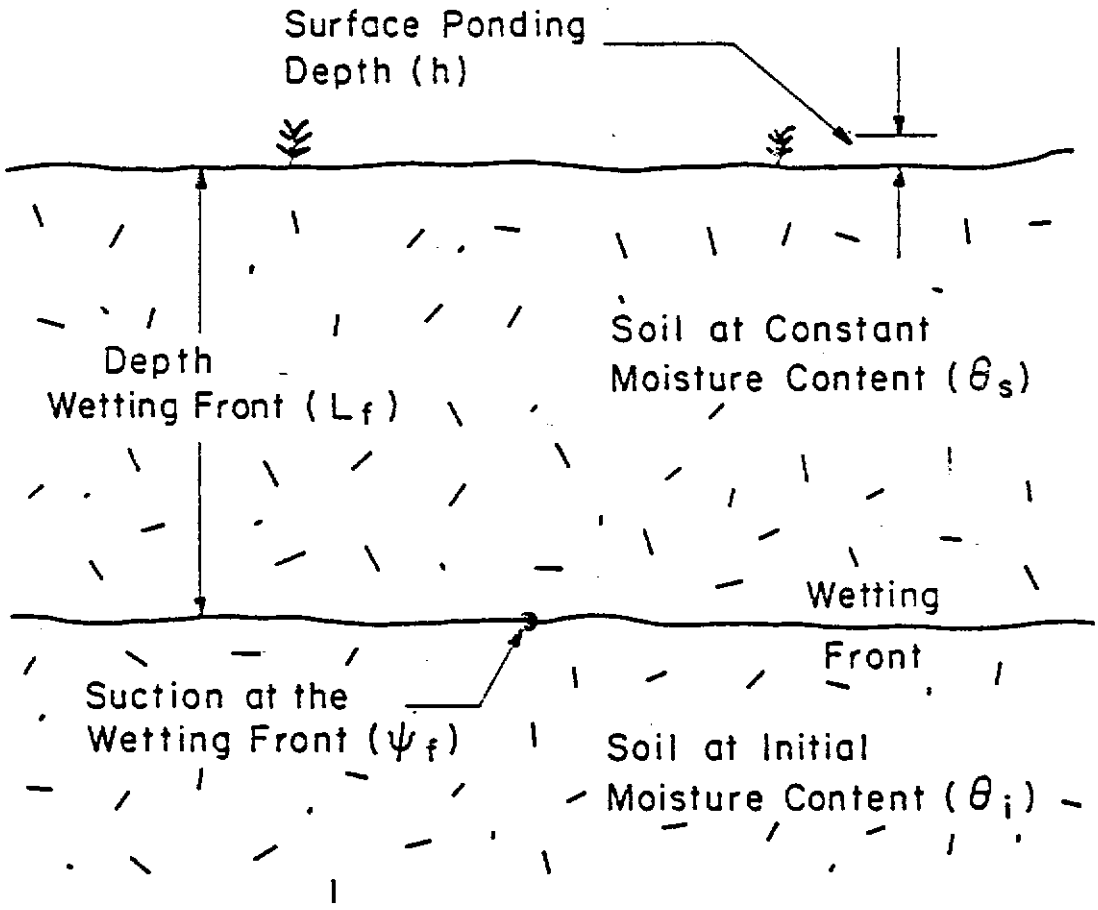

Fig. 4.1 Green and Ampt Model Variables

$$v = f = K(h + L_f + \Psi_f)/L_f \qquad (4.1)$$

where

f = infiltration rate (equal to velocity due to the one-dimensional analysis) (length/time),

h = depth of surface ponding (length),

L_f = depth to wetting front (length), and

Ψ_f = wetting front suction pressure (length).

Several assumptions were necessary to write Darcy's law in the form of Eq. 4.1, namely (Overton and Meadows, 1976):

1) There exists a distant and precisely definable wetting front.

2) Suction pressure, Ψ_f, at the wetting front remains essentially constant, regardless of the time and depth.

3) Above (behind) the wetting front, the soil is uniformly wet (constant moisture content, θ_s) and has a constant hydraulic conductivity, K.

4) Below (in front of) the wetting front, the soil moisture content is relatively unchanged from its initial moisture content, θ_i.

The above assumptions, when checked against the actual infiltration soil moisture profile (Bodman and Colman, 1943), illustrate the approximate nature of the Green and Ampt model (see Fig. 4.2)

The accumulated infiltration, F, can be obtained by integrating Eq. 4.1, i.e.,

$$f = dF/dt = K(h + L_f + \Psi_f)/L_f \qquad (4.2)$$

or directly from

$$F = (\theta_s - \theta_i)L_f = \delta\theta L_f \qquad (4.3)$$

where θ_s is the saturated moisture content and θ_i is the initial moisture content. The measure of moisture content, θ, is a volumetric measure, therefore, $\delta\theta$ is calculated by the relationship

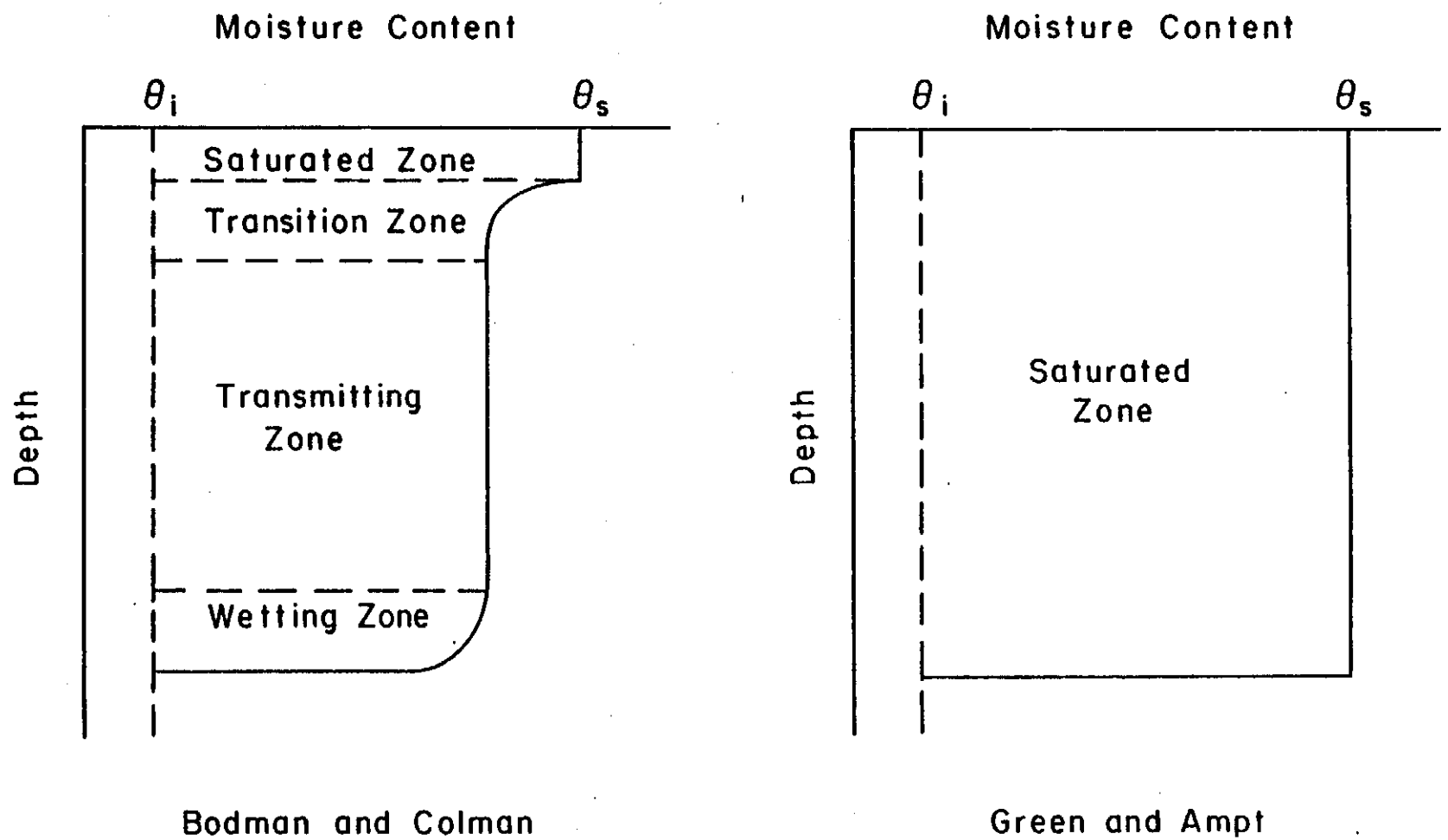

Fig 4.2 Comparison of Green-Ampt Moisture Profile to Bodman - Colman Profile

$$\delta\theta = (\theta_s - \theta_i) = \phi(1 - S_i)$$

where ϕ is the porosity and S_i is the initial degree of saturation. Substituting for L_f from Eq. 4.3 into Eq. 4.2 leads to

$$dF/dt = K(F + \delta\theta h + \delta\theta\Psi_f)/F \tag{4.4}$$

In applying the Green and Ampt model, it is often assumed that the depth of ponded water, h, is negligible and the resulting Eqs. are somewhat simplified. In the model presented here, h is retained in order to be consistent with the overland flow routing procedure.

Rearranging Eq. 4.4 gives

$$FdF/(F + \delta\theta h + \delta\theta\Psi_f) = Kdt \tag{4.5a}$$

which can also be written as

$$dF\ (1 - 1/((F + \alpha)/\alpha)) = Kdt \tag{4.5b}$$

where $\alpha = \delta\theta h + \delta\theta\Psi_f$. Substituting $u = (F+\alpha)/\alpha$ into Eq. 4.5b gives

$$dF - \alpha\ du/u = Kdt \tag{4.6}$$

Integrating both sides of Eq. 4.6 yields

$$Kt = F_t - \alpha \ln (1 + F_t/\alpha)$$

$$= F_t - (\Psi_f\delta\theta + h_t\delta\theta) \ln (1 + F_t/(\Psi_f\delta\theta + h_t\delta\theta)) \tag{4.7}$$

where F_t is the cumulative infiltration at time t and h_t is the surface ponded depth at time t.

Eq. 4.7 is implicit in both F and t. To avoid an iterative solution for values of F at any time, an incremental cumulative infiltration equation must be developed. First, writing Eq. 4.7 at time $t+\Delta t$ gives

$$K(t+\Delta t) = F_{t+\Delta t} - (\Psi_f \delta\theta + h_t \delta\theta) \ln \left(1 + \frac{F_{t+\Delta t}}{\Psi_f \delta\theta + h_t \delta\theta}\right) \tag{4.8}$$

where

Δt = increment of time

$$F_{t+\Delta t} = F_t + \Delta F \tag{4.9}$$

ΔF = increment in cumulative infiltration from time t to time $t+\Delta t$

(Note that in writing Eq. 4.8, the variation in h with time is assumed to be negligible with respect to the infiltration equation. Otherwise, an iterative infiltration-overland flow solution would be required). Subtracting Eq. 4.7 from Eq. 4.8 and substituting Eq. 4.9 gives

$$\begin{aligned} K\Delta t &= \Delta F - \alpha[\ln (1 + (F_t+\Delta F)/\alpha) - \ln (1+F_t)/\alpha] \\ &= \Delta F - \alpha \ln[1 + \Delta F/(\alpha + F_t)] \end{aligned} \tag{4.10}$$

Using the first term of the logarithmic series expansion

$$\ln (1 + x) = 2[x/(2+x) + 1/3(x/(2+x)^3 + \ldots]$$

in Eq. 4.10 leads to the following approximation:

$$\Delta F = \frac{K\Delta t - 2F_t}{2} + \sqrt{\left(\frac{2F_t - K\Delta t}{2}\right)^2 + 2K\Delta t(\alpha + F_t)}$$

$$= \frac{K\Delta t}{2} - F_t + \sqrt{\left(\frac{2F_t - K\Delta t}{2}\right)^2 + 2K\Delta t(h_t \delta\theta + \Psi_f \delta\theta + F_t)} \tag{4.11}$$

Eq. 4.11 is the desired incremental cumulative infiltration equation from which the infiltration increments can be obtained directly. The approximation error in Eq. 4.11 is approximately eight percent (8%) due to truncation of the logarithmic series expansion to only the first

term. The advantage of Eq. 4.11 in comparison with the more exact Eq. 4.10 is that Eq. 4.11 is an explicit representation of the cumulative infiltration increment, whereas Eq. 4.10 is a implicit relationship.

The cumulative infiltration at the end of each time increment is

$$F_{t+\Delta t} = F_t + \Delta F, \text{ if } \Delta F < i\Delta t + h_t \qquad (4.12a)$$

$$= F_t + i\Delta t + h_t, \text{ if } \Delta F > i\Delta t + h_t \qquad (4.12b)$$

where i is the rainfall rate and h_t is the surface ponded water depth. Eq. 4.12a implies that ponded water remains after infiltration is exerted over a given time increment; consequently, overland flow occurs. In case of Eq. 4.12b, the infiltration increment is large enough such that both the surface ponded water and the rainfall during the time increment are absorbed into the soil. Therefore, no ponded water remains, and there is no overland flow for the time increment.

The incremental cumulative infiltration equation, Eq. 4.11, was developed assuming uniform soil properties. However, it can be applied to layered soils, assuming each layer has uniform properties. The required soil properties, i.e., K_s, Ψ_f, ϕ and S_i and the thickness, d, must be known for each layer. Then after each infiltration computation, the computation, the cumulative infiltration volume, F, is compared with the storage capacity of that particular layer. The storage capacity of that particular layer. The storage capacity of layer one is $d_1\delta\theta$. If F exceeds $d_1\delta\theta$, the next infiltration calculations are performed using the soil properties of the next layer. Then F is compared with $d_1\delta\theta$, + $d_2\ \delta\theta_2$ before a third layer data is used. Similarly for four or more layers.

Even though the Green and Ampt model is a simplification of the

actual infiltration process, parameter estimation is required. Methods of parameter estimation have been presented by Bouwer (1969), Brakensiek (1977) and Brakensiek and Engleman (1979).

Bouwer (1969) defined the Green and Ampt parameter K to be "the actual hydraulic conductivity in the wetted zone," which is less than the saturated hydraulic conductivity, K_s . He concluded, based on previous work (Bouwer, 1966), that K may be taken as about $0.5\ K_s$.

Brakensik (1977) presented an estimate of the Green and Ampt parameter ψ_f , effective capillary pressure at the wetting front, as

$$\psi_f = \frac{\eta}{\eta - 1} \frac{\psi b}{2} \tag{4.13}$$

where ψ_b (bubbling pressure) and $\eta (\eta = 2+3\ \lambda;\ \lambda$ - pore size distribution index) are estimated based on the description soil moisture-tension data of Brooks and Corey (1966). The ratio $\psi_b/2$ in Eq. 4.13 is used to approximate the air exit pressure h_e. Eq. 4.13 can be generalized as

$$\psi_f = \frac{\eta}{\eta - 1} h_e \tag{4.14}$$

where $h_e = \psi_b/2$ for desorption data and h_e can be directly determined for absorption data. Consequently, the use of actual absorption data, for the areas to be analyzed, is the preferred method for determining ψ_f (Eq. 4.14). A laboratory determination of K_s is also preferred. However, in most cases absorption data will not be available, and it may not be feasible to determine K_s for all areas to be analyzed. To overcome these difficulties, Brakensiek and Engleman (1979) presented equations for both ψ_f and K_s as functions of the soil textural class. Using a total of 1085 sets of soil moisture characteristics for soils in various textural classes, they determined the constants of the Brooks and Corey function. Then ψ_f was determined using Eq. 4.13 (Brakensiek,

1977). By relating the average paramenter values to the mean percent of clay, sand, and silt in each test area, the following relationships were developed:

$$\ln \Psi_f = 3.4948 - 0.0146 \text{ (\%Sand)}; \; r = -0.874 \tag{4.15}$$

$$\ln K_s = -11.9661 - 1.9784 \ln \text{(\%Clay/100)}; \; r = -0.982 \tag{4.16}$$

where r^2 gives the fraction of the data that fit each equation. If, for a given soil, the percents of sand and clay are known, these values can be entered directly into Equations 4.15 and 4.16. If only a general soil grouping is known, the average values of percent sand and clay are entered. Average values can be obtained from the United States Department of Agriculture soil textural triangle (Fig. 4.3). Referring to Fig. 4.3, it can be seen that use of a general soil textural classification could result in large errors in the percent of sand and clay compared to the actual values.

4.3 Kinematic Wave Approximation

The governing differential equations for overland flow are assumed to be the kinematic wave equations. The two equations used in the kinematic wave approximation (KWA) are the continuity and momentum equations. The continuity equation for a variable width plane is

$$w \frac{\partial h}{\partial t} + \frac{\partial Q}{\partial x} = w \, i_e \tag{4.17}$$

and the momentum equation is

$$S_f = S_o \tag{4.18}$$

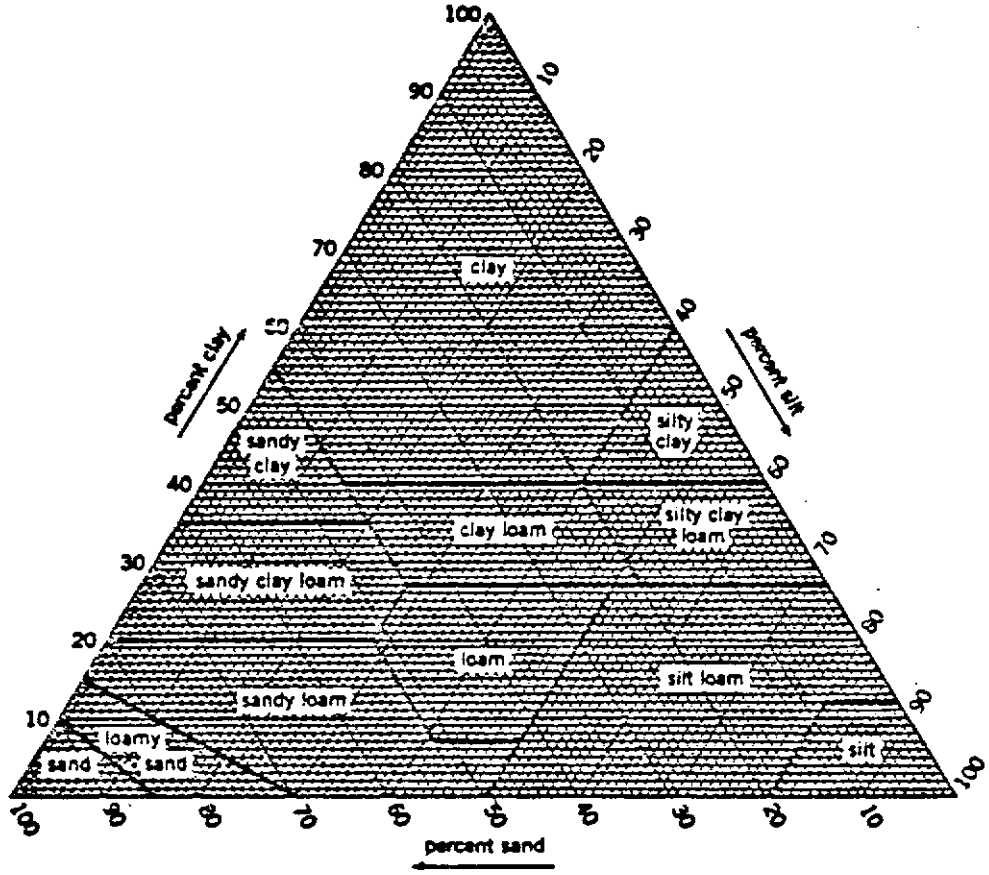

Fig. 4.3 United States Department of Agriculture, Soil Textural Triangle

where

w - width of flow plane (length)

h - flow depth (length)

Q - flowrate (length /time)

$i_e = i - f$

$= i - \Delta F/\Delta t$

- excess rainfall intensity (length/time)

S_f - friction slope (length/length)

S_o - bed slope of flow plane (length/length)

t - time

x - distance along plane (length)

Use of the KWA (Equations 4.17 and 4.18) allows the flowrate to be to be described by a uniform flow resistance equation. This resistance equation can be written as

$$Q = \alpha h^m \tag{4.19}$$

where $\alpha = 1.486 \sqrt{S_o}\, w/n$, $m = 5/3$ and n is Manning's friction factor for Manning's turbulent flow approximation. For laminar flow $\alpha = gS_o /3\nu$, $m = 3$ and ν is the kinematic viscosity (Chow, 1959). Jayawardena and White (1977) used $\alpha = \sqrt{S_o}/n$ and $m = 2$ to approximate the flowrate. In this chapter the variable width Manning resistance equation is utilized.

Extensive studies into the use of the KWA for approximating the motion of water in open channels has led to the consideration of two criteria for flow to be classified as kinematic:

(1) Lighthill and Whitham (1955) resolved for kinematic flow to be applicable, the Froude number should be less than two. The Froude number is defined as

$$F = V/\sqrt{gh} \qquad (4.20)$$

where V = discharge velocity

g = acceleration due to gravity and

h = normal flow depth.

Lighthill and Whitham also found that the KWA is best when $F > 1$ (supercritical flow). However, subcritical kinematic flow is theoretically possible and has been observed (Overton and Meadows, 1976).

(2) In addition, Woolhiser and Liggett (1967) developed a dimensionless kinematic flow parameter, k:

$$k = \frac{L S_o g}{V^2} \qquad (4.21)$$

where

L = length of flow plane,

S_o = bed slope, and

V = discharge velocity.

The parameter k represents the magnitude of slope and friction effects; e.g., high values of k indicate that the slope and friction dominate the flow, therefore the KWA is accurate (Kibler and Woolhiser, 1970). For k = 10, Woolhiser and Liggett found a maximum error of about ten percent in approximating the complete equation solutions (i.e., the Saint-Venant equations) with the KWA. For $k > 10$, the KWA exhibits a rapid decrease in error as k increases.

Eagleson (1970) suggests both these conditions hold for unsteady flow to be classified as kinematic. However, Al-Mashidani and Taylor (1974) proved the Froude number can be greater than two provided the kinematic flow number is large. Ross et al, (1979) gives an extensive

list of investigators who have verified the applicability of the kinematic wave approximation for overland flow. For example, Woolhiser and Liggett (1967) concluded that the KWA is a good approximation for most overland flow situations, because k rarely falls below 10. Furthermore, they determined that much of the experimental work on overland flow has been carried out under essentially kinematic conditions.

4.4 Finite Element Formulation

The goal of any finite element formulation is to establish a system of algebraic equations which can be solved to obtain the nodal field variable values. The five basic steps for establishing the overland flow algebraic equations are: 1) approximation of the field variable behavior; 2) construction of integral relationships corresponding to the the governing equation; 3) establishment of the element equations; 4) time integration, and; 5) assembly of the element equations into the set of global equations.

The field variable is the flow depth, h. The behavior of h is approximated by an interpolation function (polynominal) written in terms of the nodal values of h. In this report, one-dimensional Lagrangian interpolation is used to represent the flow depth variation. The program can use either linear, quadratic or cubic Lagrangian elements. Fig. 4.4 shows a cubic Lagrangian element and the corresponding shape functions and shape function derivatives. Letting $\overline{h}$ be the interpolant which approximates h, the cubic Lagrangian element approximation can be written as

$$\overline{h} = N_1 h_1 + N_2 h_2 + N_3 h_3 + N_4 h_4 = \lfloor N \rfloor \{h\} \qquad (4.22)$$

where $\lfloor N \rfloor$ is the row vector of shape functions and $\{h\}$ is the column

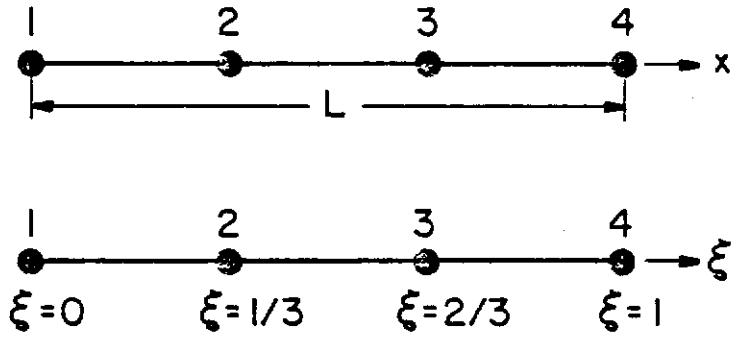

(a) Element

$$N_1 = 1 - 5.5\xi + 9\xi^2 - 4.5\xi^3, \text{ Where } \xi = x/L$$

$$dN_1/dx = (-5.5 + 18\xi - 13.5\xi^2)/L$$

$$N_2 = 9\xi - 22.5\xi^2 + 13.5\xi^3$$

$$dN_2/dx = (9 - 45\xi + 40.5\xi^2)/L$$

$$N_3 = -4.5\xi + 18\xi^2 - 13.5\xi^3$$

$$dN_3/dx = (-4.5 + 36\xi - 40.5\xi^2)/L$$

$$N_4 = \xi - 4.5\xi^2 + 4.5\xi^3$$

$$dN_4/dx = (1 - 9\xi + 13.5\xi^2)/L$$

(b) Shape Functions and Derivatives

Fig. 4.4 Cubic Lagrangian Element

vector of nodal h values. The same interpolation is used for the other spatially varying quantities, i.e.,

$$\begin{aligned} w &= [N]\{w\} \\ i_e &= [N]\{i_e\} \\ Q &= [N]\{Q\} \\ \dot{h} &= \frac{dh}{dt} = [N]\{\dot{h}\} \end{aligned} \tag{4.23}$$

The interpolant given by Eq. 4.22 does not exactly satisfy the governing differential equation (Eq. 4.17). Rewriting Eq. 4.17 as

$$D(h) = 0$$

and substituting h from Eq. 4.22 gives

$$D(\bar{h}) = R \neq 0$$

where R is the residual. The residual is obtained due to the approximation $\bar{h}$ to the actual solution h. To improve the accuracy of the approximation, an integral formulation of the problem is developed using the method of weighted residuals (MWR).

The MWR uses a set of weighting functions to make the integral of the residual equal to zero, i.e.,

$$\int_{\Omega} WF_j \, D(\bar{h}) \, d\Omega = 0 \; ; \; j=1,2,\ldots,m \tag{4.24}$$

where Ω is the solution domain, WF_j is the j^{th} weighting function and m is the number of weighting functions. In this paper, the integral form is written over each element and the Galerkin method is used, whereby the element shape functions are also used as the weighting functions. Consequently, the element level integral relationships are written as

$$\int_{\Omega^e} \{N\} \, D(\bar{h}) \, d\Omega = 0 \tag{4.25}$$

where Ω^e represents an element domain and $\{N\}$ is the column vector of

shape functions, i.e., the Galerkin method weight functions. Substituting $\bar{h}$ into Eq. 4.17 to obtain $D(\bar{h})$, and then into Eq. 4.25 gives

$$\int_{\Omega^e} \{N\} \left(w\frac{\partial \bar{h}}{\partial t} + \frac{\partial Q(\bar{h})}{\partial x} - wi_e\right) d\Omega = 0 \tag{4.26}$$

Including the element variations, Eqs. 4.22 and 4.23, in Eq. 4.26 gives gives

$$\begin{aligned} &\int_{\Omega^e} \{N\} \left(\lfloor N \rfloor \{w\}\right) \lfloor N \rfloor \, d\Omega \, \{\dot{h}\} \\ &\quad + \int_{\Omega^e} \{N\} \frac{d\lfloor N \rfloor}{dx} \, d\Omega \, \{Q\} \\ &\quad = \int_{\Omega^e} \{N\} \left(\lfloor N \rfloor \{w\}\right) \lfloor N \rfloor \, d\Omega \, \{i_e\} \end{aligned} \tag{4.27}$$

Writing Eq. 4.27 in matrix form gives

$$[a]\{\dot{h}\} + [b]\{Q\} = [a]\{i_e\} = \{\hat{i}_e\} \tag{4.28}$$

Due to the inclusion of $\{w\}$, the vector of nodal widths, matrix [a] may change from one element to another. Numerical integration, using Gaussian quadrature data (5-point data for cubic elements), is used to evaluate [a] for each element. Matrix [b] does not contain element dependent values, therefore, it was close-form evaluated and included in the program as a constant data block.

Since the overland flow model is time-dependent, the time dimension must be included in the formulation. Assuming a linear variation in time,

$$\{\dot{h}\} = \frac{\{h\}_{t+\Delta t} - \{h\}_t}{\Delta t} \tag{4.29}$$

where the subscripts $(t+\Delta t)$ and t denote the times at which the flow depth vectors occur and Δt is the chosen time increment. Fig. 4.5

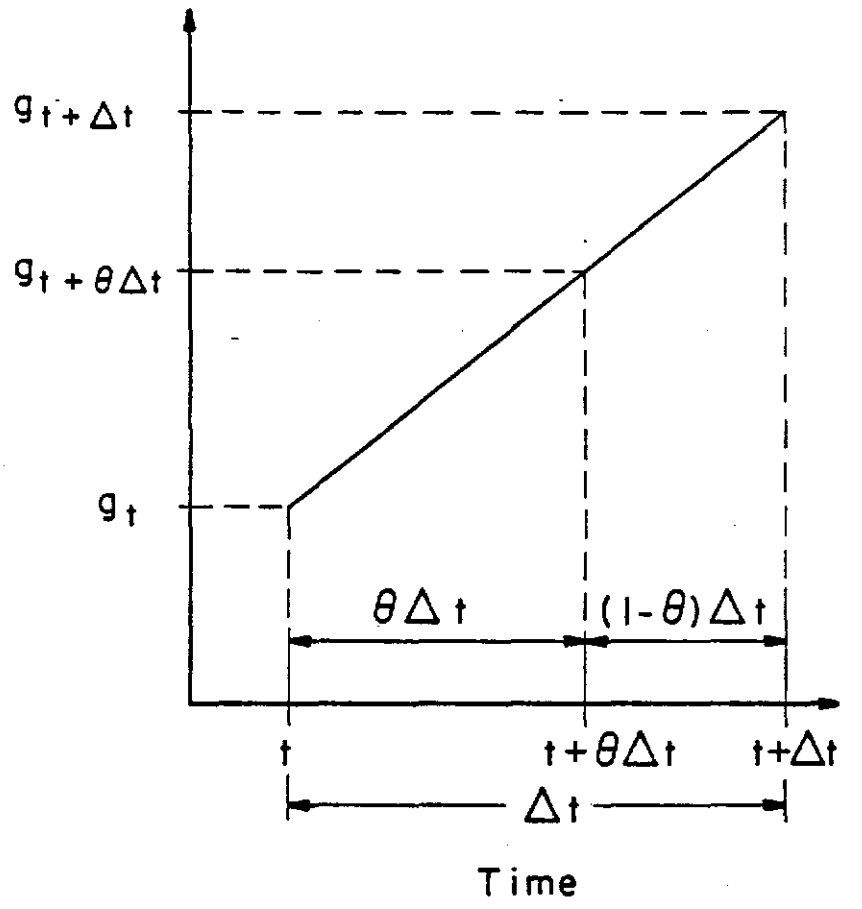

Fig. 4.5 Linear Time Interpolation

illustrates development of the following expressions for $\{Q\}$ and $\{i_e\}$ at time equal to $t+\theta\Delta t$ for the linear time variation

$$\{Q\}_{t+\theta\Delta t} = \theta \{Q\}_{t+\Delta t} + (1-\theta) \{Q\}_t \tag{4.30}$$

$$\{i\}_{e\ t+\theta\Delta t} = \theta \{i\}_{e\ t+\Delta t} + (1-\theta)\{i\}_{e\ t} \tag{4.31}$$

Using Eqs. 4.29, 4.30, and 4.31 to write Eq. 4.28 at time $t+\theta\Delta t$ and rearranging to isolate $\{h\}_{t+\Delta t}$ gives

$$\begin{aligned}[a]\{h\}_{t+\Delta t} &= [a]\{h\}_t - \Delta t\theta[b]\{Q\}_{t+\Delta t} \\ &- \Delta t\,(1-\theta)[b]\{Q\}_t + \Delta t\theta\{\hat{i}_e\}_{t+\Delta t} \\ &+ \Delta t\,(1-\theta)\{\hat{i}_e\}_t\end{aligned} \tag{4.32}$$

Eq. 4.32 is the element level recurrence scheme. The time weighting coefficient, θ, can be varied from 0 to 1 resulting in various time marching schemes. Due to the occurrence of $\{Q\}_{t+\Delta t}$ on the right hand side of Eq. 4.37, a nonzero value of θ results in an implicit scheme. If $\theta = 0$, Eq. 4.32 is a explicit Euler forward difference scheme. If $\theta = 1/2$, $2/3$ or 1, Eq. 4.32 is a Crank-Nicholson, Galerkin or implicit backward difference scheme, respectively.

Having generated the element matrix equations, Eq. 4.32, the element equations are assembled to represent the total solution domain. The element assembly procedure is designed to ensure continuity of flow depth, h, at the element junctions. The assembly process can be described as

$$A_{ij} = \sum_{e=1}^{n^e} \int_{\Omega^e} N_i\,([N]\{w\})\,N_j\,d\Omega$$

$$B_{ij} = \sum_{e=1}^{n^e} \int_{\Omega^e} N_i\,\frac{dN_j}{dx}\,d\Omega$$

$$C_i = \sum_{e=1}^{n^e} \int_{\Omega^e} N_i\,([N]\{w\})\,[N]\{ie\}d\Omega$$

where the coefficients of the global matrices A_{ij}, B_{ij} and vector C_i are assembled from the contributions of the total n^e elements in the domain. Simple assembly procedures would result in an NxN system of equations, where N is the total number of nodes. However, the dimensions of the overland flow matrices are reduced by one because the flow depth at node point one is a prescribed boundary value (see Blandford, Peters and Meadows, 1983). Furthermore, due to the sparseness and bandedness of the matrix equations, assembly and solution procedures based on a fully populated system of equations would be inefficient. Consequently, assembly is executed in a manner consistent with the symmetric profile solution technique developed by Taylor (1977). Taylor's technique operates on the coefficients within the symmetric profile only and these coefficients are compactly stored as a vector.

Eq. 4.32 can be symbolized in a global assembled form as

$$[A]\{H\}_{t+\Delta t} = \{C\}_t - \Delta t\theta[B]\{Q(H)\}_{t+\Delta t} \qquad (4.33)$$

where the upper case letters represent assembled matrices and $\{C\}_t$ includes all of the known vectors on the right hand side of Eq. 4.32.

4.5 Solution Strategy

As discussed previously, a nonzero value of the time weighting coefficient, θ, results in an implicit form of Eq. 4.33. The implicit form of Eq. 4.33 requires both an initial estimate for the vector $\{H\}_{t+\Delta t}$ and an iterative scheme to generate an accurate solution. A modified Newton-Raphson iteration scheme is used herein.

The modified Newton-Raphson solution scheme can be described as follows:

$$[A]\{H\}^{i+1}_{t+\Delta t} = \{C\}_t - \Delta t\theta[B]\{Q(H)^{i}_{t+\Delta t}\}_{t+\Delta t} \tag{4.34}$$

where the superscripts i and i+1 represent the i^{th} and $i+1^{st}$ estimates of $\{H\}_{t+\Delta t}$.

The first estimate for nodal flow depth values is obtained by using a forward in time, backward in space finite difference approximation (see grid point 2 of Fig. 4.6) of Eq. 4.17. The explicit finite difference approximation for the advanced time step node point flow depths is

$$h_4 = h_2 + \Delta t ie_2 - \frac{\Delta t}{W_2}\,\frac{Q_2 - Q_1}{\Delta x} \tag{4.35}$$

Eq. 4.35 is used to obtain the vector of initial h values which is substituted into the right hand side of Eq. 4.34 for the first iteration cycle. For subsequent iteration cycles, the computed values of $\{H\}_{t+\Delta t}$ are used in the right hand side of Eq. 4.34.

The iteration procedure of Eq. 4.34 is continued until the convergence criterion is satisfied, i.e.,

$$\left| \frac{h^{i+1}_{t+\Delta t} - h^{i}_{t+\Delta t}}{h^{i+1}_{t+\Delta t}} \right| < \varepsilon$$

where ε is the prescribed relative error (0.001), for every nonprescribed flow depth node. The program stops execution if the maximum number of iterations (50) is exceeded prior to obtaining a converged solution. A schematic representation of the iteration scheme is shown in Fig. 4.7.

In general, the overland flow equations are assumed to apply to planes with constant slopes. Consequently, the program was designed to accommodate overland flow planes with varying slopes. The varying slope

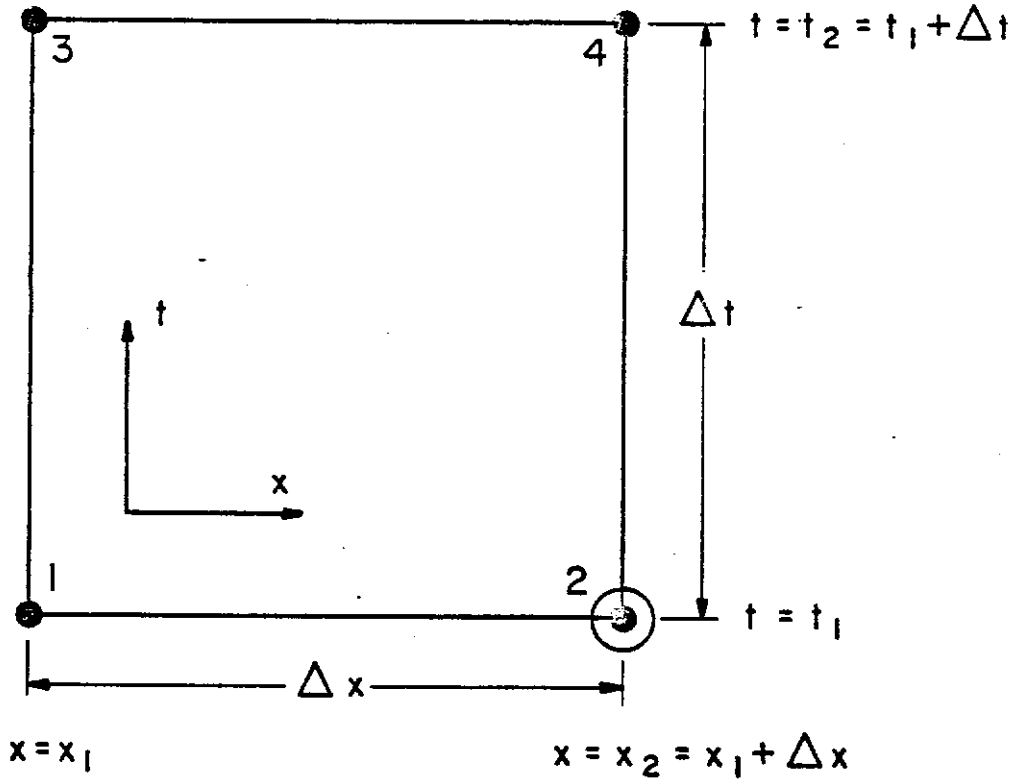

Fig. 4.6 Finite Difference Grid

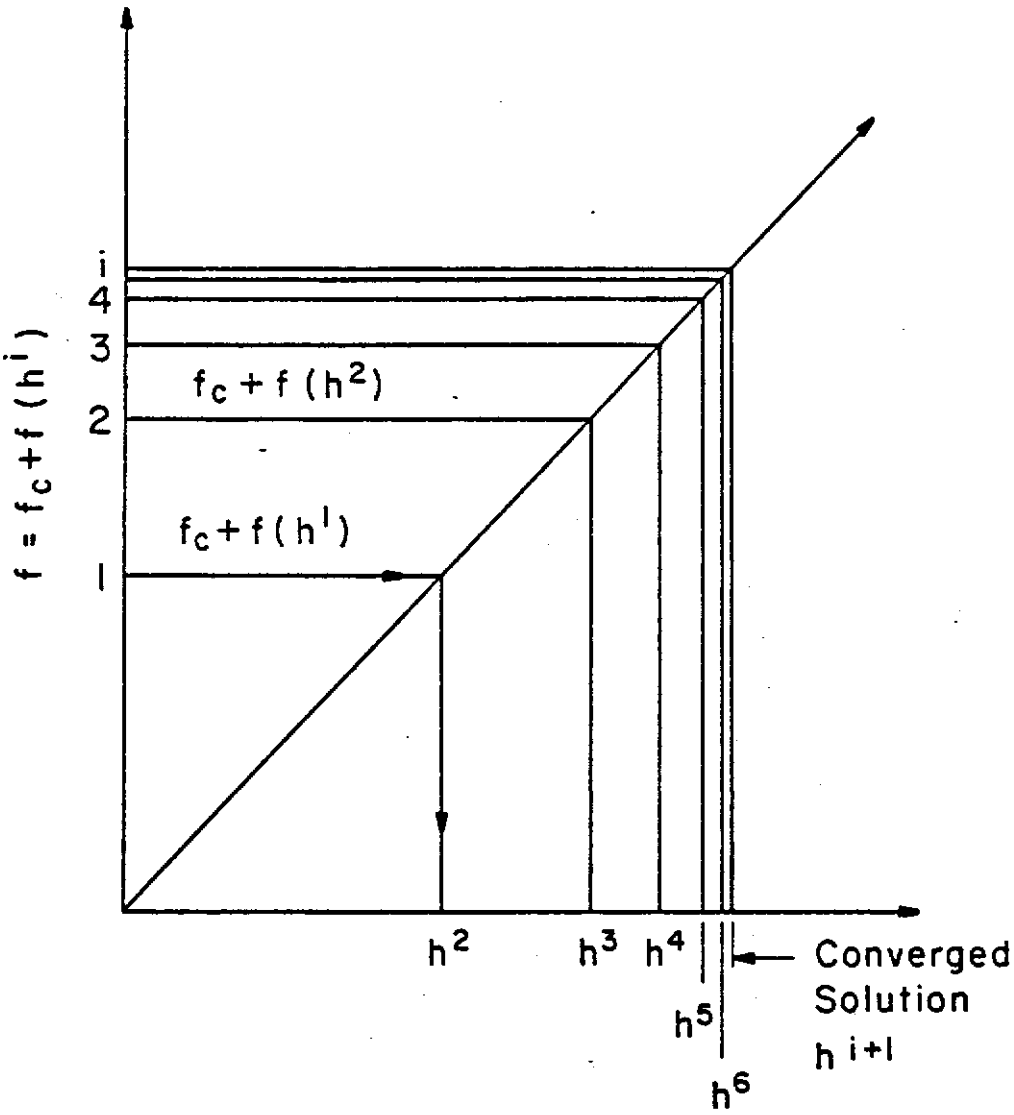

Fig. 4.7 Schematic of the Iteration Procedure for a Problem with a Single Degree of Freedom

planes are modeled as a series of constant slope planes. The series of planes is solved sequentially from the upstream to downstream and continuity of flow rate, Q, is imposed at plane junctions. The upstream flow rate and the new properties of the downstream plane (S_o and/or n) are substituted into Manning's equation to obtain the flow depth at the first first node of the downstream plane. The calculated flow depths at node one become prescribed boundary values for the plane.

Further details on the overland flow model are presented in Blandford, Peters and Meadows, (1983). In the following section several sample problems will be presented demonstrating the applicability/accuracy of the developed model.

4.6 Sample Results

The overland flow model was tested on data from both impervious and pervious controlled watersheds (Blandford, Peters and Meadows, 1983). In this section sample results are presented for an impervious plane problem and for a small agricultural experimental watershed maintained by the United States Department of Agriculture - Agriculture Research Service (USDA - ARS).

4.6.1 Impervious Plane - Izzard's Run # 138

Data reported by Izzard (1946) was used to test the ability of the model to simulate rainfall events on impervious surfaces. Run # 138 consists of two steady intensities; 1.83 in/hr for the first eight minutes and 3.55 in/hr for the next eight minutes. The runoff surface was an asphalt plane with the following physical characteristics;

L = 72.0 ft (length of plane)

Manning n = 0.024

S_o = 0.01 ft/ft

This rainfall event produced a maximum Froude number of 0.55 and a minimum kinematic flow number of 156; consequently, well within the classification of kinematic flow. A single cubic Lagrangian element was utilized for the finite element discretization and a Δt = 30 seconds was chosen which is within the Courant condition time increment of 37 seconds (Blandford, Peters and Meadows, 1983).

Fig. 4.8 shows the computed hydrograph along with the observed hydrograph. Both the Crank-Nicholson (θ=1/2)and Galerkin (θ=2/3) time interpolation schemes exhibit slight oscillations about the observed equilibrium discharges. Table 4.1 gives the computed and observed times to equilibrium and the equilbrium flow rates corresponding to the time interpolated results of Fig. 4.8. Table 4.1 shows that the θ= 1/2 and θ=2/3 time interpalation schemes resulted in a more accurate reflection of the observed response.

Table 4.2 presents the simulated runoff volumes, V_Q, and ponded water volumes, V_P , for the various time interpalation schemes. Examination of Table 4.2 reveals that the mass balance errors are smallest for θ=½ with increasing error as θ is increased. However, even the mass balance error of 1.29% for θ=1 (backward difference) should be considered insignificant. The combined results of Tables 4.1 and 4.2 show that only the Crank-Nicholson and Galerkin schemes should be used for surface runoff simulations.

4.6.2 Pervious Plane - Hastings Watershed 5H

The results presented in the previous section demonstrated the applicability of the model to simulate kinematic overland flow. In this section, the combined infiltration - overland flow model will be tested on a small natural watershed.

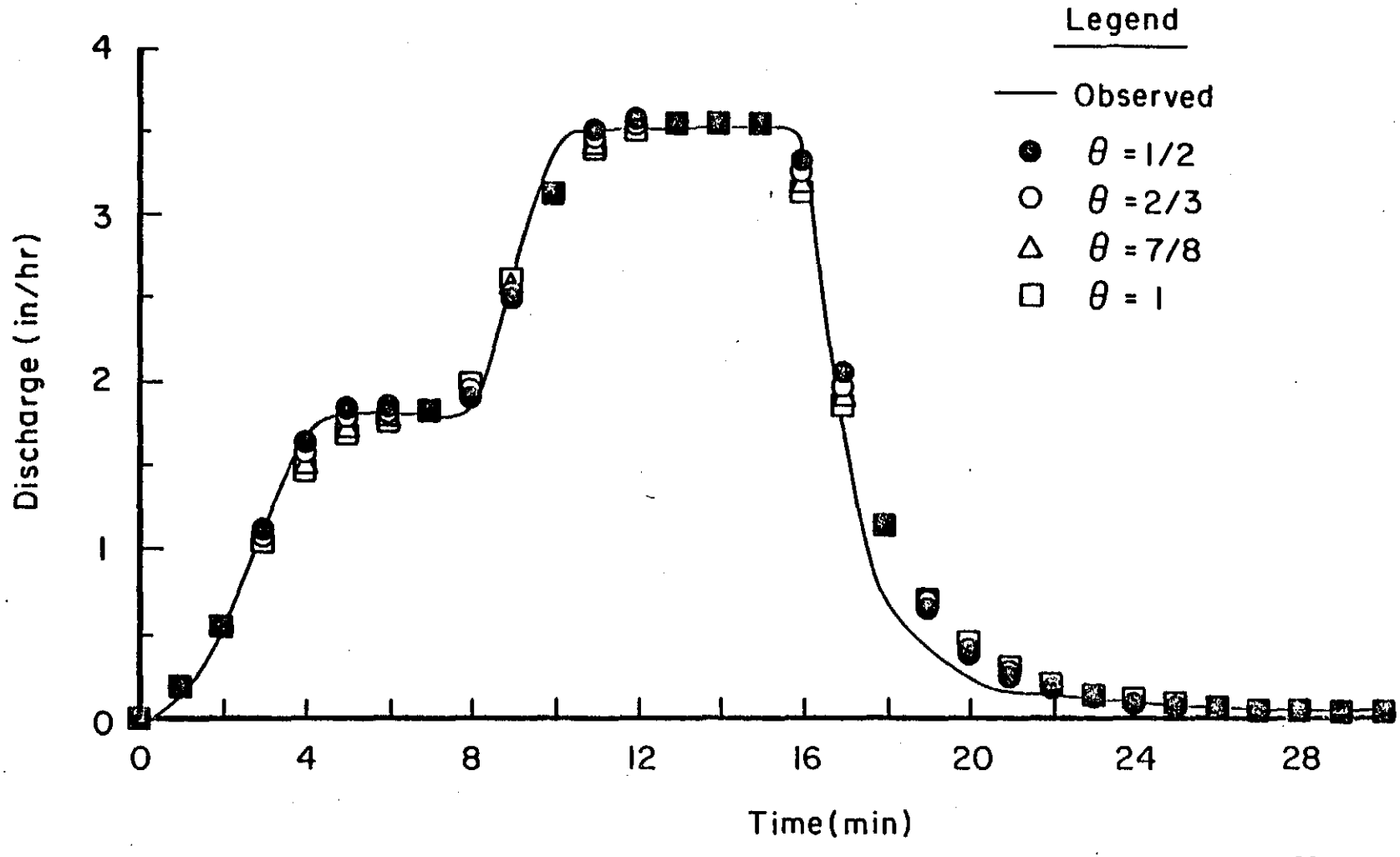

Fig. 4.8 Izzard's Run #138 - Hydrographs Computed Using One Cubic Element and Δt = 30 seconds

Table 4.1 - Izzard's Runn # 138 - Times to 1st and 2nd Equilibrium Flow (T_{e1} and T_{e2}) and the Equilibrium Flow Rates (q_{e1} and q_{e2})*

θ	T_{e1} (min)	T_{e2} (min)	q_{e1} (in/hr)	q_{e2} (in/hr)
1/2	4 1/2	11 1/2	1.839	3.555
2/3	5	12	1.831	3.551
7/8	5 1/2	12 1/2	1.818	3.548
1	6	13	1.816	3.546

*Observed T_{e1} = 5 min.

Observed T_{e2} = 11 min.

Observed q_{e1} = 1.83 in/hr

Observed q_{e2} = 3.55 in/hr

Table 4.2 - Izzard's Run # 138 - Simulated Runoff and Ponded Volumes

θ	$V_Q(ft)^3$	$V_P(ft)^3$	%error*
1/2	4.289	0.005821	0.21
2/3	4.273	0.006095	0.58
7/8	4.254	0.006418	1.01
1	4.242	0.006606	1.29

*Rainfall Volume = 4.304 ft

Data was obtained from the USDA-ARS (undated) for experimental watersheds located in Hastings, Nebraska. A small watershed, identified as Hastings 5H, was selected for study. The watershed was classified as pasture land and consisted of the same three soil types; Hastings silt loam, Hastings silty clay loam and Colby silt loam. Each soil occurred in layers, but infiltration did not proceed beyond the first layer (5 inches) in any of the storm events analyzed. Therefore, properties are given only for the first layer of each soil type. After obtaining the Green and Ampt parameters for each soil type, area-weighted averaging was used to estimate a single, overall set of watershed parameters.

The Green and Ampt parameters for each soil were obtained from Meadows et al. (1983). Meadows et al. determined the wetting front suction, Ψ_f after Brakensiek (1977) using Eq. 4.13, with the Brooks and Corey (1966) parameters determined from desorption data reported by the ARS. The ARS data included the moisture content, at various soil depths, corresponding to capillary pressures of 0.1, 0.3, 0.6, 3.0 and 15.0 bars. The porosity, ϕ , of each soil was determined from ARS bulk density data. Table 4.3 lists ϕ and Ψ_f for each soil type. Table 4.3 also gives the percent composition of watershed 5H for each soil type.

Unlike Ψ_f, the saturated hydraulic conductivity, K_s , could not be determined directly from given ARS data. For a given soil type, the ARS reported a large range of K_s values. After numerous optimization studies, which considered only infiltration volume, Meadows et al. (1983) concluded that K_s was variable due to the swelling nature of the soil. (This conclusion is confirmed by Smith (1970) who also analyzed a Hastings experimental watershed). The swelling behavior is the result of the clay content of the soil. It was determined that the overall

Table 4.3 - Summary of Green and Ampt Parameters for Watershed 5H with the Percent of Each of the Soil Types

Soil Type:	Hastings Silt Loam	Hastings Silty Clay Loam	Colby Silt Loam
ϕ	.5509	.630	.550
$\Psi_{f(ft)}$	.812	.787	1.780
Percent	87	7	6

K_s (averaged over the three soil types) could vary from 0.15 in/hr to 0.58 in/hr depending upon the initial moisture content, θ_i. Initially wet soil would be swollen, thereby having a smaller saturated hydraulic conductivity. Data obtained from Meadows et al. indicated the maximum (for each soil type) for which the average K_s would not be decreased from 0.58 in/hr. The data also indicated the lowest θ_i for which a wet, swollen soil would retain a K_s of 0.15 in/hr.

The ARS data also did not contain extensive initial moisture content data for the historical events recorded on the Hastings watersheds. To overcome this difficulty, Meadows et al. (1983) obtained bimonthly data, giving moisture content versus depth, for what was considered to be a model rainfall year. This data was then used as a general trend to estimate θ_i for a given rainfall event. If antecedent moisture conditions were described as wet, the estimated θ_i was adjusted accordingly. Such a rational procedure for estimating θ_i is necessary in order to analyze past rainfall events for which θ_i was not recorded. However, the procedure is, at best, an educated guess of the initial moisture content of the soil.

The Hastings 5H watershed is shown in Fig. 4.9. Hastings 5H was chosen because it does not possess irregularities which would make application of the one-dimensional overland flow model difficult. The watershed is relatively flat at the upstream end, but converges toward a definite flow path. The watershed was modeled as a series of three constant slope planes, and each plane was discretized using one cubic Lagrangian element as shown in Fig. 4.9. The flow plane width for each of the three subplanes was approximated with a cubic polynomial along the flow path (see Fig. 4.9 and Eq. 4.23)

The finite element-Green and Ampt analyses were performed for two

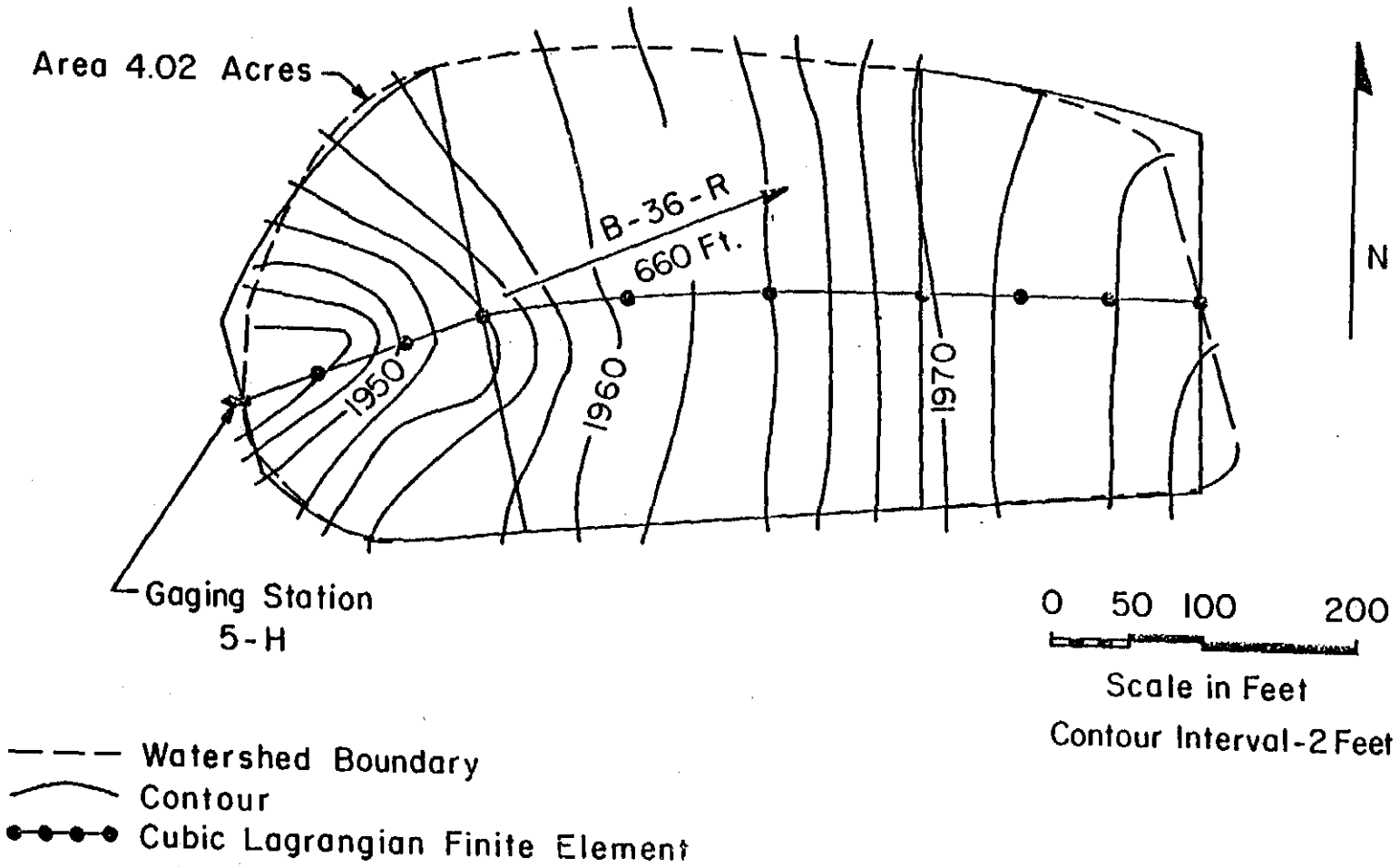

Fig. 4.9 Hastings Watershed 5H

rainfall events. Table 4.4 presents each event with the corresponding value of K and the initial moisture content, θ_i, for each soil type. Table 4.5 summarizes the rainfall data for each event. Figs. 4.10 and 4.11 show the computed runoff hydrograph (for $\Delta t = 15$ sec and $\theta = 1/2$) and the observed hydrograph for each event.

The first event, August 11, 1961 on watershed 5H, was used to determine an optimum value of Manning's roughness coefficient, n. Manning's n was chosen to obtain a computed hydrograph similar in shape to the observed hydrograph. A value of n = 0.035 was found to yield the optimal hydrograph shape. This value of n corresponds to the value given by Chow (1959) for flood plains in pasture land. Table 4.3 gives the values of ϕ and Ψ_f used for all events. Values of K_s and θ_i for each event were suggested by Meadows et al. (1983). As explained previously, however, θ_i was simply an educated guess. Therefore, θ_i was varied to optimize the calculated peak runoff and runoff volume within the limits of values discussed previously.

Fig. 4.10 shows the hydrographs for the August 11, 1961 event on watershed 5H. The computed hydrograph initiated runoff within two minutes of the observed hydrograph and was very similar in shape to the observed hydrograph. However, the computed time to peak missed the observed time to peak by six minutes and the computed hydrograph ceased runoff several minutes prior to the observed hydrograph. Fig. 4.11 shows the results for the July 26, 1964 event on watershed 5H. In this case, the computed hydrograph peaked within 1/4 of a minute of the observed hydrograph, but initiated runoff three minutes early and ceased runoff over thirty minutes too soon.

A characteristic exhibited by both computed hydrographs is early

Table 4.4 - Summary of K_s and θ_i Values Used for the Watershed 5H Analyses

Event	K_s (in/hr)	θ_i Hastings Silt Loam	θ_i Hastings Silty Clay Loam	θ_i Colby Silty Loam
8/11/61	0.58	0.255	0.213	0.255
7/26/64	0.58	0.150	0.137	0.156

Table 4.5 - Summary of Rainfall Data for Hastings 5H Events

August 11, 1961		July 26, 1964	
Time (hr. min)	Accumulated Rain (in)	Time (hr. min)	Accumulated Rain (in)
0.26	0.00	16.44	0.00
0.38	0.74	16.51	0.78
0.42	0.76	16.55	1.07
0.52	1.50	16.58	1.28
1.00	1.61		
1.30	1.70		
1.50	1.71		

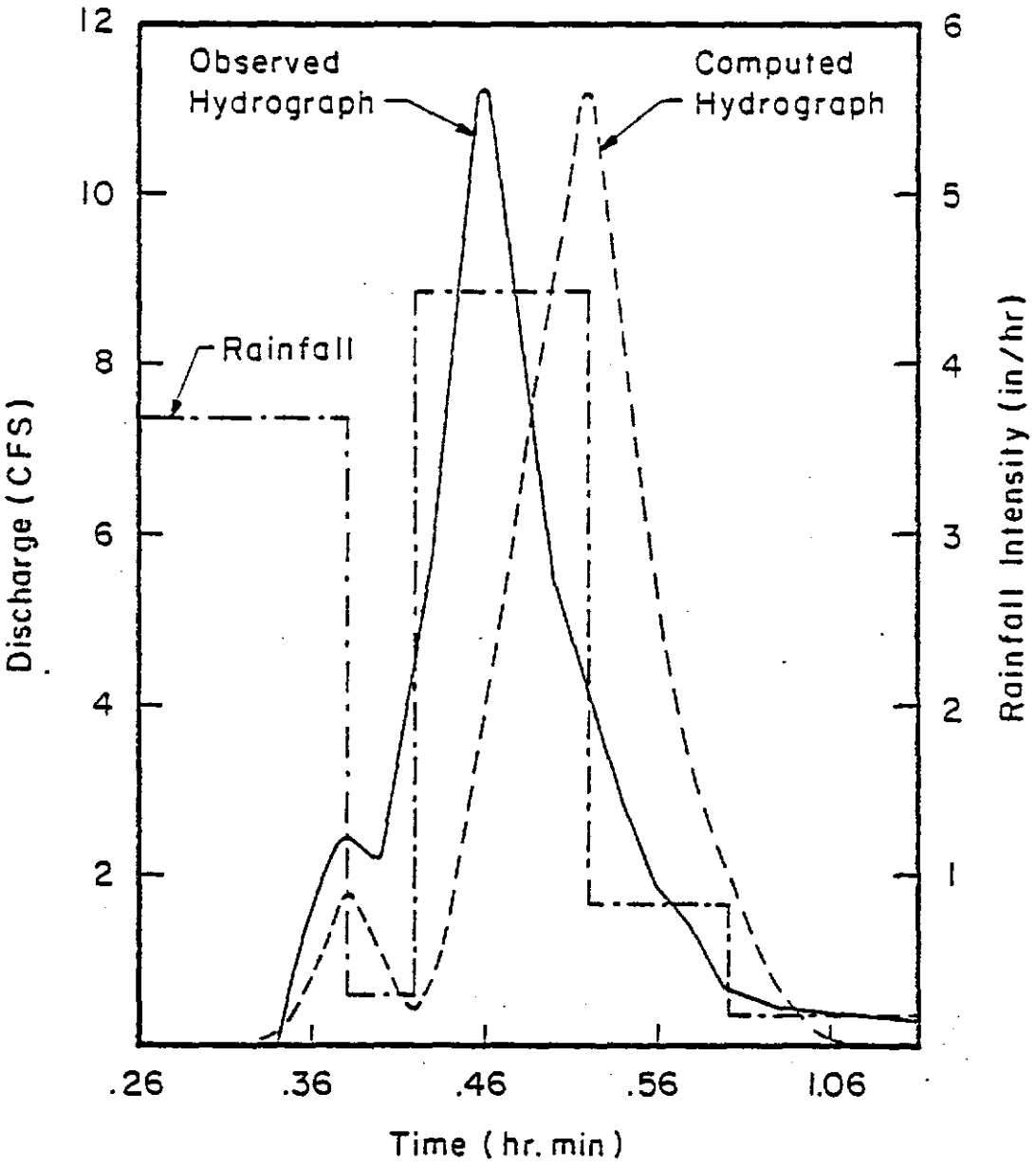

Fig. 4.10 August 11, 1961 Event on Watershed 5H - Simulated Using $\theta = 1/2$ and $\Delta t = 15$ seconds

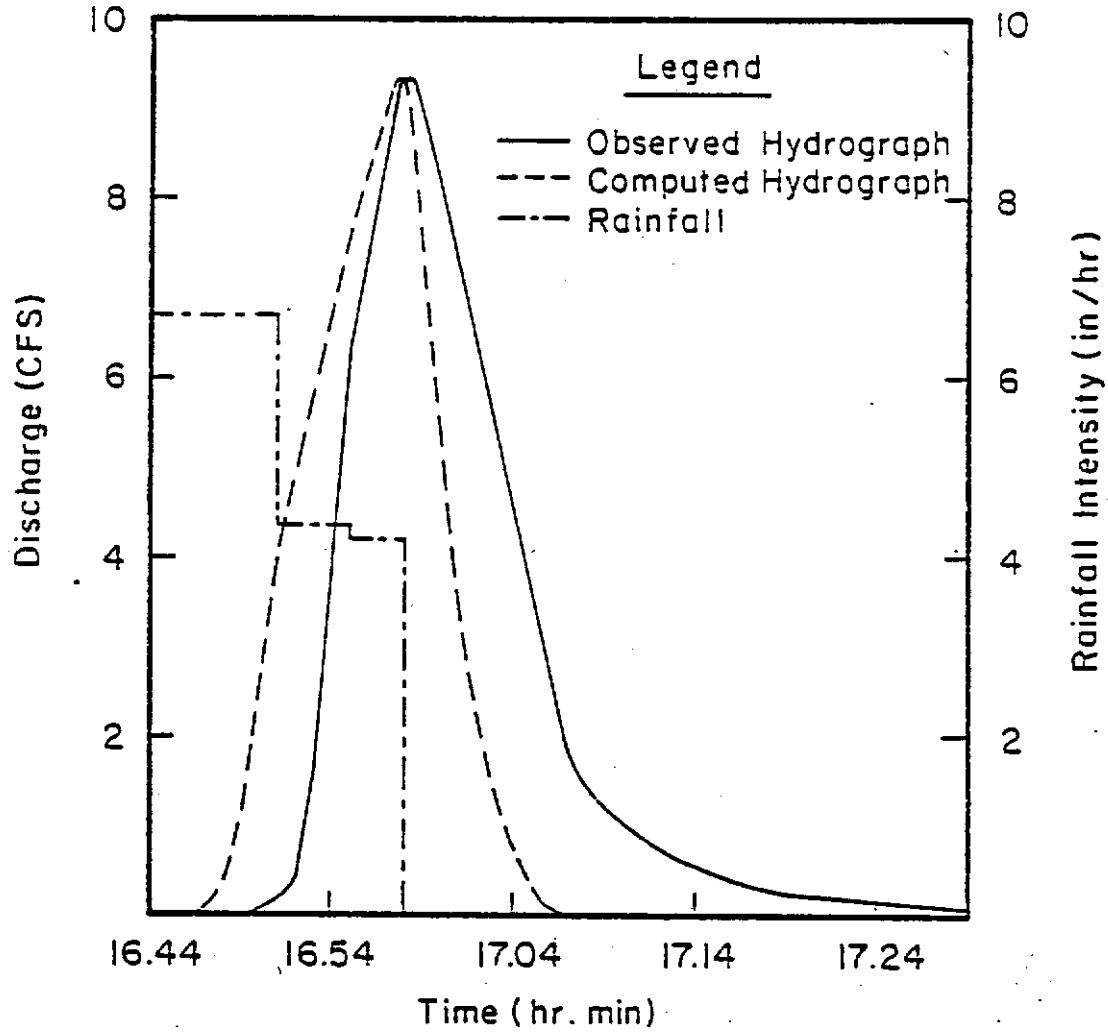

Fig. 4.11 July 26, 1964 Event on Watershed 5H - Simulated Using $\theta = 1/2$ and $\Delta t = 15$ seconds

prediction of both the initiation and the cessation of runoff. A likely explanation for this behavior is that a one-dimensional flow model was applied to a natural surface. Channelized flow, which is not represented by the one-dimensional model, occurs to various extents over the natural watersheds. In the upper planes, where the terrain is relatively flat, small flow channels will form because the plane is not perfectly uniform in slope. This channelization causes the actual watershed response to be delayed somewhat, in comparison to the computed, because flow is initially moving toward the channels, rather than directly toward the watershed outlet. In the third plane the terrain causes the flow paths to converge toward a larger main flow channel. The extended recession limb of the observed hydrographs probably represents the drainage of the main channel which occurs after rainfall ceases. At the end of rainfall on the natural watersheds, most of the flow is channelized and infiltration is occurring over a very small percent of the total watershed area. However, the one-dimensional model calculates infiltration over the entire watershed area, causing the ponded water to be absorbed relatively quickly after rainfall ceases. In addition to channelization, formation of a surface seal may also serve to extend the actual recession limb further than the calculated hydrograph.

Additional error in the computed hydrographs may result from error in the rainfall data. Rainfall data, which was used as input to the finite element program, was obtained from one raingauge near the watershed. Therefore, due to lack of better information, each intensity during the storm event was assumed to apply uniformly over the whole watershed. But the observed hydrograph is the measured response of the watershed to the actual rainfall pattern, which, in all probability, had some degree of spatial variability over the watershed area.

4.7 Applicability to Surface Mined Watersheds

Specific simulations of stormwater runoff from surface coal mined watersheds were not performed. The primary reason is that sufficient data (particularly soil data required for the Green-Ampt infiltration model) has not been published and field data collection was beyond the scope of this report. However, the agricultural watershed events considered are typical of mining disturbed watersheds. For example, areal mining procedures are used in topographic regions similar to the Hastings watershed. Areal mining is practiced on relatively flat or gentle rolling terrain which is similar in scope to the Hastings watershed (three to seven percent slopes). Areal mining is extensively utilized in midwestern prime farmland areas and in western regions of the United States (Barfield, et al., 1981).

The coupled Green-Ampt infiltration-finite element overland flow model is applicable for assessing both the pre-mining and post-mining (reclaimed) hydrologic responses. The physically based Green-Ampt infiltration model is ideal for representing infiltration on reclaimed mining disturbed watersheds, as well as watersheds in various stages of disturbance. Furthermore, significant historical records are not required to utilize the coupled infltration-overland flow model.

CHAPTER 5

SUMMARY AND RECOMMENDATIONS

5.1 Summary

Surface mining often is conducted in a harsh environment, usually disturbs a large area, can involve major changes in topography, ground cover and soil profile, and often is performed in an area where little or no hydrologic information is available. As such, mathematical models that account for the changes in watershed hydrologic response due to these modifications are required for planning and evaluating the effectiveness of management strategies. Most available models were developed and calibrated on data from agricultural, forested or urban watersheds. Thus, there are problems with using these models for surface mine simulation. First, key component model parameters, such as the SCS curve number, have not been evaluated for surface mined land use. Second, too few comparision studies evaluating the capability of models to simulate stormwater runoff in the absence of calibration data have been published. Consequently, the user is confronted with a range of models for a given situation and has little direction on which one to choose. Once the choice is made, there are still the problems of how to interpret the parameter values and how best to apply the model. The purpose for this research was to develop improved methods and guidelines for modeling stormwater runoff from surface mined lands.

Available rainfall simulation data from natural and reclaimed spoil sites at two mines in Wyoming were evaluated for runoff curve numbers. The results suggest that proper reclamation can be effective in returning a disturbed site to its natural surface runoff potential. The computed curve numbers were compared with published values to relate

them to known agricultural, forested, and urban land use curve numbers. Generally, the reclaimed curve numbers were equivalent to cultivated land. Until better data are available with which to quantify surface mined curve numbers, the appropriate agricultural land use curve number is recommended.

Four popular synthetic unit hydrograph models were tested to determine their regional applicability. This is considered a necessay first step to applying existing models to a different land use. The models tested were the SCS curvilinear (Haan), SCS single triangle, Williams, and TVA double triangle unit hydrographs. The data base included event data from 38 USDA experimental watersheds in 14 physiographic provinces. In all, each model was tested on over 270 events. Event curve numbers were used, i.e., for each event, the curve number that preserved continuity between recorded rainfall and runoff was used. Though inconclusive due to the limited number of events analyzed, test results indicated a regional tendency for each model, with the SCS curvilinear unit hydrograph method generally performing best overall. Since event curve numbers were used, hydrograph volumes were predicted exactly. For all models, simulated shapes compared well with observed shapes; but, predicted peaks and times varied as much as 50 percent from observed.

A second test was conducted using only the SCS curvilinear unit hydrograph to test the hypothesis that the prediction errors were due to the rainfall excess pattern simulated with the curve number model. Forty-eight events on 11 small watersheds at the Central Great Plains Experimental Watershed at Hastings, Nebraska, were selected. A theoretical analysis of the curve number model equation suggests it should perform best with short duration rainfall events without lulls or

extended periods of rainfall less than the soil saturated hydraulic conductivity. The test results supported this concept, particularly on watersheds dominated volumetrically by surface runoff. In contrast, the curve number model, in conjunction with the SCS curvilinear unit hydrograph model, does not perform well on watersheds dominated hydrologically by subsurface flow. Analysis of data from the New River basin in Tennessee for watersheds up to 20 percent mined, but under the old mining practices that did not require return to contour, indicated subsurface, or analogous, dominance of the runoff hydrograph. This indicates the SCS curvilinear unit hydrograph does not apply in these and similar watersheds.

To overcome the difficulties of applying available models to new land use or on ungaged watersheds where the model parameter prediction equations do not hold, a procedure that used the time area method and the two parameter gamma distribution to develop a unit hydrograph was presented. Limited tests on Pony Mountain Branch watershed in Culpepper County, Virginia, showed significant improvement in simulation accuracy compared to the SCS curvilinear unit hydrograph model results. This method is recommended for ungaged watersheds, or watersheds undergoing land use change, where available unit hydrograph techniques do not apply.

A coupled Green-Ampt infiltration-finite element kinematic wave model for multi-plane watersheds has been presented. An infiltration equation was developed based on the physics of Darcy's law and the assumptions of Green and Ampt infiltration modeling. The explicit Green-Ampt infiltration model is numerically evaluated using the finite difference method. Parameter estimation techniques for the

deterministic Green-Ampt infiltration model were presented.

A Galerkin finite element approximation using linear, quadratic and/or cubic Lagrangian elements was presented for the spatial discretization of the overland flow model. A linear time variation was used to represent the temporal variations. With the linear time variation, both explicit and implicit time marching algorithms are available. The choice of explicit or implicit time integration scheme depends on the choice of time weighting coefficient.

Choosing an implicit time discretization requires an initial estimate of the nodal flow depths at the advanced time step ($t + \Delta t$). A forward in time, backward in space, finite difference solution of the kinematic wave equation was used to generate the initial flow depth estimates at time $t + \Delta t$. The final converged flow depth profile was obtained using a modified Newton-Raphson procedure on the system of finite element equations.

The coupled Green-Ampt infiltration-finite element kinematic wave model was tested using impervious plane data (Izzard's Run #138) and pervious multi-plane data for two storm events (Hastings Watershed 5H). The impervious surface results demonstrated that the finite element model is an excellent method for simulating overland flow. In general, the impervious plane simulation demonstrated that cubic Larangian elements and Crank-Nicholson ($\theta = 1/2$) or Galerkin ($\theta = 2/3$) time integration schemes should be used for finite element simulation of overland flow (further demonstration of this is given in Blandford, Peters and Meadows, 1983).

The coupled Green-Ampt infiltration-finite element kinematic wave overland flow model simulations using Hastings 5H data verified the applicability of the model to simulate storm events on pervious plane

watersheds. However, there are several problems associated with the developed model for simulating stormwater runoff from general watersheds. First, the model assumes unidirectional sheet flow. Consequently, channelized flow or two-dimensional overland flow is not represented and for watersheds where these effects may be dominant the developed model should not be used. Secondly, Green and Ampt infiltration does not represent lateral subsurface flow. Therefore, the model should not be used for watersheds where lateral subsurface flow (interflow) is significant. Third, the model assumes a uniform flow resistance, e.g., Manning's turbulent resistance equation. The model does not include the possibility of various resistance equations depending on the flow depth. This means some empirical adjustment or parameter optimization may be required to simulate the wide range of flow resistance which may occur for an unsteady storm event of long duration. Consequently, selection of Manning's friction factor (n) and flow depth exponential (m) in Eq. 4.19 should be selected to represent the dominant mode of flow (i.e., laminar, transition or turbulent) anticipated for a given storm event on a given watershed.

5.2 Recommendations

Future research to adapt existing stormwater models to surface mined land use conditions or to develop new models will require a quality data base collected under controlled conditions where land use, soils, mining schedule and reclamation practices are known. The data presently being collected under permit requirements are incomplete and therefore not useable for model verification studies. The available data identified during this study were collected under mining practices prior to the current regulations and also are not useable for developing

models descriptive of present mining and reclamation practices. Several federal agencies, such as the U.S. Geological Survey and the USDA-ARS, have identified study watersheds and are collecting the necessary hydrologic and land use data. They are encouraged to publish the data and to make them accessible to all researchers.

It is recommended that research be conducted to develop and test a statistical based method for determining curve numbers from short periods of record and from mixed land use records.

Further work is required to understand more fully the effect of the rainfall pattern on unit hydrograph simulation accuracy. The results of this study indicate that model simulation is poor for rainfalls with lulls or prolonged periods near the cessation of rain when the rainfall intensity is less than the soil saturated hydrologic conductivity. No rule of thumb was identified which would aid the model user in applying a model to such a rainfall event. This is important because many of the synthetic design rainfall patterns have periods when the rainfall intensity is low.

The proposed method for unit hydrograph development using the time area method and the two parameter gamma function should be tested on more watersheds representing a wide range of land use and hydrologic conditions. In particular, it should be tested on watersheds where the stormwater hydrograph is dominated volumetrically by subsurface flow.

The deterministic finite element model should be modified to include potential overland flow sources into the watershed channels and the modeling of the channelized flow. Other modifications include using a two-dimensional Richard's equation formulation to represent both infiltration and lateral subsurface flow in saturated-unsaturated porous

media. The use of a variable, depth dependent surface flow resistance equation should also be implemented. Once the proposed modifications have been implemented into the finite element model, further testing for a variety of watershed conditions would be necessary.

REFERENCES

Alley, W.M., Dawdy, D.R., and Schaake, J.C., Jr. (1980), "Parametric-Deterministic Urban Watershed Model," ASCE, J. Hydr. Div., Vol. 106, No. HY5, pp. 679-690.

Al-Mahidani, G. and Taylor, C. (1974), "Finite Element Solutions of the Shallow Water Equations--Surface Runoff," Finite Elements in Flow Problems, UAH Press, Huntsville, AL.

Ardis, C.V., Jr. (1972), "A Storm Hydrograph Model for the Response of Small Rural Watersheds," thesis presented to the University of Wisconsin, at Madison, Wisconsin, in partial fulfillment of the requirements for the degree of Doctor of Philosophy.

ASCE (1983), "Quantification of Land Use Change Effects Upon Hydrology," by the Task Committee on Quantifying Land Use Change Effects, R.P. Betson, Chmn., presented at the July 20-22, 1983, ASCE Irrigation and Drainage Division Specially Conference, held at Jackson, Wyoming.

Barfield, B.J., Warner, R.C. and Hahn, C.T. (1981), Applied Hydrology and Sedimentology for Disturbed Areas, Oklahoma Technical Press, Stillwater, OK.

Betson, R.P., Bales, J., and Pratt, H.E., (1980), "Users Guide to TVA-HYSIM, A Hydrologic Program for Quantifying Land Use Change Effects," EPA-600/7-80-048, Tennessee Valley Authority, Water Systems Development Branch, Norris, Tennessee.

Betson, R.P., Bales, J., and Deane, C.H. (1981), "Methodologies for Assessing Surface Mining Impacts," Report No. WR28-1-550-108, Tennessee Valley Authority, Water Systems Development Branch, Norris, Tennessee.

Blandford, G.E., Peters, N., II and Meadows, M.E. (1983), Development of Models for Simulating Stormwater Runoff from Surface Coal Mined Lands - Finite Element Simulation of Overland Flow, Report No. G5115213, Vol. II, U.S. Dept. of the Interior, Office of Surface Mining, Division of Research, Washington, D.C.

Bloomsburg, G.L. (1960), "A Hydrograph Equation," presented at the October 19-20, A.G.U. Pacific Northwest Section Meeting, held at Moscow, Idaho.

Bodman, G.B. and Colman, E.A. (1943), "Moisture and Energy Conditions During Downward Entry of Water into Soils," Proc. Soil Sci. Soc. Am., 7, pp. 116-122.

Bouwer, H. (1969), "Infiltration of Water into Nonuniform Soil," J. of the Irr. and Drainage Div., ASCE, Vol. 95, No. IR4, pp. 451-462.

Brakensiek, D.L. (1977), "Estimating the Effective Capillary Pressure in the Green and Ampt Infiltration Equation," Water Resources Res., Vol. 13, No. 3, pp. 680-682.

Brakensiek, D.L. and Engleman, R.L. (1979), "Relating Initial Abstraction, I_a, to Soil Infiltration," SCS-AR Cooperative Research on Hydrologic Modeling: Progress Report.

Brooks, R.H. and Corey, A.T. (1966), "Properties of Porous Media Affecting Fluid Flow," J. of the Irr. and Drainage Div., ASCE, Vol. 92, No. IR2, pp. 61-88.

Chow, V.T. (1959) Open Channel Hydraulics, McGraw-Hill, NY, p. 113.

Curwick, P.B., and Jennings, M.E. (1981), "Evaluation of Rainfall-Runoff Models for Hydrologic Characterization of Surface Mined Lands," presented at the May 18-21, 1981, International Symposium on Rainfall-Runoff Modeling, held at Mississippi State University, Starkville, Mississippi.

Damushkodi, V. (1979), "Flood Flow Frequency by SCS TR-20 Computer Program," ASCE, J. Hydr. Div., Vol. 105, No. HY9, pp. 1123-1135.

Delleur, J.W. (1964), Discussion of "Design Hydrographs for Small Watersheds in Indiana," by I-Pai Wu, Journal of the Hydraulics Division, ASCE, Vol. 90, No. HY4, pp. 318-320.

Dooge, J.C.I. (1973), "Linear Theory of Hydrologic Systems," U. S. Department of Agriculture, Agricultural Research Service, Tech. Bull. No. 1468.

Dunne, T. (1978), "Field Studies of Hillslope Flow Processes," in Kirkby, M.J. (Ed.), Hillslope Hydrology, John Wiley and Sons, New York.

Eagleson, P.S. (1970), Dynamic Hydrology, McGraw-Hill, NY.

Edson, C.G. (1951), "Parameters for Relating Unit Hydrographs to Watershed Characteristics," Transactions American Geophysical Union, Vol. 32, No. 4, pp. 591-596.

Golding, R.L. (1979), discussion of "Runoff Curve Number with Varying Site Moisture," R.H. Hawkins, J. Irrigation Drainage Div., ASCE, Vol. 105, No. IR4, pp. 441-442.

Gray, D.M. (1961), "Synthetic Unit Hydrographs for Small Watersheds," Journal of the Hydraulics Division, ASCE, Vol. 87, No. HY4, pp.33-54.

Haan, C.T. (1970), "A Dimensionless Hydrograph Equation," File Report, Agricultural Engineering Department, University of Kentucky, Lexington, Kentucky.

Hawkins, R.H. (1980), "Infiltration and Curve Numbers: Some Pragmatic and Theoretic Relationships," in Proceedings, ASCE Symposium on Watershed Management, Boise, Idaho, July 21-23, pp. 925-937.

Himmelblau, D.M. (1972), Applied Nonlinear Programming, McGraw-Hill, New York, 1972.

Izzard, C.F. (1946), "Hydraulics of Runoff from Developed Surfaces," Highway Res. Board, Proc. 26th Annual Meeting, pp. 129-150.

Jayawardena, A.W. and White, J.K. (1977), "A Finite Element Distributed Catchment Model, I. Analytical Basis," J. of Hydrology, Vol. 34, pp. 269-286.

Jayawardena, A.W. and White, J.K. (1979), "A Finite Element Distributed Catchment Model, II. Application to Real Catchments," J. of Hydrology, Vol. 42, pp. 231-249.

Johanson, R.C., Imhoff, J.C. and Davis, H.H., Jr. (1980), "Users Manual for Hydrlogical Simulation Program-Fortran (HSPF)," EPA-600/9-8-015, Environmental Research Laboratory, Office of Research and Development EPA, Athens, Georgia, 677 pp.

Judah, O.M., Shanholtz, V.O. and Contractor, D.N. (1975), "Finite Element Simulation of Flood Hydrographs," Trans. ASAE, Vol. 18, No. 3, pp. 518-522.

Kibler, D.F. and Woolhiser, D.A. (1970), "The Kinematic Cascade as a Hydrologic Model," Hydrology Paper No. 39, Colorado State University, Fort Collins, CO.

Lighthill, M.H. and Whitham, G.B. (1955), "On Kinematic Waves, I. Flood Movement in Long Rivers," Proc. Royal Soc. London, Ser. A, 229, pp. 281-316.

Lusby, G.C., and Toy, T.J, (1976), "An Evaluation of Surface Mine Spoils Area Restoration in Wyoming Using Rainfall Simulation," Earth Surface Processes, Vol. 1, pp. 375-386.

McCuen, R.H., and Bondelid, T.R. (1983), "Estimating Unit Hydrograph Peak Rate Factors," Journal of Irrigation and Drainage Engineering, ASCE, Vol. 109, No. 2, pp. 238-250.

Meadows, M.E., Howard, K.M. and Chestnut A. (1983), "Development of Models for Simulating Stormwater Runoff from Surface Coal Mined Lands: Unit Hydrograph Models, Report No. G5115213, Vol. I, U.S. Dept. of the Interior, Office of Surface Mining, Diviion of Research, Washington, D.C.

Medina, M.A., Jr., and Mohns, L.R. (1978), "Kinematic Wave Approximation to Forested Overland Flow with Urban Hydrologic Models," in Proceedings, International Symposium on Urban Stormwater Management, University of Kentucky, Lexington, Kentucky, July, 1978, pp. 63-72.

Mein, R.G. and Larson, C.L. (1971), "Modeling Infiltration Component of the Rainfall-Runoff Process," Bulletin 43, Water Resources Res. Center, University of Minnesota, Minneapolis, MN.

Mein, R.G. and Larson, C.L. (1973), "Modeling Infiltration During a Steady Rain," Water Resources Res., Vol. 9, No. 2, pp. 384-394.

Minshall, N.E. (1980), "Predicting Storm Runoff on Small Experimental Wastersheds," Journal of the Hydraulics Division, ASCE, Vol. 86, No. HY8, pp. 17-38.

Overton, D.E. (1980), "Computer Program TENN II, a Nonlinear Model for Simulating Stormwater Runoff Volumes, Hydrographs, and Pollutant Yields for Small Watersheds: Users Manual," D.E. Overton and Associates Consulting Engineers, Knoxville, Tennessee, 21 pp.

Overton, D.E. and Meadows, M.E. (1976), Stormwater Modeling, Academic Press, New York, 351 p.

Nash, J.E. (1959), "Systematic Determination of Unit Hydrograph Parameters," Journal of Geophysical Research, Vol. 64, No. 1, pp. 111-115.

Ponce, V.M., Li, R. and Simons, D.B. (1978), "Applicability of Kinematic and Diffusion Models," J. of the Hydr. Div., ASCE, Vol. 104, No. HY3, pp. 353-360.

Rallison, R.E. (1980), "Origin and Evolution of the SCS Runoff Equation," in Proceedings, ASCE Symposium on Watershed Management, Boise, Idaho, July 21-23, 1980, pp. 912-924.

Ross, B.B. (1978), "A Spatially Responsive Catchment Model for Predicting Stormwater Runoff from Ungaged Watersheds," Ph.D. Thesis, Virginia Polytechnic Institute and State University, Blacksburg, VA.

Ross, B.B., Shanholtz, V.O., Contractor, D.N., and Can, J.C. (1978), "A Model for Evaluating the Effects of Land Uses on Flood Fows," Bulletin 85, Virginia Water Resources Center, VPI and SU, Blacksburg, Virginia, 137 pp.

Ross, B.B., Contractor, D.N. and Shanholtz, V.O. (1979), "A Finite-Element Model of Overland and Channel Flow for Assessing the Hydrologic Impact of Land-Use Change," J. of Hydrology, Vol. 41, pp. 11-30.

Sherman, L.K. (1932), "Streamflow from Rainfall by the Unit Graph Method," Engineering News Record, Vol. 108, pp. 501-505.

Smith, R.E. (1970), "Mathematical Simulation of Infiltrating Watersheds," Ph.D. Thesis, Colorado State University, Fort Collins, CO.

Soil Conservation Service (1969), "Computer Program for Project Formulation, Hydrology," SCS Technical Release 20, Supplement No. 1.

Soil Conservation Service (1972), "National Engineering Handbook, Section 4: Hydrology," Washington, D.C.

Soil Conservation Service (1975), "Urban Hydrology for Small Watersheds," Technical Release No. 55.

Stoker, J.J. (1953), "Numerical Solution of Flood Prediction and River Regulation Problems - Report I - Derivation of Basic Theory and Formulation of Numerical Methods of Attack," Report No. IMM-200, Institute of Mathematical Sciences, New York University, New York, NY.

Taylor, R.L. (1977), in O.C. Zienkiewicz, The Finite Element Method, Third Edition, McGraw-Hill, NY, Chapter 24.

Tennessee Valley Authority (1973), "Storm Hydrographs Using A Double Triangle Model," Division of Water management, Research Paper NO. 9, Knoxville, Tennessee.

USDA-ARS (undated), "The Central Great Plains Experimental Watersheds: A Summary of Thirty Years of Hydrologic Research."

Ward, A., Haan, C.T. and Tapp, J. (1979), The DEPOSITS Sedimentation Pond Design Manual, Prepared for the Institute for Mining and Mineral Research Laboratory, Lexington, Kentucky.

Williams, J.R. (1968), "Runoff Hydrographs from Small Texas Blacklands Watersheds," U.S. Department of Agriculture, Agricultural Research Service, ARS 41-143.

Williams, J.R. and Hann, R.W. (1973), "HYMO: Problem-Oriented Computer Language for Hydrologic Modeling Users Manual," U.S. Department of Agriculture, Agricultural Research Service, ARS-S-9.

Woolhiser, D.A. and Liggett, J.A. (1967), "Unsteady One-Dimensional Flow Over a Plane--The Rising Hydrograph," Water Resources Res., Vol. 3, No. 3, pp. 753-771.

Wu, I-Pai (1963), "Design Hydrographs for Small Watersheds in Indiana," Journal of the Hydraulics Division, ASCE, Vol. 89, No. HY6, pp. 35-66.

Zienkiewicz, O.C. and Cheung, Y.K. (1965), "Finite Elements in the Soution of Field Problems, Engineer, Sept. 1965.